

DISSERTATION

A SURFACE PROTEASE OF LYME DISEASE BACTERIA DEGRADES HOST
EXTRACELLULAR MATRIX COMPONENTS AND INDUCES INFLAMMATORY
CYTOKINES *IN VITRO*

Submitted by

Theresa Michelle Tidd Russell

Department of Biochemistry and Molecular Biology

In partial fulfillment of the requirements

For the Degree of Doctor of Philosophy

Colorado State University

Fort Collins, Colorado

Fall 2012

Doctoral Committee:

Advisor: James R. Bamberg

Co-Advisor: Barbara J.B. Johnson

Karolin Luger

Robert E. Cohen

Claudia Gentry-Weeks

Copyright by Theresa Michelle Tidd Russell 2012

All Rights Reserved

ABSTRACT

A SURFACE PROTEASE OF LYME DISEASE BACTERIA DEGRADES HOST EXTRACELLULAR MATRIX COMPONENTS AND INDUCES INFLAMMATORY CYTOKINES *IN VITRO*

For nearly two decades, the paradigm in Lyme disease research has been that *Borrelia burgdorferi* does not produce proteases capable of damaging host molecules. Lyme disease has been considered, therefore, to be the consequence of an exuberant inflammatory response to infecting bacteria. This prevailing concept, however, has created a conundrum for the field. The bacterial burden in infected tissue is low, but the degree of inflammation is remarkable and seemingly out of proportion to this burden. The studies described in this dissertation provide evidence that, contrary to current thinking, *B. burgdorferi* does possess a protease that degrades numerous molecules of the host extracellular matrix (ECM). In addition to destabilization of the ECM which would be expected to benefit the organism, characterization of this proteolytic activity demonstrates that ECM fragments are produced that are known to be pro-inflammatory. These bioactive fragments may amplify the inflammatory processes triggered by the presence of the bacteria itself. When this hypothesis was tested directly by exposing chondrocytes to the borrelial protease in vitro, inflammatory cytokines and chemokines that are hallmarks of Lyme disease were

induced. The studies herein suggest a new model for the pathogenesis of Lyme disease and offer an explanation for the paradox of debilitating inflammatory disease in the presence of few infecting organisms. Lastly, in contrast to current serology-based Lyme disease diagnostic tests, the activity of this protease *in vitro* may generate diagnostic biomarkers enabling detection of active *B. burgdorferi* infection.

ACKNOWLEDGEMENTS

This dissertation is dedicated, first and foremost, to my family:

to my brilliant and astonishingly supportive husband, Larry, who believed in me long before I believed in myself,

to our equally brilliant children, Sam and Claire, who remind me every day that life is *only* about filling the moments with love and laughter,

to my twin sister, Janine, who has inspired me for decades with her indomitable spirit and her quest for knowledge.

It's been a wild ride! Thanks for taking it with me and for encouraging me to stick with it.

The work described in this dissertation could only have been accomplished with the sagacious guidance of my mentors, Dr. Barbara J.B. Johnson and Dr. James R. Bamburg. Yours are the shoulders upon which I've stood. Thank you for sharing with me your wisdom and your love for the art of science.

TABLE OF CONTENTS

ABSTRACT	ii
LIST OF TABLES	ix
LIST OF FIGURES	x
CHAPTER 1: Introduction	1
CHAPTER 2: Lyme Disease	4
Epidemiology	4
Zoonotic Cycle	6
Signs and Symptoms	6
Diagnosis	7
Treatment.....	8
Post-Treatment Lyme Disease Syndrome	9
Pathogenesis of Lyme Disease.....	9
Borrelial Factors Involved in the Pathogenesis of Lyme Disease	9
Borrelial Immune Evasion Strategies	14
Host Factors Involved in the Pathogenesis of Lyme Disease.....	15
CHAPTER 3: Lyme Arthritis.....	20
Clinical Features of Lyme Arthritis	21
Radiographic and Histopathologic Features of Advanced Lyme Arthritis	21
Antibiotic-Refractory Lyme Arthritis.....	22
Persistent <i>Borrelia burgdorferi</i>	22
Molecular Mimicry	24
Other Forms of Inflammatory Arthritis	25
Osteoarthritis	26
Rheumatoid Arthritis.....	27
Septic Arthritis	29
Reactive Arthritis	30

Comparison of LA With Other Forms of Inflammatory Arthritis	33
CHAPTER 4: Extracellular Matrix Degradation and Proteases in Arthritis. 36	
Aggrecan.....	36
Host Proteases in Arthritis.....	39
Aggrecanases	39
Matrix Metalloproteinases.....	40
HtrA1	41
Bacterial Proteases in Disease	45
Bacterial HtrA Homologs	46
Proteases in Lyme Disease	48
Host Proteases in Lyme Disease	48
Borrelial Proteases in Lyme Disease.....	50
CHAPTER 5: Materials and Methods	51
Characterization of Commercial Aggrecan by Dot Blots	51
Bacterial Strains and Growth Conditions	51
Fluorescence Labeling of Aggrecan.....	51
Analysis of Borrelial Interaction with Aggrecan	52
Fluorescent Aggrecan Labeling of Intact Borrelia.....	52
Affinity Chromatography.....	52
Mass Spectrometric Analysis of Aggrecan-Binding Proteins	54
Amino-Terminal Sequence Analysis.....	55
Characterization of BbHtrA	55
Generation of Recombinant BbHtrA and BbHtrA ^{S226A}	55
Determination of Endotoxin Units	56
Polyclonal Rabbit Anti-BbHtrA.....	56
Immunoblot Analysis of Borrelial Lysates	58
Zymography	59
Proteinase K Assays	59
Surface Biotinylation.....	60

Analysis of Human Sera for Antibodies to BbHtrA ^{S226A}	60
Proteolysis Assays	61
Immunoblot Analysis of Recombinant Aggrecan Proteolytic Fragments	62
Evaluating Inflammatory Cytokine Responses to BbHtrA Activity	63
Mesenchymal Stem Cell Culture	63
Chondrogenesis and Aggregate Formation.....	63
Chondrocyte Cytokine Induction.....	64
Cytokine Assays.....	65
Analysis of Cytokine Pixel Density	65
Mass Spectrometry of Fibronectin Fragments.....	66
CHAPTER 6: Results	69
Characterization of the Aggrecan Used in These Studies.....	69
Examination of the Interaction of Intact Borrelia with Aggrecan.....	74
Identification of <i>B. burgdorferi</i> Aggrecan-Binding Proteins.....	76
Agarose-Based Affinity Chromatography Using <i>B. burgdorferi</i> Clonal Isolate A3.....	76
Agarose-Based Affinity Chromatography Using Non-Clonal <i>B. burgdorferi</i>	81
Polyacrylamide-Based Affinity Chromatography of Non-Clonal <i>B. burgdorferi</i>	88
Mass Spectrometric Identification of <i>B. burgdorferi</i> Aggrecan-Binding Proteins	90
Characterization of BbHtrA	98
In Silico Analysis of Homology between BbHtrA and Selected Orthologs ...	98
Expression and Purification of Recombinant BbHtrA and BbHtrAS226A ..	103
BbHtrA is Auto-catalytic, Cleaving between Phe89-Phe90.....	105
Recombinant BbHtrA is Proteolytically Active	105
Examination of Surface Exposure of BbHtrA.....	108
BbHtrA is an Early Immunogenic Protein	111
HtrA is Conserved Among Lyme Disease Spirochetes	113
Characterization of the Interaction Between BbHtrA and Aggrecan.....	115

BbHtrA Degrades Recombinant and Native Aggrecan	115
Cleavage of Aggrecan at the Aggrecanase 374ARGS Site.....	117
Degradation of Hyalactins, Small Leucine-Rich Proteoglycans, and Fibronectin	120
BbHtrA Generates Pro-inflammatory Fibronectin Fragments	123
In Vitro Consequences of BbHtrA Activity in a Cartilage-like System	123
BbHtrA Stimulates Chondrocyte Release of Inflammatory Cytokines	126
CHAPTER 7: Discussion.....	135
A New Model for Borrelial Pathogenesis.....	145
CHAPTER 8: Future Directions	148
Detailed Characterization of BbHtrA	148
Diagnostic Potential of BbHtrA-Generated ECM Fragments.....	148
REFERENCES	150

LIST OF TABLES

Table 1 Borrelial adhesins and host ECM ligands	13
Table 2 Potentially antigenic BbHtrA peptides.....	57
Table 3 Summary of BbHtrA and Bgp mass spectrometry data	93
Table 4 Homology of selected HtrA orthologs and homologs with BbHtrA determined by BLAST analysis	99
Table 5 Pixel densities of cytokines altered by test conditions	132
Table 6 Statistical significance of differences in cytokine expression between chondrocyte culture conditions	134

LIST OF FIGURES

Figure 1 Confirmed cases of Lyme disease in the United States in 2010.....	5
Figure 2 Clinical Manifestations of Confirmed Lyme Disease Cases-United States, 2001-2010.....	20
Figure 3 Schematic of aggrecan structure and cleavage within the interglobular domain (IGD).	37
Figure 4 Purification of bovine aggrecan by Sigma supplier.....	71
Figure 5 Dot blots of Sigma aggrecan A1960 Lot 089K4071 to assess composition, integrity, and purity.....	73
Figure 6 Confocal microscopy of intact <i>B. burgdorferi</i> with fluorescently labeled aggrecan.....	75
Figure 7 <i>B. burgdorferi</i> B31 A3 proteins eluted from an agarose-based aggrecan column	78
Figure 8 <i>B. burgdorferi</i> B31 A3 proteins eluted from two agarose-based aggrecan columns.	80
Figure 9 Immunoblot of aggrecan-binding proteins within lysates of non-clonal <i>B. burgdorferi</i> B31	83
Figure 10 Immunoblot of non-clonal <i>B. burgdorferi</i> B31 aggrecan-binding proteins retained under stringent wash conditions on an agarose-based affinity column	85
Figure 11 Aggrecan-binding proteins identified by tandem mass spectrometry .	87
Figure 12 Affinity chromatography demonstrating <i>B. burgdorferi</i> aggrecan binding proteins.....	89
Figure 13 Proteins with a minimum of 2 unique peptides identified in eluates from chromatography columns.....	92
Figure 14 Mass Spectrometry data for BbHtrA identified in aggrecan affinity chromatography eluates	94
Figure 15 Mass Spectrometry data for Bgp identified in aggrecan affinity chromatography eluates	95
Figure 16 Protein Sequence Alignments of Amino Acids 1-300 for Selected HtrA Orthologs Demonstrating Conservation	100

Figure 17 Protein Sequence Alignments of Amino Acid 301 to Carboxyl Terminus For Selected HtrA Orthologs Demonstrating Conservation.....	101
Figure 18 Structural model of BbHtrA.....	102
Figure 19 Purity of recombinant BbHtrA and BbHtrA ^{S226A} and auto-degradation of BbHtrA	104
Figure 20 Analysis of BbHtrA proteolytic activity in various reaction conditions	107
Figure 21 Surface biotinylation of BbHtrA.....	109
Figure 22 BbHtrA surface exposure on intact spirochetes assessed by sensitivity to proteinase K.....	110
Figure 23 BbHtrA is an immunogenic protein expressed during human disease	112
Figure 24 HtrA expression and activity is conserved among the major genospecies of Lyme disease spirochetes	114
Figure 25 BbHtrA degradation of aggrecan	116
Figure 26 Amino terminal sequence analysis of BbHtrA-generated aggrecan fragments	119
Figure 27 BbHtrA degradation of proteoglycans and fibronectin	122
Figure 28 Identification of cytokines induced in chondrocyte cultures	125
Figure 29 Comparison of cytokine responses induced in chondrocytes by BbHtrA, heat-denatured BbHtrA and LPS	128
Figure 30 Comparison of cytokine responses induced in chondrocytes by wild type BbHtrA, mutant BbHtrA ^{S226A} and LPS.....	130
Figure 31 Box plots of pixel density data for induced cytokine responses	133
Figure 32 Model of potential consequences of BbHtrA-mediated ECM degradation.....	147

CHAPTER 1: Introduction

Lyme disease became a Nationally Notifiable disease in 1991 and ranked 5th on this list of infectious diseases in the United States in 2009. In the US, reported cases have tripled since reporting began and are continuing to rise with over 30,000 cases being reported in 2010. Lyme disease is also an important public health problem in Europe with over 65,000 cases of Lyme borreliosis being reported annually (1) and is an emerging public health problem in Asia (2).

The infectious agent, the spirochete *Borrelia burgdorferi*, is transmitted to humans during the bite of an infected tick. Efforts to understand the molecular basis of Lyme disease pathogenesis have been hindered because few bacteria are deposited into the skin of a host and few organisms colonize affected tissues (3). The mechanism(s) by which *B. burgdorferi* disseminate from sites of infection, penetrate the extracellular matrix (ECM) of connective tissues, and enter the vasculature are poorly understood. Systemic infection develops as *Borrelia* migrate through tissue extracellular matrices (ECM) to colonize various parts of the body including joints. This infection results in multi-organ system illness that, left untreated, can result in significant pathologies that may involve the skin, neural tissue, joints and the heart (2). The diverse pathologies induced by *B. burgdorferi* have not been traced to direct activities of the spirochetes. Instead, Lyme disease is thought to arise from host inflammatory responses stimulated by a relatively small number of organisms (4).

Here, we identify and characterize a surface-exposed protease of *B. burgdorferi* (BbHtrA) which is expressed during human disease and is conserved

among the major spirochetal genospecies that cause Lyme disease. BbHtrA degrades fibronectin and numerous proteoglycans found in skin, joints and neural tissues. BbHtrA proteolysis of fibronectin generated known pro-inflammatory fibronectin fragments FnIII₁₃₋₁₄ and Fnf-29. Consistent with these results, BbHtrA proteolytic activity stimulated release of inflammatory cytokines (sICAM-1 and IL-6) and chemokines (CXCL1, CCL1, CCL2, CCL5, and IL-8) *in vitro*. These data demonstrate that *B. burgdorferi* possess proteolytic machinery capable of degrading the host ECM and which may enable their direct participation in their dissemination. Additionally, the inflammatory response to BbHtrA-generated ECM damage may contribute to the inflammation-related pathologies observed in Lyme disease.

This dissertation describes a previously uncharacterized *B. burgdorferi* protease, BbHtrA, which may reshape our understanding of the pathogenesis of this bacterial infection and offer opportunities to develop new diagnostic tests for Lyme disease.

Chapter 2 provides a general overview of Lyme disease including epidemiology, commonly associated symptoms of the disease and a discussion of the known host and pathogen factors that contribute to the pathogenesis. In Chapter 3, Lyme arthritis (LA), the most common rheumatologic late manifestation of Lyme disease, is compared and contrasted to other common forms of inflammatory arthritis. The degenerative changes in arthritic joints are a consequence of proteolytic activity; thus, proteases involved in the tissue destruction seen in arthritis are described in Chapter 4.

The original scientific contributions of this dissertation are described in detail in Chapters 5-6. The significance of the results described in this report is then discussed in the context of the observed pathologies in Lyme disease in general and LA in particular. A new model for the pathogenesis of Lyme disease based on the observations of this work is proposed in Chapter 7.

CHAPTER 2: Lyme Disease

Epidemiology

In 1977, an unusual geographic and seasonal clustering of diagnoses of juvenile rheumatoid arthritis (RA) prompted an epidemiological investigation in Lyme, Connecticut and two surrounding towns (5). This arthritis involved short and recurrent episodes of pain and swelling usually affecting a large joint and most commonly the knee. Prior to development of arthritis, 25% of patients recalled having an expanding rash, often with central clearing and accompanying flu-like symptoms. These findings were recognized as those common to insect bites and one patient remembered having been bitten by a tick at the site of the rash. Similarities between the rashes observed in these patients and those experienced by European patients bitten by Ixodid ticks led to the hypothesis that Lyme disease (LD) was likely caused by an infectious agent transmitted by an arthropod vector. Black-legged ticks (*Ixodes dammini*, now called *Ixodes scapularis*) were posited as the likely vectors. In 1981, Burgdorfer *et al.* isolated a spirochete from the midgut of an *I. scapularis* tick and subsequently showed that these bacteria, *Borrelia burgdorferi*, were transmitted to naïve animals during tick feeding (6). *B. burgdorferi* were isolated from the blood of two LD patients in 1983, thus establishing the link between these bacteria and Lyme disease (7). One species of *Borrelia*, *B. burgdorferi*, is responsible for Lyme disease within the United States. In Europe and Asia, *B. burgdorferi*, *Borrelia afzelii* and *Borrelia garinii* are the major genospecies causing disease.

Zoonotic Cycle

B. burgdorferi is an obligate parasite that exists in a zoonotic cycle between small mammals and birds and the *Ixodid* ticks that feed on them (4). *Peromyscus leucopus* (white-footed mouse) is the preferred mammalian host, although various other small mammals and birds are also competent reservoirs for *Borrelia* and remain persistently infected without obvious pathology. The white-tailed deer (*Odocoileus virginianus*) is an important amplifying host for the tick.

Ixodid ticks require a blood meal at each stage of their two year life cycle and may feed on an infected mammal and acquire *Borrelia*. A previously infected tick, searching for its next meal, may bite a human instead of a competent host (9). The blood meal changes the midgut environment for *Borrelia* by altering the temperature, pH and providing other unknown factors which alter the regulation of more than 100 borrelial genes (10). After a minimum of 24 hours of tick feeding, these changes stimulate and allow for borrelial migration from the tick midgut to the salivary glands and deposition into the host skin at the site of tick attachment (11).

Signs and Symptoms

Early in the disease, usually 7-9 days after transmission while the bacteria are still localized in the skin, roughly 70% of those infected develop a painless red expanding rash (erythema migrans) at the site of the tick bite (12). Flu-like

symptoms (headache, fever, muscle and joint pain) are also common at this point in the infection.

If the infection is not recognized and treated with appropriate antibiotics, a systemic infection is established as the bacteria spread through the skin and enter the blood vessels. Weeks to months later a broader range of symptoms are observed and can vary depending on the infecting genospecies, the site of colonization and host factors. Rheumatologic (myalgia and arthralgia), neurologic (meningitis, radiculopathies, Bell's palsy), and cardiac (arrhythmias and carditis) symptoms are among the clinical findings in the early disseminated stage. Late manifestations of Lyme disease (arthritis or neurologic conditions such as encephalopathy) develop months to years after dissemination.

Diagnosis

In an endemic area, the diagnosis of Lyme disease is made based on a patient history with likely tick exposure and varies depending on patient symptoms (13). The presence of erythema migrans (EM) is very indicative of borrelial infection and allows for the diagnosis of Lyme disease in endemic areas without further evaluation (14). In later disease, a two-tiered analysis of antibody responses provides both sensitivity and specificity. The first tier utilizes enzyme-linked immunosorbent assays (ELISA) using whole-cell antigens of culture-grown *B. burgdorferi* or a peptide antigen called C6. If the ELISA is positive or indeterminate, a second tier immunoblot analysis of IgM or IgG antibodies (Western or striped blots) recognizing recombinant immunodominant antigens is

performed. The choice of IgM or IgG analysis is determined by the length of infection which reflects the likelihood of a specific antibody response having been developed. An IgM immunoblot requires the presence of 2 of 3 diagnostically significant bands and an IgG immunoblot requires 5 of 10 diagnostically significant bands (13). It is important to note that many of the signs and symptoms of Lyme disease may arise from causes other than infection with *B. burgdorferi*. Consequently, when serology is deemed appropriate, both ELISA and immunoblot analysis must be performed for the sensitivity and specificity required to accurately diagnose Lyme disease.

Treatment

Treatment for Lyme disease depends on disease manifestations and is based on guidelines published by the Infectious Diseases Society of America (15). Early Lyme disease, characterized by the presence of erythema migrans, is treated with 2-3 weeks of oral doxycycline or amoxicillin. Up to 4 weeks of intravenous ceftriaxone is indicated for patients with cardiac or neurologic involvement. LA is treated with 4-8 weeks oral antibiotics and may be followed with 4 weeks of IV therapy if joint swelling persists. LA remains unresolved for 10% of patients who have completed recommended courses of antibiotics. Long-term antibiotic therapy has been evaluated for treatment of this “antibiotic-refractory” arthritis and found to be ineffective. Thus, disease modifying anti-rheumatic drugs (DMARDS) and those targeting the inflammatory response are recommended.

Post-Treatment Lyme Disease Syndrome

After antibiotic therapy of the recommended type and duration (15), 10-20% of Lyme disease patients continue to experience subjective symptoms such as fatigue, musculoskeletal pain or memory impairment (16). These symptoms usually abate within 6 months of completion of antibiotic treatment; however, they can last for several years in some patients (17). “Post-Treatment Lyme disease syndrome” (PTLDS) is used to describe these symptoms if they last beyond 6 months. Four placebo-controlled double-blinded studies were unable to demonstrate the efficacy of long-term antibiotic therapy in impacting the duration or severity of PTLDS symptoms (17, 18). Thus it seems unlikely that persistent symptoms are due to persistent infection but rather to aberrant or slowly resolving immune responses. Nonetheless, this is a controversial topic and an area of active research. As with most infectious diseases, there is no validated and standardized test of cure of *B. burgdorferi* infection.

Pathogenesis of Lyme Disease

Borrelial Factors Involved in the Pathogenesis of Lyme Disease

Genospecies

There are three closely related major borrelial genospecies which cause Lyme disease: *Borrelia burgdorferi*, *Borrelia garinii* and *Borrelia afzelii*. These three genospecies, collectively known as *B. burgdorferi sensu lato*, are responsible for the vast majority of Lyme disease cases (2). Infrequently, other species of *Borrelia* have been isolated from patients (*B. bavariensis*, *B.*

lusitaniae, *B. spielmanii*, *B. valaisiana* and, by PCR only, *B. bisettii*) (19). However, their burden with regard to public health is uncertain and apparently low.

B. burgdorferi is the sole agent known to cause Lyme disease in North America whereas all three species cause human disease in Eurasia (2, 20). There is overlap in many of the clinical manifestations resulting from infection by these sub-types of Lyme disease spirochetes. However, there are trends in some of the most commonly observed pathologies. Arthritis is most commonly associated with infection by *B. burgdorferi* and, as mentioned earlier, is a more common clinical finding in the US (30%) than in Europe (15.4%)(21). Neurologic symptoms, most commonly Bell's palsy, meningitis or radicular pain, occur with all genospecies, although are most frequent subsequent to infection with *Borrelia garinii* (2). The vast majority of cases of borreliosis lymphocytoma and acrodermatitis chronica atrophicans are associated with *B. afzelii* infections (2).

***B. burgdorferi* RST Type**

Restriction-fragment length polymorphism (RFLP) analysis of the DNA in the 3kb spacer region between the 16S and 23S ribosomal genes is used to genotype *B. burgdorferi* strains (22). Three major genotypes have been identified (rRNA spacer types 1-3) in spirochetes isolated from field infected ticks and human samples. RST1 has been most frequently isolated from blood cultures and from patients with multiple erythema migrans skin lesions (23). In comparison with RST3 in a mouse model, RST1 strains were more invasive

(measured by dissemination rate to peripheral tissues) and more arthritogenic (measured by the degree of ensuing inflammation) (23, 24).

***B. burgdorferi* OspC Type**

Variations in the gene for outer surface protein C (OspC) are also used to type strains of *Borrelia* (9). OspC, one of the many borrelial plasminogen-binding proteins (25), is required for mammalian infection. Twenty-one OspC variants have been detected, 16 of which have been found within the US. Four types (A, B, I and K) are associated with invasive disease (26). RST types and OspC types are genetically linked (9); RST1 strains contain OspC types A and B, RST2 strains contain OspC types F, H, K and N. The rest of the OspC variants are associated with RST3 strains (25). In comparison of plasminogen binding between OspC variants, types A and B have 3-fold greater affinity for plasminogen than do types F and H. Since types A and B are also more invasive in mice and more commonly isolated from human blood samples, Lagal *et al.* (2006) concluded that the enhanced spirochetaemia may be attributable to plasminogen binding capability (25). However, *Borrelia* disseminate to all organs within plasminogen-deficient mice (27) indicating that OspC provides undiscovered contributions to pathogenesis.

***B. burgdorferi* Plasmid Content**

The genome of *B. burgdorferi* strain B31 is comprised of a megabase chromosome and 21 plasmids, both linear and circular. Comparison of the plasmid profile for clinical isolates has demonstrated variable plasmid content

between strains (28). Linear plasmid 25 (lp25) is present in all clinical isolates, required for experimental infection of mice, and consequently is thought to be required for human infection as well (29-32). Restoration of BBE22, a nicotinamidase gene present on lp25, is sufficient to restore infectivity of lp25 deficient strains. Linear plasmid 28-1 (lp28-1) contains the gene for VlsE, the variable surface lipoprotein involved in antigenic variation and evasion of the host immune system. Lp28-1 is also required for infectivity in mice (33).

Adhesins

Bacterial adhesin molecules are important virulence factors allowing for the colonization of host tissues. The vast array of ECM targets underscores the observed borrelial predilection for connective tissues (Table 1). The relatively recent ability to genetically manipulate *Borrelia* has permitted studies with deletion mutants of several of these adhesins. *Borrelia* ECM interactions are important for maximal borrelial transmission (34), dissemination (35) and persistence (36) within the host. However, none of these interactions alone have been found to be critical for borrelial survival within a host suggesting that the functional redundancy of these interactions is also protective.

Table 1 Borrelial adhesins and host ECM ligands

Borrelial ECM-Binding Proteins		
ECM Ligand	Borrelial Adhesin	Reference
Decorin	DbpA & DbpB	Guo et al., 1995
Fibronectin	BBK32 RevA & RevB	Probert et al., 1998 Brissette et al., 2009
Integrin	P66 BBB07	Coburn et al., 1999 Behera et al., 2008
Laminin	ErpX BmpA	Brissette et al., 2009 Verma et al., 2009
Glycosaminoglycans		
Heparan sulfate	Bgp	Parveen et al., 2000
Dermatan sulfate	Bgp	Parveen et al., 2000
	BBK32	Probert et al., 1998
Chondroitin sulfate	DbpA & DbpB	Guo et al., 1995
	Bgp	Parveen et al., 2000
	DbpB	Fischer et al., 2003
	BBK32	Fischer et al., 2006

Borrelial persistence within the ECM of joint tissue suggests that *Borrelia* likely come into contact with aggrecan, the most abundant proteoglycan in joint tissues. *B. burgdorferi* binding to aggrecan has not been specifically addressed in the literature. Guo et al. (1995) used aggrecan as a competitive inhibitor in binding assays between *B. burgdorferi* strain N40 and another proteoglycan, decorin. They found that aggrecan was able to partially inhibit borrelial binding to decorin which is consistent with subsequent findings that DbpB (decorin binding protein B) also binds to one of the chondroitin sulfate side chains found on aggrecan (chondroitin-6-sulfate; Fischer et al. 2003). Additionally, Leong et al. (1998) found that aggrecan chondroitin sulfates (chondroitin-4-sulfate (CS-A) and chondroitin-6-sulfate (CS-C)), which differ in the position of their sulfate group, also differ in their ability to inhibit borrelial interactions with Vero and 293 cells *in vitro*. These studies established the foundation for the hypothesis that *borrelia* interact with aggrecan.

Borrelial Immune Evasion Strategies

B. burgdorferi are obligate parasites whose life cycle requires persistent infection of a mammalian host, tick acquisition during a blood meal and then transmission to another mammalian host (10). Bacterial persistence within an immune-competent host requires numerous mechanisms to evade both the innate and the adaptive immune system. Toll-like receptors are pivotal components of innate immunity that stimulate the activation of innate immune cells and the subsequent involvement of adaptive immunity. Flagellar proteins are recognized by TLR5; however, sequestration of borrelial flagella within the

periplasmic space reduces interaction with this TLR. Binding of complement-inhibitory factor H to at least 7 borrelial surface proteins (37) as well as inhibitory C4b (38) may increase avoidance of the complement arm of innate immunity. Antigenic variation of variable surface lipoprotein (VlsE) reduces antibody recognition of the spirochete and is required for mammalian infection (39). Phase variation of outer surface proteins A and C (OspA and OspC) also contributes to borrelial evasion of adaptive immunity. OspA is expressed within the tick and down-regulated during the blood-meal, whereas OspC is up-regulated during the late stage of tick feeding. OspC is again down-regulated soon after mammalian infection. Several antibodies against Osps A and C are directly borrelicidal in a complement-independent fashion (40). Consequently, the limited exposure of these antigens to the adaptive immune system is thought to be protective for *Borrelia* (41).

Host Factors Involved in the Pathogenesis of Lyme Disease

Inflammatory Responses to *B. burgdorferi*

Mammalian reservoir hosts are persistently infected with *Borrelia* for life without obvious pathology (42) pointing to differences in non-reservoir host immune responses. Substantial activation of innate and adaptive immune responses occurs very early in Lyme disease. Both branches of immunity are crucial for controlling the infection and eventually eradicate the spirochete. Unlike reservoir hosts, however, humans infected with *Borrelia* experience significant pathology which is attributed to the vigorous inflammatory response triggered by this pathogen.

Macrophages and dendritic cells are very early responders to sites of *Borrelia* infection and produce pro-inflammatory cytokines and chemokines to recruit and activate responding lymphocytes, monocytes and neutrophils (43, 44). Recognition of the spirochetes is mediated, in part, by activation of “Toll-like receptors” (TLRs) which recognize various borrelial “pathogen associated molecular pattern” molecules (PAMPS) (45-47). Most TLRs form a complex with the adaptor protein MyD88 whereas TLR3 utilizes the adaptor TRIF. TLR4 can use either adaptor. These complexes stimulate signal transduction cascades leading to the release of cytokines and chemokines which coordinate immune responses by recruiting appropriate innate and adaptive immune cells to sites of infection. Borrelial tri-acylated lipoproteins, of which there are more than one hundred, are recognized by heterodimers of TLR1/TLR2 which stimulate release of inflammatory cytokines and chemokines such as IFN γ , IL-12, IL-6, CCL2, and CXCL1 (48, 49). Pro-inflammatory signaling has also been observed in response to borrelial RNA and unidentified non-nucleic acid components in spent borrelial growth media (50). Though *B. burgdorferi* lack the prototypical TLR4 ligand LPS, macrophages from TLR4^{+/+} mice released higher concentrations of TNF α upon exposure to *Borrelia* than did macrophages from TLR4^{-/-} mice (51). Thus, TLR4 engagement by a borrelial or host component subsequent to *B. burgdorferi* infection was suggested.

Several studies have addressed the relative importance of TLR signaling in animal models of LA. It was expected that TLR2 deficiency, by eliminating the lipoprotein induced signaling, would reduce the severity of arthritis. However,

TLR2 deficiency resulted in altered cytokine and chemokine production, altered immune cell trafficking to joints, greater bacterial loads and more severe arthritis (52, 53). It was expected, therefore, that studies with *Borrelia*-infected MyD88-deficient mice would also demonstrate more severe arthritis. Even higher bacterial loads are observed in MyD88^{-/-} mice (54-56). However, unlike TLR2 deficient mice, arthritis severity was unchanged in MyD88^{-/-} mice (55, 56). Thus, spirochetal burden is not the driving force in arthritis development in mice. Additionally, in the absence of MyD88-dependent TLR signaling, tissue-specific alterations in cytokines and chemokines were observed (54-56). TLR signal transduction cascades fine tune tissue-specific responses via cytokine and chemokine release and immune cell recruitment and activation.

Immunomodulation in Lyme Disease

Interleukin-10 (IL-10) is a potent anti-inflammatory cytokine that induces regulatory T cells (TRegs) which limit host immune responses to prevent excessive inflammation-related damage. Several studies *in vitro*, *in vivo*, and *ex vivo* have demonstrated IL-10 up-regulation in response to *B. burgdorferi* (57). The IL-10 response has been well characterized in the murine model for LA. C57BL/6 mice, which normally experience only mild arthritis in response to borrelial infection, produce more IL-10 and fewer inflammatory cytokines than arthritis susceptible C3H mice (58). Additionally, IL-10 deficient C57BL/6 mice develop more severe arthritis. The IL-10^{-/-} mice had fewer bacteria within the joint suggesting that arthritis development is not dependent on bacterial burden in the IL-10^{-/-} model. Although increased antibody production was observed in the IL-10^{-/-}

^{-/-} mice, a follow-up study demonstrated no qualitative differences between the antibodies of wild type and IL-10^{-/-} mice (59). Comparisons of microarray data between infected joints of arthritis-susceptible C3H mice and C57BL/6 IL-10^{-/-} mice and arthritis-resistant C57BL/6 mice point to significantly different inflammatory responses (60). Transcriptomes of the arthritis susceptible mice revealed a pro-inflammatory profile with a predominance of IFN-inducible genes. The arthritis resistant C57BL/6 mouse induction profile involved genes important in wound repair and epidermal differentiation. Mice in these models experience the same bacterial load within joint yet mount very different inflammatory responses suggesting that the loss of anti-inflammatory IL-10 results in an IFN-inducible profile and the development of arthritis.

Consistent with these studies, comparisons between wild type, IL-10^{-/-}, and mice treated with neutralizing antibody for IFN γ demonstrated that the loss of IL-10 results in both local (joint) and systemic increases in IFN γ and chemokines (61). Additionally, increased IFN γ and chemokine levels led to elevated numbers of immune cells within arthritic joints. It was determined that CD4⁺ T cells and macrophages were responsible for the local increase in IFN γ , which has long been appreciated as a pivotal cytokine in the development of LA (62, 63). These and other immune cells recruited to the joint are activated by the high levels of this very potent cytokine and release additional signaling molecules potentially setting up a positive feedback loop for inflammatory responses. Thus, the IL-10 deficient mice initially benefit from an increased inflammatory response and pathogen clearance. However, the inability to down-regulate that inflammatory

response ultimately leads to greater tissue damage. Extending these observations to human disease, these authors suggest that differences in IL-10 regulation may play a role in treatment resistant or slowly resolving LA in humans (61).

Human Leukocyte Antigen (HLA)

Major histocompatibility complex proteins (MHC), also referred to as human leukocyte antigens (HLA), are surface-expressed proteins which present peptide antigens to T cells. Several diseases are associated with particular MHC alleles. With regard to arthritis, RA is strongly associated with HLA-DR4 genes whereas reactive arthritis and ankylosing spondyloarthritis are associated with HLA-B27 (64). Studies conducted in the US and Europe comparing HLA types between Lyme disease patients and healthy controls do not show significant differences in HLA types between these groups (65, 66). Neither is there a difference between those with Lyme arthritis and those with other symptoms of Lyme disease (65, 67). However, within groups of Lyme arthritis patients, one group has reported a tendency for those with antibiotic-refractory arthritis to have higher frequencies of HLA-DRB*04 alleles than those with antibiotic responsive arthritis (65, 67, 68). Antibiotic-refractory LA is further discussed in Chapter 3.

CHAPTER 3: Lyme Arthritis

A CDC review of clinical findings from 213,515 Lyme disease cases reported between 2001-2010 revealed physician-diagnosed arthritis in 30% of these cases (Fig. 2) (69). In Europe, joint involvement occurs in 15.4% of cases (21). LA develops months to years after systemic spread of the bacteria. Arthritis subsequent to borrelial infection can be divided into two categories: an atypical septic arthritis due to the presence of viable *Borrelia* within the joint and an “antibiotic-refractory” arthritis that remains after clearance of the spirochetes.

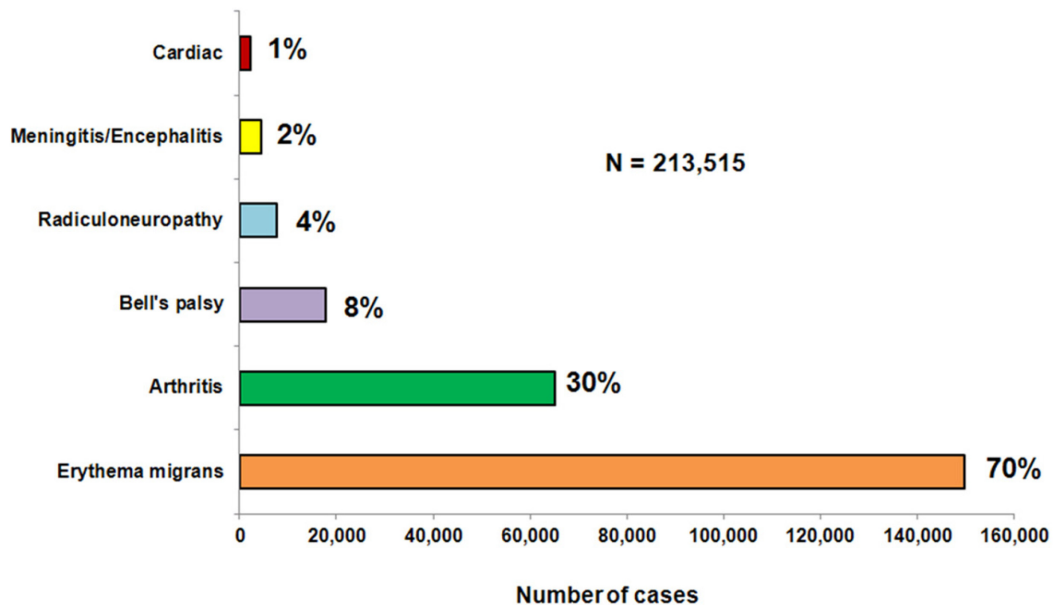


Figure 2 Clinical Manifestations of Confirmed Lyme Disease Cases-United States, 2001-2010.

CDC figure, public domain.

Clinical Features of Lyme Arthritis

The vast majority of LA patients (90%) have a septic arthritis in which symptoms resolve after antibiotic therapy (70-72). Arthritis begins long after the initial infection of the joint by the bacterium, lasts for weeks to months at a time and can recur over a period of several years (73). Spirochetal DNA is detectable in 50-70% of synovial fluid samples (74). The most common clinical picture is one of large joint swelling and pain, frequently of one knee, with significant joint effusions accompanied by lower than expected levels of pain (5, 70). This is contrasted with classical septic arthritis in which patients often present with guarding of an exceedingly painful joint (75, 76).

As with reactive arthritis, LA eventually resolves spontaneously in untreated patients (43). However, given the possibility for progression to irreversible joint damage and the development of other serious manifestations of Lyme disease, immediate treatment with an appropriate antibiotic follows the diagnosis of LA. Conjunctivitis and urethritis are not unknown in LA, but they are uncommon findings in Lyme disease.

Radiographic and Histopathologic Features of Advanced Lyme Arthritis

Pathologic features typical of inflammatory, and in advanced cases, of erosive arthritis occur in response to the presence of *B. burgdorferi* within the joint (44, 77, 78). Radiographic analysis of 25 untreated patients with advanced chronic LA demonstrated involvement of all tissues within the joint (17). Cartilage loss or calcification, tendon calcification, osteoporosis, bone erosion and bone spurs were frequent findings. Soft tissue abnormalities were evident as an

inflamed synovial lining (synovitis) with proliferating synovial cells (hyperplasia), villous formation (hypertrophy) and angiogenesis. An encroachment of the hyperplastic and hypertrophic synovium onto the joint surface (pannus) was also frequently observed. Also remarkable within the synovium was the presence of very large numbers of T cells, B cells and plasma cells so densely arranged that they resembled secondary lymph tissue (79). Macrophage and mast cells were also abundant within synovial tissue whereas neutrophils were only sparsely observed (79). Neutrophils and T cells are abundant in normal synovial fluid (80).

None of the features mentioned above are exclusive to LA and are seen in varying degrees in other forms of inflammatory arthritis (81, 82). As mentioned, these similarities led to the frequent misdiagnosis of RA until the bacterial etiology of LA was established (5, 73).

Antibiotic-Refractory Lyme Arthritis

Roughly 1 in 10 LA patients treated with standard and/or extensive antibiotic therapy continue to suffer from recurrent bouts of arthritis (18), a condition known as antibiotic-refractory LA. There are several potential causes for persistent symptoms after antibiotic therapy for Lyme disease, including 1) persistent infection; 2) autoimmunity arising from molecular mimicry; and 3) slowly-resolving inflammatory responses either to retained borrelial antigens or resultant damage to tissues (42).

Persistent *Borrelia burgdorferi*

The antibiotic regimen recommended for treatment of Lyme disease is detailed in Chapter two and based on guidelines published by the Infectious

Diseases Society of America (15). The issue of borrelial persistence is an active area of research in the field and is very much unresolved.

Persistence within dogs and mice, after antibiotic therapy analogous to doses received by humans, has been demonstrated by PCR, microscopy and by the acquisition of *Borrelia* by naïve ticks after feeding on antibiotic treated mice (xenodiagnosis) (83-85). In one of the xenodiagnosis studies, the infected ticks were able to transmit the spirochetes to naïve SCID mice; however, the mice had very low bacterial burdens and no observable pathology (85). In all cases, the organisms were non-cultivable by standard methods. These persistent forms are clearly viable as they are able to sense a chemotactic gradient and migrate to the site of tick attachment to be acquired by a naïve tick. Likewise, viability is required to be able to migrate from the midgut to the salivary glands of the tick to be transmitted into the SCID mice.

To address the viability question, a recent study used quantitative PCR to analyze borrelial DNA, 16S ribosomal RNA and mRNA in synovial fluids from 11 antibiotic-refractory patients (86). The hypothesis was that ribosomal and mRNA would be detectable from metabolically active bacteria. Results demonstrated that 3/11 synovial fluid samples were positive for borrelial DNA, the same patients were also positive for 16S rRNA. All samples were negative for mRNA.

Collectively, these observations are the basis for the widely held belief within the research community that, though a small number of spirochetes may persist after antibiotic therapy, these spirochetes are greatly attenuated, non-pathogenic, and ultimately cleared by the host immune system (87). Support for

this assertion comes from and the lack of pathology observed in persistently infected SCID mice post-antibiotic treatment (84, 85) and clinical observations that antibiotic-refractory LA resolves in all patients (67).

While apparent non-virulence makes these spirochetes clinically less interesting, the models demonstrating attenuated spirochetes post-antibiotic therapy offer a unique opportunity to study borrelial virulence. One possible explanation is that long-term survival after antibiotic therapy required the loss of plasmid DNA. A full plasmid profile was not established for the xeno-transferred *Borrelia*; however, Bockenstedt *et al.* (84) were able to demonstrate a lack of linear plasmid lp25 and diminished presence of lp28-1. These plasmids are both required for full infectivity in the murine model of Lyme disease (30).

Molecular Mimicry

Molecular mimicry occurs when endogenous peptide epitopes are similar enough to pathogen peptide epitopes to allow for antibody cross-reactivity. During the septic phase of LA, CD4+ T cells become appropriately sensitized to specific borrelial peptides and stimulate B cell production of antibodies. Coincidence of OspA antibody responses with the flares of chronic LA prompted the study of OspA as a potential molecular mimic (68). However, follow-up studies have demonstrated that, if molecular mimicry is involved in antibiotic-refractory LA, OspA is very likely not the source of the triggering peptides (88, 89).

Other Forms of Inflammatory Arthritis

Arthritis is the most common cause of disability in the United States (CDC) and accounts for 15% of visits to family medicine practices (90). At the simplest level, arthritis is a consequence of an imbalance in the homeostasis within the joint that causes stiffness, pain, swelling, and redness. There are over 100 different forms of arthritis with causes ranging from injury to autoimmunity that stimulate different combinations, severity and duration of these symptoms. At times, this imbalance is driven by resident cells responding to local stimuli and at other times it is from responding immune cells.

The similarities between rheumatoid arthritis (RA) and Lyme arthritis (LA) prompted the misdiagnosis of RA until the bacterial etiology of LA was established. Unlike arthritis caused by other bacterial infections, which is evident and destructive in a matter of days, RA and LA develop over months to years (91). Significant joint effusions, synovitis and pannus formation are common to both. Cartilage loss and subsequent bone destruction are much more prevalent in RA; however, with prolonged disease they are also observed in LA. In contrast to RA, LA does not lead to systemic involvement

While the etiologies of other inflammatory arthritides differ from LA, the downstream consequences of inflammatory responses within the joint are similar. Consequently, lessons learned from studies of this pathogen-induced arthritis may have mechanistic implications for other forms of inflammatory arthritis.

A brief discussion of the major forms of arthritis will aid in distinguishing the unique characteristics of LA and, perhaps, provide mechanistic insights.

Degenerative processes within an arthritic joint are the result of proteolytic activity which degrades the extracellular matrix of cartilage and remodels bone. Chapter 4 will discuss the proteases involved in arthritis in detail.

Osteoarthritis

Osteoarthritis (OA) is the most common form of arthritis affecting more than 27 million Americans. Large weight-bearing joints and small bones in the hands are most frequently affected with degenerative changes characterized by cartilage loss and the development of bony growths called osteophytes. OA usually develops over a period of years with risk factors including age, injury, excess body weight, and genetics (~50%) though the underlying cause of OA remains unknown.

OA is considered primarily a disease of cartilage with secondary bone and synovial involvement (92). Cartilage is a complex connective tissue consisting of glycosaminoglycans, proteoglycans, and proteins existing in an extracellular matrix synthesized and maintained by chondrocytes. In OA, there is an imbalance of extracellular matrix synthesis and degradation by chondrocytes, resulting in cartilage loss or calcification and, often, osteophyte formation and other bone changes (93). These changes usually occur without excessive inflammation, leading to the historical classification of OA as a non-inflammatory degenerative arthritis. It has long been appreciated that low-grade inflammation stimulates the pathology observed within the OA joint by both up-regulating proteases which mediate the destruction and down-regulating matrix synthesis (94-96). However, the source of this inflammation was considered to be cells

within the synovial lining and the altered chondrocyte metabolism was thought to be in response to these external stimuli (97). There is increasing evidence that chondrocytes within the cartilage of the affected joint actively generate and respond to the inflammatory signaling observed (98-101). For example, when stimulated with IL-8, CXCL1 or CCL2, chondrocytes respond by decreasing synthesis of aggrecan and collagen, as well as increasing expression of several MMPs (26-31).

In brief, the chronic low-grade inflammation of OA drives the imbalance between anabolism and catabolism by altering the homeostasis of all cell types within the joint.

Rheumatoid Arthritis

Rheumatoid arthritis (RA) is an autoimmune systemic inflammatory disease of unknown etiology. HLA-DR4, an allele of the major histocompatibility class II complex, is strongly associated with RA (~50%) and with more severe courses of the disease (102). Smoking is a significant environmental risk factor for HLA-DR4 positive individuals (103). Arthritis is the most common clinical finding and typically presents with bilateral joint swelling, redness and pain accompanied by morning stiffness and a positive “rheumatoid factor” test (autoantibodies). Symptoms of RA usually occur rather suddenly over a period of weeks to months and expand as the disease progresses.

After the onset of RA, the synovial membrane that lines the joint is chronically inflamed and abnormally proliferative leading to a thickening of the lining (synovial hyperplasia). This hyperplastic membrane eventually encroaches

on and attaches to the cartilage, at which point it is called a pannus. The pannus develops villous projections ultimately invading and destroying the cartilage and underlying bone (104). Pannus is a tumor-like tissue composed largely of synovial fibroblasts with migratory capabilities that can leave the affected joint and migrate to unaffected joints in the body. Thus, although initially involving one or a few joints, RA eventually affects most joints in the body (105). It should be noted that, while most frequently discussed in the context of RA, pannus is a consequence of prolonged synovial inflammation and is observed in many forms of inflammatory arthritis (106-108) including Lyme arthritis. The frequency and severity of pannus formation in RA points to the degree of inflammation observed in this disease.

The synovial cells secrete numerous inflammatory cytokines including TNF α , IL-6, and IL-1 β . These potent cytokines stimulate additional inflammatory responses from neighboring cells within the joint and, indeed, systemically leading to a range of pathologies (102). Within the joint, synovial fibroblasts, chondrocytes and osteoclasts respond by releasing proteases responsible for the destruction of cartilage and bone. Numerous chemokines increased in RA joints have been demonstrated to be specifically responsible for the recruitment of monocytes (CCL5), neutrophils (CXCL1, IL-8), and T cells (CCL2, CCL5) (109). Additionally, IL-6 is a pivotal cytokine in the balance between anabolic and catabolic chondrocyte responses and is very well studied in the context of RA. The synovial hyperplasia and cartilage destruction characteristic of RA are

attributed to exuberant expression of IL-6 and IL-6 blockade is a recently approved therapeutic approach (25).

Distinct patterns are observed within the cellular infiltrates in hyperplastic synovial membranes. The infiltrates are predominantly CD4+ T cells and macrophages into the synovial membrane, whereas neutrophils are abundant in the synovial fluid. Additionally, B-cells are stimulated to produce autoantibodies directed at the Fc portion of IgG antibodies and citrullinated matrix components (103). The responding cells may be either randomly associated between resident cells within the membrane or organized into partially or fully functional germinal centers. Germinal centers are aggregates of immune cells similar to those seen in lymph nodes and utilized for antibody production and immune cell proliferation (109). The abundance of antibody complexes in RA leads to the activation of the complement cascade which contributes to the tissue damage observed.

The changes observed within the joint are directly attributable to the prolonged highly inflammatory RA environment as demonstrated by the efficacy of anti-TNF α , anti-IL-1 and anti-IL-6 therapies. However, the underlying causes for this inflammatory state remain unclear.

Septic Arthritis

Bacterial infection of a joint occurs after hematogenous spread from a primary site of infection or, less commonly, with direct inoculation during trauma or surgery. The synovial lining is richly vascularized and lacks a basement membrane, thus bacterial entry into the joint is relatively unimpeded (110) and a fulminant infection can quickly become established. Septic arthritis is a medical

emergency associated with a high mortality rate (10-15%) and a permanent loss of function in 50% of patients in a matter of hours to days (76, 90). Pre-existing arthritis, age, and joint prostheses are among the greatest risk factors. Staphylococcal, streptococcal and gonococcal infections account for the majority of septic arthritis cases (76).

The degree of joint damage depends greatly on the pathogenic mechanisms of the infecting organisms and the host response (75, 76, 110, 111). Bacterial secretion of cytotoxins or enzymes, such as proteases, hyaluronidases or lipases, damage or kill cells of the joint and destroy cartilage. Lipopolysaccharide and other strongly inflammatory bacterial components stimulate cytokine and chemokine release from resident cells and an influx of recruited immune cells. The responding macrophages and neutrophils release reactive oxygen species and both resident and responding cells release matrix degrading proteases and which further damage the tissues. If these and other measures are not adequate to control the infection, the high levels of bacterial toxins and cytokines can stimulate a systemic inflammatory response leading to septic shock and death (110).

Reactive Arthritis

Reactive arthritis (ReA, Reiter's syndrome, post-infectious arthritis) is a sterile arthritis arising secondary to an infection elsewhere in the body and most commonly subsequent to gastrointestinal or genitourinary infections. The classic triad of symptoms- an inflamed joint, conjunctivitis and urethritis/cervicitis- occurs in 30% of patients with ReA, usually within 4 weeks of infection (112). Skin

involvement, a painless red rash with waxy blisters (keratoderma blennorrhagica) frequently on the hands or soles of the feet, occurs in nearly 15% of patients. There is evidence of vertebral involvement in 10-30% of patients. Malaise, fatigue and fever are common clinical findings. Spontaneous resolution of ReA frequently occurs within 3-12 months but can take a chronic course in 15-30% of patients with recurrent arthritis flares (113).

Chlamydia trachomatis, which causes an estimated 2.8 million genitourinary infections each year in the US, is the most common cause of ReA with 4-15% of patients developing ReA (114, 115). Implicated enteric pathogens include but are not limited to *Campylobacter*, *Salmonella* and *Yersinia*. Common features of these triggering pathogens are that they are all gram-negative, LPS-containing and intracellular pathogens. ReA associations with HLA-B27 vary considerably in the literature. Earlier reports, based on hospital data and representing more severe cases, estimated HLA-B27 association up to 80% (114). Subsequent population-based analyses of epidemics found only slight associations between HLA-B27 and the subsequent occurrence of ReA (116, 117). However, HLA-B27 is strongly associated with the severity and duration of ReA (118).

The inflammation in ReA is attributed to the deposition or retention of immune complexes or bacterial products within the joint which trigger a local immune response (112). In animal models of ReA, antigens within the joint are commonly observed at avascular structures such as the cartilage surface, ligaments and tendons (119).

Sterile arthritis is best exemplified by *Yersinia*-induced ReA. *Yersinia enterocolitica* antigens, frequently outer membrane proteins, are found in joints in the absence of evidence of bacterial presence by either culture or PCR analysis. The continued presence of these antibody-antigen complexes indicates that persistent organisms are continuing to shed components which make their way to the affected joint (114). One possible mechanism for transport is macrophage recruitment to the joint with previously phagocytized bacteria. Lymph nodes are an organ of persistence in rat models of *Yersinia*-induced ReA (120). Once the outer membrane proteins are in the joint, both TLR2 and TLR4 receptors are triggered leading to inflammatory responses which could drive the development of arthritis (121).

A difficulty in diagnosing ReA is establishing the aseptic nature of the arthritis. Low-grade infection of a joint, such as occurs with *B. burgdorferi*, *Tropheryma whippelii* or *Mycobacterium tuberculosis* infections among others, may be particularly difficult to identify and thus difficult to distinguish from truly reactive arthritis (112). Additionally, viable but metabolically inactive *C. trachomatis* have been isolated from synovial membrane samples of ReA patients after antibiotic therapy (122, 123). These findings suggest that arthritis secondary to low-grade infections or those with organisms capable of persisting in a metabolically inactive state might actually be low-grade chronic septic arthritis. Instead of a reaction to products of dead bacteria then, arthritis would be the consequence of chronic low-level stimulation of the inflammatory response (115, 122). Several placebo-controlled studies of extended single-antibiotic

treatment have demonstrated that prolonged courses of antibiotic therapy are ineffective in treating chronic ReA. However, in support of the persistence hypothesis, a recent placebo-controlled double-blinded study of *Chlamydia*-induced ReA demonstrated that combination antibiotic therapy, instead of the single antibiotic therapy usually used to treat chlamydial infections, was able to reduce pain and inflammation in 17/27 (63%) ReA patients compared to 3/15 (20%) of those in the placebo group (124). Chlamydia presence in synovial tissue samples and peripheral blood mononuclear cells were likewise reduced. Additionally, 16/26 (62%) patients with a related arthritic disease (undifferentiated spondyloarthritis) were chlamydia positive (125). Despite the small size of these studies, these results suggest that post-chlamydial arthritis is caused by unresolved infection in some patients.

Comparison of LA With Other Forms of Inflammatory Arthritis

It was recognized more than 25 years ago that based on symptoms, clinical course and a post-infectious etiology, LA is most similar to reactive arthritis (82). Intermittent, asymmetric and large joint involvement with significant joint effusions are features of both forms of arthritis. HLA-B27 is not associated with the occurrence of either ReA or LA, although this MHC allele is more common in patients with severe and protracted ReA. Clinical observation of ReA occurs most frequently subsequent to *C. trachomatis* infection and in 4-15% of patients (115, 117). LA is observed in ~30% of Lyme disease patients and estimated to develop in ~60% of patients without appropriate antibiotic therapy. Thus, *B. burgdorferi* seem to be relatively more arthritogenic although this could

reflect the relative efficiency of joint colonization and persistence rather than inherent arthritogenicity.

Arthritis caused by borrelial infection differs from classic septic arthritis in several important respects. First, septic arthritis is associated with large numbers of bacteria within the joint which are easily observable in synovial fluid samples. *Borrelia* have only twice been isolated from synovial fluid (126, 127) and, when found in synovial tissues, are present in very low numbers deep within the connective tissue of the synovial lining (44, 128). Second, unlike arthritis caused by other bacteria which is typically evident in hours to days after joint infection, LA develops weeks to several years after *Borrelia* colonize the joint. Third, many arthritogenic bacteria secrete tissue-damaging enzymes into the joint space which can quickly cause irreversible damage including joint destruction. With the exception of the studies in this report, *Borrelia*-induced damage has been solely attributed to the up-regulation of host proteases during the inflammatory response. Most importantly, septic arthritis progresses to life-threatening sepsis in 10-15% of patients (76). In contrast, though permanent joint damage can occur in a very small number of cases, LA is a self-limiting infection that eventually resolves in all patients without extra-articular complications (43). Consequently, though LA is a bacterially induced arthritis, it is significantly different from typical septic arthritis.

The similarities between rheumatoid arthritis (RA) and Lyme arthritis (LA) prompted the misdiagnosis of RA until the bacterial etiology of LA was established. Significant joint effusions, synovitis and pannus formation are

common to both. Cartilage loss and subsequent bone destruction are much more prevalent in RA and, with prolonged disease, are also observed in LA. However, as mentioned above, these features are common to all forms of inflammatory arthritis.

While the etiologies of other inflammatory arthritides differ from LA, the downstream consequences of inflammatory responses within the joint are similar. Degenerative processes in arthritis are the result of proteolytic activity which degrades the extracellular matrix of cartilage and remodels bone.

CHAPTER 4: Extracellular Matrix Degradation and Proteases in Arthritis

Joint homeostasis is maintained by contributions from resident cells within the synovium, cartilage and bone as well as by transient immune cells. Increased concentrations of inflammatory cytokines and chemokines within an arthritic joint alters the biology of these cells, increases the immune cell presence and activation within the joint and, if the inflammatory signaling is persistent, ultimately leads to the destruction of joint tissues.

Aggrecan

Cartilage is a complex connective tissue consisting of glycosaminoglycans, proteoglycans, and proteins existing in an extracellular collagen matrix synthesized and maintained by chondrocytes. In addition to cartilage, aggrecan is expressed in tendons, ligaments, the synovial lining, perineuronal nets in the brain and in the central nervous system (129, 130). Aggrecan is the most abundant proteoglycan in cartilage and is so named for the very large aggregates that it forms with hyaluronic acid (131). The aggregates are composed of a hyaluronic acid back-bone to which are attached an average of 100 aggrecan monomers. The aggrecan monomer is an enormous molecule with a mass of approximately 2500 kilodaltons (kD). The core protein is 220 kD and contains three globular domains; G1, G2, and G3 (Fig. 3A). The first globular domain reversibly associates the aggrecan monomer with hyaluronic acid and link protein. The function of the G2 domain is unknown. The G3 domain has many important interactions with proteins and other aggrecan monomers that act to confer additional stability to the extracellular matrix (132). Between the G2 and

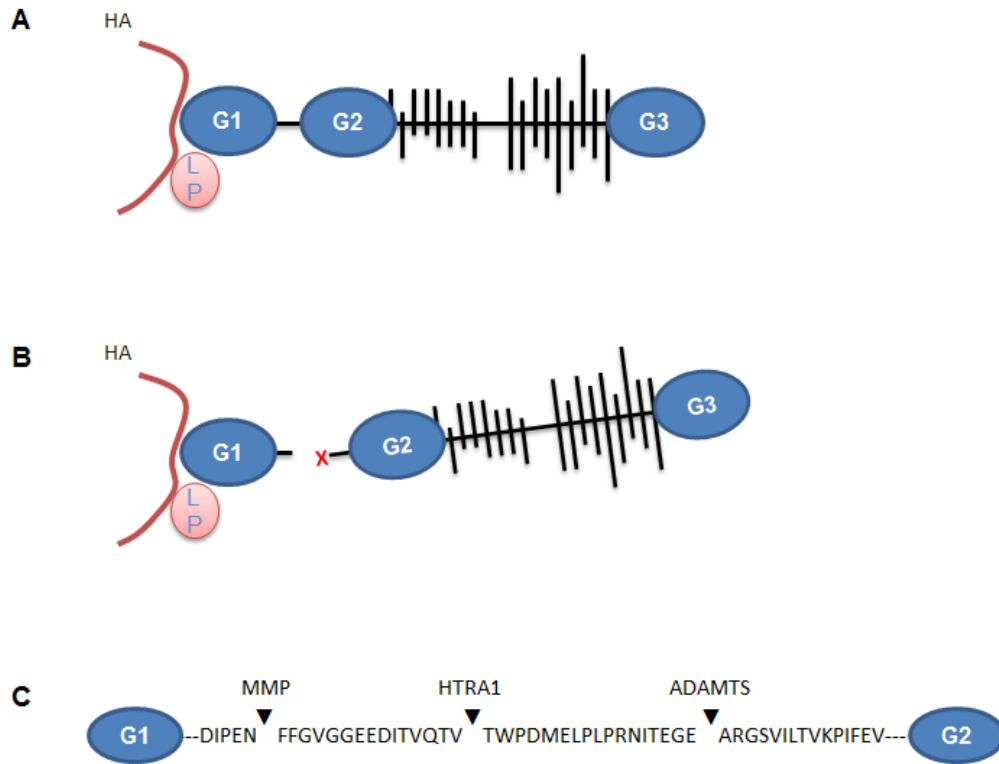


Figure 3 Schematic of aggrecan structure and cleavage within the interglobular domain (IGD).

A. Intact aggrecan showing three globular domains and the glycosaminoglycan attachment region between domains two and three. Globular domain one associates with hyaluronic acid (HA) and link protein (LP) to tether aggrecan to the ECM. G1-3, globular domains 1 through 3. **B.** Aggrecan cleavage within the IGD between G1 and G2 releases the G2 to G3 fragment from the ECM. The G1 fragment is retained. **C.** Expanded view of the IGD showing the position of specific protease cleavage sites.

G3 domains are the glycosaminoglycan (GAG) regions to which are attached roughly 40 keratan sulfate and 100 chondroitin sulfate (CS) side chains accounting for 90% of the mass of aggrecan. The GAG chains are polymers of highly negatively charged sulfated disaccharides which attract sodium ions to balance these charges and, consequently, water is osmotically drawn into cartilage. The ability of aggrecan GAG chains to attract water into cartilage is directly responsible for its ability to resist compression and for the resiliency required to resume its natural shape as the water returns after compressive force (133).

In healthy cartilage, there is a balance of anabolic and catabolic processes which results in a steady state of aggrecan presence in the ECM (134). In normal turnover, aggrecan is cleaved at a variety of positions in the chondroitin sulfate region of the GAG domain between G2 and G3. In pathologic processes, cleavage occurs in the interglobular domain (IGD) between G1 and G2 (Fig.3B). The result of this scission is that G2, the entire GAG domain, and G3 are released from the monomer and diffuse out of the extracellular matrix (10). The remaining G1-IGD fragment is devoid of the hydrophilic GAG chains and the stabilizing properties of the G3 domain and, consequently, normal cartilage function is lost.

Aggrecan degradation is a hallmark of arthritic diseases. Aggrecan loss is an early and reversible event in the progression of erosive arthritis. As mentioned previously, the cartilage damage observed in arthritis is a consequence of proteolytic degradation of the extracellular matrix. Inflammatory cytokines such

as IL-1 β stimulate upregulation of the proteases responsible for the majority of the ECM degradation. IL-1 β also profoundly affects chondrocytes by suppressing the synthesis of cartilage components, thereby compounding the problem.

Host Proteases in Arthritis

Aggrecanases

Several classes of enzymes, including cathepsins, MMPs, HtrA1 and ADAMTS proteases are capable of cleaving aggrecan *in vitro*. However, ample evidence has demonstrated that ADAMTS proteinases are responsible for the majority of aggrecan degradation in arthritic diseases (135, 136). There are over 20 members of the ADAMTS family of zinc-dependent proteinases. Of these, ADAMTS-1, 4, 5, 8, 9, and 15 are capable of degrading aggrecan at NITEGE³⁷³ in the interglobular domain (136-138). ADAMTS-4 and 5 are thought to be the most important aggrecanases in arthritis as they have been isolated from arthritic cartilage and have the highest activities against aggrecan *in vitro* (139, 140). ADAMTS-5 is constitutively expressed whereas ADAMTS-4 expression is significantly induced by inflammatory cytokines including IL-1 β and TNF- α (134, 139). Consequently, ADAMTS-4 is considered the principle aggrecanase in degenerative disease in humans.

ADAMTS proteases are secreted as inactive zymogens requiring proteolytic processing for activation and are primarily activated intracellularly by PACE4, a furin-like serine protease that is also up-regulated in erosive arthritis (135). Aggrecanases are able to cleave aggrecan core protein at 5 distinct sites, 4 of which occur in the GAG regions between G2 and G3 and generate fragments

equally abundant in healthy and diseased cartilage. As mentioned, cleavage at the site within the IGD destroys aggrecan function. Aggrecan fragments cleaved at this site are much more abundant in samples of arthritic cartilage than in healthy individuals, leading to the understanding that cleavage at this site occurs predominantly during pathologic processes (141). Studies of recombinant ADAMTS-4 and 5 with cartilage explants or purified aggrecan have demonstrated that aggrecanases preferentially cleave aggrecan within the GAG domains (142, 143). These observations are partially explained by ADAMTS-4/5 interactions with the chondroitin sulfate GAG chains on aggrecan which may direct aggrecanase activity to these regions (144). Additional aggrecanase regulation comes from interaction with TIMP-3 (tissue inhibitor of metalloproteinases 3), the only known endogenous inhibitor of ADAMTS-4 and 5. TIMP-3 inhibition of ADAMTS-4 is increased 20-fold in the presence of CS GAGS (145) further underscoring the protective role that CS GAGs play in preventing degradation within the IGD. TIMP-3 and other protease inhibitors are repressed at the protein level during arthritis allowing for unregulated aggrecanase activity (138).

Matrix Metalloproteinases

During inflammatory arthritis chondrocytes and cells of the synovium express increased amounts of several MMPs in response to elevated levels of TNF α and IL-1 β (109). There are 25 zinc-dependent matrix metalloproteinases which, collectively, have the ability to degrade all components of the ECM and function in a variety of processes from development to wound healing (146). MMP zymogens are processed to their active form by plasmin, MMP-3 other

MMPs. In arthritis, MMPs are most noted for their irreversible degradation of collagens. Other important ECM targets include a wide array of matrix proteins including fibronectin, laminins and aggrecan which they cleave at DIPEN³⁴¹ within the IGD (147). Collagenases (MMP-1, 8, 13) degrade intact collagens while partially degraded collagens are proteolyzed by the gelatinases (MMP-2, 9). The stromelysins (MMP-3, 10, 11) have the broadest substrate specificity. MMP-1, 3, 9 and 13 are responsible for the majority of MMP-related ECM damage observed in arthritis (135). MMPs are efficiently inhibited by TIMPS 1-4; however these inhibitors are decreased in arthritic diseases (147) leading to deregulated MMP activity. It is also now clear that MMPs modulate inflammation by activating or degrading inflammatory cytokines and chemokines (109, 148).

HtrA1

HtrA serine proteases are highly conserved, ATP-independent, dual-function protease/chaperones with homologs found in organisms from bacteria to mammals (149). These proteases contain a variable amino terminal region and a chymotrypsin-like catalytic domain which is followed by one or more substrate recognition PDZ domains (postsynaptic density protein 95-discs large-zona occludens 1) (150). Proteolytic activation usually requires substrate binding to the PDZ domain. However, PDZ independent activity has also been observed (151).

Mammals express four HtrA proteins, HtrA1-4. HtrA1 is widely expressed and is involved, both intracellularly and extracellularly, in a myriad of processes including bone development, angiogenesis and placental maturation (152-155). HtrA1 is only minimally expressed in healthy cartilage. Expression is increased 7

fold in RA and 3 fold in osteoarthritis (156). HtrA1 activity may impact the homeostasis of the joint several ways: 1) direct degradation of ECM components, 2) generation of pro-inflammatory ECM fragments that up-regulate MMPs and stimulate the release of inflammatory cytokines and chemokines, 3) degradation of inhibitors of the complement cascade and 4) interference with growth-factor regulated homeostasis potentially contributing to the observed imbalance between anabolism and catabolism.

Insights about the consequences of increased HtrA1 activity can be gained from considering HtrA1 activity during ossification. During development, as the cartilage template is replaced by skeletal bone, HtrA1 is strongly expressed by terminally differentiated hypertrophic chondrocytes near the ossification center – those destined to be replaced by bone (157, 158). HtrA1 is actively involved in cartilage resorption by degrading numerous ECM components including proteoglycans (158, 159), fibronectin (156), aggrecan (160), fibulin (161), and collagens type I, II and VI (156, 162). In contrast to this physiologic process, pathologic chondrocyte hypertrophy and expression of HtrA1 also occurs in degenerative arthritis (159, 163-165). Cells within the inflamed synovium and some responding immune cells also contribute to elevated HtrA1 levels within the joint (166). As in development, HtrA1-mediated matrix degradation ensues.

Degradation of the ECM generates fragments including those derived from fibronectin, proteoglycans, collagens and hyaluronic acid which are inflammatory by virtue of their interactions with TLR-2, TLR-4, DDR2, CD44 receptors and

others (167-172). These interactions lead to the upregulation of aggrecanases, MMPs, cytokines and chemokines (162, 169, 173). Fibronectin fragments (Fn-f) stimulate significant cellular responses including: a reduction of proteoglycan synthesis and increased proteoglycan degradation (174); release of inflammatory cytokines and chemokines (175-177); and MMP-1, 3 and 13 upregulation (156, 170, 178).

Two studies on HtrA1 involvement in macular degeneration have examined the responses to HtrA1-generated Fn-fs. Elevated levels of chemokine CCL2, cytokines IL-6 and TNF α , as well as MMP-3 and MMP-9 were observed in retinal pigment epithelial (RPE) cells exposed to HtrA1 Fn-fs (179). Transgenic mice specifically overexpressing HtrA1 in RPE cells had higher levels of Fn-fs and ECM degradation than their wild type littermates (161). Additionally, in osteoarthritis human synovial fibroblasts, elevated levels of MMP-1 and MMP-3 were observed on exposure to HtrA1-generated Fn-fs (156). Like Fn-fs generated by other proteases, HtrA1-generated fibronectin fragments are bioactive and stimulate catabolic responses.

Understanding of a novel role for HtrA1 in regulation of the complement cascade is developing. Clusterin and vitronectin, major inhibitors of the membrane attack complex in the complement cascade, were identified in a peptide library as potential substrates of HtrA1 (180). Mass spectrometric analysis of conditioned media from HtrA1-treated RPE cells also revealed clusterin degradation which was later confirmed with recombinant proteins (181). Fibromodulin, another HtrA1 substrate within the ECM (158), binds and activates

C1q (182). Fibromodulin was also underrepresented in the HtrA1 RPE treated cells. HtrA1 degrades biglycan, decorin and fibronectin which bind the “tails” of C1q and inhibit in the classical pathway of the complement cascade (183, 184). Thus, HtrA1 degradation of inhibitors and activators of the complement cascade may impact the regulation of innate immunity within the joint.

In addition to its role in matrix remodeling, HtrA1 contributes to the homeostasis of a variety of tissues by proteolytically modulating levels of critical proteins such as tumor suppressors or the TGF β family of growth factors (152, 157). Loss of HtrA1 leads to unregulated TGF β signaling which contributes to the metastatic transformation of some cancers (152, 155, 185) and CARASIL (cerebral autosomal recessive arteriopathy with subcortical infarcts and leukoencephalopathy) (186), whereas excessive HtrA1 leads to TGF β depletion which contributes to age-related macular degeneration (187) and osteoarthritis (188). For example, chondrocyte terminal differentiation, the point at which ECM production is halted and cartilage resorption begins, is inhibited by TGF β (189).

Degradation of the ECM of cartilage is a sequential process initiated by aggrecanases, which remove the proteoglycan matrix, followed by MMPs which irreversibly damage the collagen framework. HtrA1 temporal involvement has not been specifically addressed. However, HtrA1 activity has been demonstrated to stimulate the release of MMP1, MMP3 and MMP13 and co-localization with MMP13 has been observed by immunohistochemistry (190).

Bacterial Proteases in Disease

Some pathogens fully exploit the host inflammatory response, not only by benefiting from the burst of host proteolytic activity, but also by secreting enzymes which directly degrade the ECM and activate the up-regulated host MMPs (191).

Periodontal disease is a consequence the inflammatory response to bacterial components which leads to excessive upregulation of host MMP- 2, MMP-8 and MMP-9. As in arthritis, down-regulation of MMP inhibitors allows for unbalanced MMP activity and degradation of gingival tissue, periodontal ligaments and the bone that support teeth (192, 193). Also like arthritis, this is a sequential process that is reversible if identified and treated early. Spirochetes comprises <1% of the bacterial population in healthy gingival tissues but over 50% of the organisms in diseased gingiva and contribute to the observed degradation (193, 194). *Treponema denticola* is the most reliably cultivable of the oral spirochetes involved in periodontal disease and thus most well characterized. Dentilisin is a *T. denticola* surface heterotrimer of lipoproteins PrcB and PrcA in complex with a chymotrypsin-like proteolytic subunit, PrtP (195). Both proteolytic and adhesion activities have been attributed to the dentilisin complex with host targets including ECM proteins and glycosaminoglycan, tight-junction proteins, complement cascade proteins, immunoglobulins and inflammatory cytokines and chemokines (195-198). MMP-2 induction and subsequent degradation of fibronectin has also been observed (192).

Staphylococcus aureus is responsible for 40-70% of septic arthritis cases in the United States (76). Full pathogenicity of *S. aureus* depends on the activities of “exo-proteases”, those secreted into the host environment. Metalloproteinase (aurolysin) and serine (SspA), cysteine (SspB) and papain-like (staphopain, ScpA) proteases are the major virulence-associated *S. aureus* exoproteases (199). Substrates within the host include ECM components, immunoglobulins and proteinase inhibitors. *S. aureus* dissemination requires a shift in phenotype from proteins required for adhesion to those allowing for invasion of host tissues (199). Shedding of surface adhesins is accomplished, in part, by SspA (200).

Bacterial HtrA Homologs

E. coli homolog DegP is the best characterized of the bacterial HtrAs. DegP is involved in the protein quality control component of the stress response. Proteins are susceptible to environmental strains such as temperature or changes in pH, changes which affect their ability to maintain a proper structure and thus a proper function. DegP contributes to normal cellular functions in adverse conditions by assisting membrane proteins in the attainment of a properly folded state, or by degradation of proteins too badly damaged to do so (201). At ambient temperatures or favorable conditions, DegP is primarily a chaperone (202). At elevated temperatures or under oxidative stress conditions, substrate binding to the PDZ domains induces 12- to 24-mer oligomerization. Conformational changes within several flexible loops align the catalytic triad and expose the active sites on the interior walls of the chamber for proteolysis (203,

204). Many bacterial HtrA homologs are indirectly involved in pathogenesis due to their chaperone activity or proteolytic processing of virulence factors (150, 201, 205).

HtrAs are surface-localized in micro-domains in gram-positive bacteria (205). Traditionally thought to be purely periplasmic in gram-negative bacteria, surface exposure (206-208) or secretion (209-212) of HtrA has been demonstrated for a growing list of gram-negative bacterial pathogens. The mechanism for export beyond the periplasm remains unknown.

HtrA proteases in some pathogenic bacteria have acquired at least one directly pathogenic “moonlighting” function (213). *Helicobacter pylori* HtrA, HpHtrA, is found in both secreted (212) and surface-exposed (208) fractions of this gram-negative pathogen. HpHtrA degrades the tight-junction protein E-cadherin to migrate across epithelial barriers (214, 215). Moreover, Hoy *et al.* recently demonstrated that HtrAs from enteropathogenic *E. Coli* (EPEC), *Shigella flexneri* and *Campylobacter jejuni* also degrade E-cadherin, whereas the HtrA from *Neisseria gonorrhoeae* did not (213). E-cadherin shedding from cells infected with the various pathogens was consistent. The authors suggest that E-cadherin degradation may be a general mechanism of pathogenesis for bacteria requiring paracellular transmigration. As *N. gonorrhoeae* utilizes transcytosis for migration, the ability to cleave E-cadherin may not be required. Although the mechanisms are unknown, borrelial migration across endothelial barriers at intercellular junctions has often been observed, (39, 216-220).

Proteases in Lyme Disease

Host Proteases in Lyme Disease

Host proteases released in response to bacterial infection degrade the ECM thereby facilitating leukocyte and lymphocyte migration into infected tissues to eradicate the bacteria (148, 191). Many pathogens take advantage of this proteolytic activity to aid in their dissemination and colonization of other sites within the host.

B. burgdorferi infection of many different cell types, cartilage explants and mice induces numerous host proteases typically observed in immune activation including ADAMTS-4 (221, 222) and MMP-1, 3, 8, 9, 10, 13 and 19 (60, 221, 223-226). Borrelial lipoproteins are recognized by TLR2 and some of the observed MMP responses are attributed to TLR2 signaling (224). However, TLR-independent MMP upregulation via integrin interactions has also been demonstrated (222).

Most of these proteases are also detected in human synovial fluid from LA patients (221, 222, 225). One study examined the MMP profile in LA synovial fluid samples before and after antibiotic treatment and observed a shift from pre-treatment expression of MMP1 and MMP3 to post-treatment expression of MMP8 and MMP9 (225). *Borrelia*-infected MMP9^{-/-} mice have unaltered bacterial loads, leukocyte profiles and cytokine and chemokine profiles compared to wild type controls (91). Interestingly, these mice develop less severe arthritis while carditis is unchanged; leading the authors to speculate that perhaps MMP9 activity releases an inflammatory factor within the joint of wild type mice. For example,

MMP9 activates the inflammatory cytokine IL-8 to a highly potent form (227). Assessing the contribution of an individual MMP will be difficult given the number of MMPs up-regulated, the overlap of their substrate specificities and the immunomodulatory functions of MMPs.

Microarray analysis has identified potential upregulation of HtrA1 *in vitro* in *Borrelia*-infected macrophages (2.68 fold) (228). Comparison of the transcriptomes of joint tissues from arthritis susceptible C3H/HeN mice and arthritis resistant C57BL/6 mice 4 weeks post infection also revealed modest HtrA1 upregulation (2.43 fold) (60). Although these findings have not been validated by quantitative PCR, HtrA1 may be up-regulated in LA as in other forms of inflammatory arthritis.

In addition to causing an increased expression of host proteases, *B. burgdorferi* coordinate host plasminogen to their surface (229, 230) with the plasminogen-binding proteins OspC (231), enolase (232, 233), and ErpP, ErpA and ErpC (234). Plasminogen, the zymogen form of the broad-spectrum serine protease plasmin, is activated by endogenous urinary (uPA) and tissue-type (tPa) plasminogen activators. Borrelial infection stimulates the upregulation of uPA in monocytes (235) which has been demonstrated in complex with plasmin on the spirochetal surface (229). *In vitro*, borrelial-associated plasmin increases spirochetal transmigration across cultured monolayers (230, 236) and enhances degradation of fibronectin, laminin and vitronectin (237, 238). In cartilage explants infected with *Borrelia*, MMP9 activation and *Borrelia*-induced GAG release was greater in the presence of plasminogen than in controls (221). *In*

vivo studies demonstrated that host-acquired plasminogen was important for borrelial migration through the tick (27). Within the murine host, while systemic dissemination was unaffected, reduced spirochetaemia was observed suggesting that plasmin may aid borrelial penetration of the vasculature. Hence, while plasmin increases the efficiency of hematogenous spread, it is not required for dissemination within the mammalian host.

Borrelial Proteases in Lyme Disease

Examination of the *Borrelia* genome has yet to identify hyaluronidases, collagenases or other proteases with significant homology to known bacterial virulence-associated proteases (39, 239). One study has demonstrated gelatinase activity associated with a high molecular weight protein (240). In assays with intact spirochetes incubated with purified substrates, no proteolytic activity against fibronectin, laminin, vitronectin or collagens type I, III or IV was observed without the addition of plasminogen (237, 238). *Borrelia* transmigration cross cell monolayers is aided by the addition of plasminogen. However, monolayer penetration occurs without added plasmin (230, 236, 241) and in the presence of inhibitors to both plasmin and ADAMTS/MMP proteases (236). Likewise, aggrecan degradation in *Borrelia*-infected cartilage explants occurred without added plasminogen and remained with treatment of plasmin, ADAMTS and MMP inhibitors (221, 242). These studies demonstrate that *Borrelia* possess proteolytic activity independent of host-acquired plasminogen or MMP activity.

CHAPTER 5: Materials and Methods

Characterization of Commercial Aggrecan by Dot Blots

Sigma aggrecan (1 μ g) was spotted onto nitrocellulose membrane strips, non-specific binding sites were blocked with Starting Block (Pierce; proprietary, partially purified milk protein, 0.5-1.5% protein content), and the membrane was probed with commercially available antibodies to aggrecan components and other proteoglycans. Primary antibodies were used at 10 μ g/ml; alkaline phosphatase labeled secondary antibodies (KPL) were used at 0.16 μ g/ml.

Bacterial Strains and Growth Conditions

The following *Borrelia* type strains were used in these studies: *Borrelia burgdorferi* (passage 4, non-clonal, infectious strain B31 and low passage, clonal, infectious strain A3), *Borrelia garinii* (unknown passage, infectious strain FR-20047) and *Borrelia afzelii* (unknown passage, infectious strain ACA-1) were grown in Barbour-Stoenner-Kelly media (BSK II) supplemented with 6% rabbit serum. *Borrelia* were cultured at 34°C for affinity chromatography and immunofluorescence microscopy. All other studies were performed with *Borrelia* cultured at 37°C.

Fluorescence Labeling of Aggrecan

Native aggrecan from bovine articular cartilage (Sigma) was labeled using an amine reactive dye following the manufacturer's protocol (3.5-fold molar excess Dylight 549, Pierce). Referred to as FL*ACAN.

Analysis of Borrelial Interaction with Aggrecan

Fluorescent Aggrecan Labeling of Intact *Borrelia*

B. burgdorferi B31 were grown to late log phase as described above, harvested by centrifugation, and washed twice (PBS, 5mM MgCl₂) to remove media components. All washes were carried out at 2,000xg for 10 min. Borrelial outer membranes were stabilized by cross-linking (2% paraformaldehyde in PBS/Mg²⁺, 40 min, room temperature with mixing) and washed twice to remove the fixative. *Borrelia* (1.4x10⁷) were blocked (TBS, 5mM CaCl₂, 3% BSA; 60 min, 37°C with mixing) and incubated with FL*ACAN (10 µg, 111nM final concentration) and monoclonal anti-FlaB (H9724, 5 µg/ml) in blocking buffer for 60 min at 37°C with mixing. Following two washes (PBS), *Borrelia* were incubated with fluorescently labeled secondary antibody (FITC goat anti-mouse, KPL, 10 µg/ml) in blocking buffer for 60 min at 37°C with mixing. *Borrelia* were washed twice more and resuspended in PBS buffer. Labeled spirochetes (2.75x10⁵) were mounted, dried, and overlaid with Prolong Gold Antifade (Invitrogen). Spirochetes incubated in the absence of FL*ACAN or with the antibodies alone served as controls. Labeled spirochetes were viewed under a Zeiss LSM5 Pascal confocal laser point scanning microscope and images were acquired and analyzed using the LSM5 Pascal image browser.

Affinity Chromatography

Aggrecan affinity columns were prepared by covalently linking 4 mg of bovine articular cartilage (Sigma, A1960) to activated aldehyde groups on polyacrylamide beads (Pierce, Ultra Link) following the manufacturer's protocol.

Control columns were generated in the same manner by omitting the aggrecan. *Borrelia* were grown to late log phase, harvested, and washed as above. Borrelial lysates were prepared by sonication in lysis buffer (20mM HEPES, pH 7.5, 150mM NaCl, 1X HALT protease inhibitor cocktail (Pierce), 0.5% Triton-X 100, and 5mM CaCl₂). Lysates were cleared by centrifugation (10,500xg, 60 min, 4°C), filter sterilized (0.22µm), and incubated with the pre-equilibrated aggrecan column overnight (4°C, with inversion). The flow through was collected and the column washed with lysis buffer to remove non-bound proteins. NaCl wash buffers (300mM and 600mM, 20mM HEPES, pH 7.5, 5mM CaCl₂) were then applied to remove non-specifically bound proteins. Chondroitin 4- and 6-sulfate glycosaminoglycans (GAGs, purified from bovine trachea; 70% chondroitin 4-sulfate, 30% chondroitin 6-sulfate; Sigma) were used as an initial elution buffer (20mM HEPES, pH 7.5, 150mM NaCl, 5mM CaCl₂) to release proteins interacting with the aggrecan GAG chains. Elution of remaining proteins was achieved with 1M NaCl (20mM HEPES, pH 7.5, 5mM CaCl₂) followed by 100mM glycine, pH 2.8. The eluates were dialyzed against water, concentrated in a centrifugal protein concentrator with a molecular weight cut off of 10,000 (Amicon Centriplus, YM-10), and adjusted to 0.5ml. SDS-PAGE was used to electrophoretically separate the eluates (10.5-14% gels, BioRad). Gels were stained with Coomassie Brilliant Blue and bands of interest were excised and sent for peptide mass fingerprinting via tandem mass spectrometry (City of Hope Beckman Research Institute, Duarte, California).

Mass Spectrometric Analysis of Aggrecan-Binding Proteins

Performed by City of Hope Beckman Research Institute, Duarte, California as follows: In-gel reduced, alkylated, and trypsin digested peptides were analyzed by LC/MS using an Agilent 6520 Q-TOF mass spectrometer with an Agilent 1200 nano-flow HPLC (Agilent Technologies, Santa Clara, CA). Separation was carried out using the Chip Cube source and a standard capacity protein identification chip. Samples were loaded onto a 40nl trapping column at 6µl/min in 99% buffer A (0.1% formic acid in water). The trapping column was then switched on line with a 75µm x 43mm analytical column and eluted directly into the mass spectrometer. The analytical gradient ran at 600 nl/min from 1% buffer B (0.1% formic acid in acetonitrile) to 50% buffer B over 8 min. The primary gradient was followed by a 1 min wash at 90% buffer B and re-equilibration to initial conditions. Mass spectra were collected in data dependent fashion. From each full mass scan, up to 6 precursor ions were selected for fragmentation. After being analyzed, each ion was placed on an exclusion list for 15 seconds. Both full mass and fragment ion spectra were collected in centroid mode at a rate of 4 Hz. Data were converted to mzData using Agilent's supplied tool. Converted data files were searched against the *B. burgdorferi* database (strain B31) and the cRap database using X!Tandem (<http://thegpm.org>). The preliminary search assumed tryptic specificity with at most one missed cleavage, quantitative carbamidomethylation of cysteine, and possible oxidation of methionine. Refinement searches considered non-tryptic cleavage, acetylation of the protein amino terminus, deamidation of asparagine and glutamine, oxidation

of tryptophan, and double oxidation of methionine and tryptophan. All searches used a mass tolerance of 25ppm for precursors and 50 ppm for fragments.

Amino-Terminal Sequence Analysis

Edman degradation was performed by the CDC Biotechnology Core Facility. Following SDS-PAGE and electroblotting onto PVDF membranes, the protein bands visualized with Coomassie Brilliant Blue were sequenced using a model cLC-Procise sequencer (Applied Biosystems, Foster City, CA) applying the manufacturer's PVDF chemistry cycles. The N-terminal sequences were identified for the main PTH signal that was assigned against the known template protein sequence.

Characterization of BbHtrA

Generation of Recombinant BbHtrA and BbHtrA^{S226A}

Recombinant wild type BbHtrA and a serine to alanine active site mutant (BbHtrA^{S226A}) were produced by GenScript USA Inc., New Jersey, USA. Full length genes with C-terminal histidine tags were codon optimized for expression in *E. coli*, synthesized, sequenced, and cloned into pUC57. For protein production, the sequences for the mature proteins (amino acids 38-474) were sub-cloned into proprietary expression vectors using the following primers: F: CTTTAAGAAGGAGATATACATATGGAAGAAAAAGATAACACCGTG; R: ATAC-AGCTGTGCGGCCGCAAGCTTTCATTAGTGATGGTGATGGTGATGAA.

Proteins were purified from the soluble cellular fraction by application to a nickel column, eluted with imidazole and dialyzed into a storage buffer (TBS, 10% glycerol). ProteoSpin endotoxin removal kits (Norgen Biotek) were used, per the

product insert, to reduce the LPS in the recombinant proteins. Proteins were aliquoted and stored at -80°C until use.

Determination of Endotoxin Units

All samples were evaluated for the relative toxicity (endotoxin units, EU) of the LPS they contained before use in cell culture. A chromogenic limulus amoebocyte lysate assay (LAL assay) was performed by Lonza Walkersville, MD. Values obtained were: Sigma LPS (lot 011M4008V), 4.5×10^3 EU/ μ g; BbHtrA^{WT}, 1.4 EU/ μ g; BbHtrA^{S226A}, 0.099 EU/ μ g.

Polyclonal Rabbit Anti-BbHtrA

A BbHtrA peptide was chosen for polyclonal antibody generation as follows. The BbHtrA amino acid sequence was analyzed, based on the method of Kolaskar and Tongaonkar (243) and using the EMBOSS antigenicity prediction algorithm (<http://bips.u-strasbg.fr/EMBOSS/>), to find potentially antigenic regions of the protein (Table 2).

Table 2 Potentially antigenic BbHtrA peptides

EMBOSS prediction of antigenic regions of BbHtrA. Peptides with scores above 1.0 are potentially antigenic. Immunogen peptide is highlighted.

<u>Residues</u>	<u>Sequence</u>	<u>Length</u>	<u>Score</u>
390-407	LPGFVVYPLVEDIKAQLN	18	1.245
370-379	NIEIVLAVRP	10	1.176
108-124	KKSLFYVVTNSHVVDKA	17	1.173
413-423	KGVVVDYIDKN	11	1.172
6-29	FSGFLLSFLALSIGFFIGMHYLA	24	1.167
293-304	SEVLKSLGVESN	12	1.155
433-442	GDVILSVNSK	10	1.138
51-82	FREVSKKILPSSVEVHATGVIKQSFPIPIFFFF	32	1.136
126-133	ELEVVSVD	8	1.129
306-324	VSAAIASLYPGSPAVKSG	19	1.127
254-262	LGFAIPVNN	9	1.125
178-201	WVMAVGSPFQFSFTVTAGIVSGLQ	24	1.111
355-366	GEKVNVEILRGN	12	1.104
331-352	IMKVNGVSMSVFQDVTSYISDF	22	1.103
450-456	FYDALEV	7	1.095
278-289	SAWLGISFYPLK	12	1.094
265-273	STVDFFLKG	9	1.086
149-155	DIALISF	7	1.084
161-167	TIKVADL	7	1.079
98-103	SGVIIG	6	1.073
44-49	VRALQD	6	1.066
228-241	GPLVNIKGEVIGIN	14	1.061
33-38	NIVFAE	6	1.050
211-218	RNLFIQTD	8	1.050

Comparative sequence analyses (BLAST) of the predicted antigenic peptides were performed to examine the BbHtrA peptides for homology with other borrelial proteins or HtrA1. To estimate surface exposure of BbHtrA candidate peptides, BLAST comparisons between BbHtrA and DegP identified the orthologous peptides in DegP. Surface exposure of the peptides was then visualized by examining the DegP peptide positions in two crystal structures of DegP (PDB codes 1KY9 and 2ZLE). BbHtrA amino acids 306-324 (VSAAIIASLYPGSPA VKSG) were selected as the peptide immunogen based on predicted antigenicity, reduced homology with other borrelial proteins or HtrA1, and potential surface exposure. GenScript USA Inc. was contracted to generate a rabbit polyclonal antibody. The peptide was synthesized and, to increase antigenicity, an amino terminal cysteine was added to allow for conjugation to keyhole limpet hemocyanin (KLH). Two white New Zealand rabbits were immunized with the KLH-peptide. Resultant antibodies were purified from polyclonal sera using affinity chromatography with the peptide immunogen.

Immunoblot Analysis of Borrelial Lysates

Borrelial lysates ($\sim 1 \times 10^8$ cells each) and recombinant BbHtrA proteins (1 μ g) were subjected to SDS-PAGE electrophoresis using pre-cast Tris-glycine gels (BioRad) and transferred to nitrocellulose (BioRad). The membrane was blocked (Starting Block, Pierce) for 60 min at room temperature and then incubated overnight with rabbit anti-BbHtrA (0.2 μ g/ml in Starting Block). The membrane was washed four times (TBS, 0.05% Tween 20) and then incubated for 60 min at room temperature with alkaline phosphatase labeled goat anti-rabbit

(Kirkegaard & Perry Laboratories (KPL), 0.05 µg/ml in Starting block). Signals were detected by chemiluminescence (PhosphaGLO, KPL).

Zymography

Borrelial lysates ($\sim 1 \times 10^8$ *B. garinii*, *B. afzelii*; $\sim 5 \times 10^7$ *B. burgdorferi*) and recombinant BbHtrA proteins (1µg) were subjected to SDS-PAGE electrophoresis using 12% β-casein Zymogram Ready Gels (Bio-Rad). Following electrophoresis, the gels were renatured in 2.5% Triton X-100 (Sigma) for 60 min at 37°C with a buffer change at 15 min. The gels were developed in Zymogram Development Buffer (BioRad) for 40h at 37°C with a buffer change at 15 min. Gels were stained (0.5% Coomassie Brilliant Blue R-250, 40% methanol, 10% glacial acetic acid) for 60 min at room temperature and then destained (40% methanol, 10% glacial acetic acid).

Proteinase K Assays

B. burgdorferi (strain B31) was cultured in complete BSK II medium to early log phase (4.5×10^6 /ml) and harvested by centrifugation at 2,000xg for 20 min. Cultures were washed twice with PBS/Mg²⁺, resuspended in the same and divided into 0.5ml samples. One sample received proteinase K (40 µg/ml, Qiagen). Samples were incubated at room temperature for 40 min with periodic inversion to mix. Samples received 1X HALT protease inhibitor cocktail (Pierce) and incubated for an additional 5 min. Samples were centrifuged as above and washed once with PBS/Mg²⁺ to remove the protease. Samples were resuspended in non-reducing SDS/PAGE sample buffer and $\sim 1 \times 10^8$ *Borrelia* were loaded per lane in pre-cast Tris-glycine gels (BioRad) . Samples were

electrophoresed, transferred to nitrocellulose and probed with the indicated antibodies. All antibodies were diluted in Starting Block and used at the following concentrations: mouse monoclonal anti-OspA (H5332, CDC collection), 1 µg/ml; mouse monoclonal anti-FlaB (H9724, CDC), 0.025 µg/ml; rabbit polyclonal anti-BbHtrA, 0.2 µg/ml; and alkaline phosphatase-conjugated secondary antibodies (KPL) at 0.05 µg/ml. Signals were detected by chemiluminescence.

Surface Biotinylation

Borrelia were grown to late log phase, harvested, and washed thrice in HBS, 5mM MgCl₂. To minimize damage to borrelial membranes, all washes were carried out at 2,000g for 10 min at 4°C. The bacteria were resuspended in HBS and half were placed on ice as the no biotinylation control. For biotinylation, *Borrelia* were incubated with Sulfo-NHS-SS-Biotin (1mM final concentration, 30 min, room temperature with mixing). The reaction was quenched (50mM Tris, pH 8.0, final concentration), *Borrelia* were washed to remove excess label, and protease inhibitors (1xHALT, Pierce) were added. *Borrelia* were sonicated, the sonicates were cleared by centrifugation (10,500g, 1 hour, 4°C) and filter sterilized (0.22µm). SDS-PAGE was used to electrophoretically separate the sonicates (10.5-14% gels (BioRad)). Silver stained bands of interest were excised and sent for peptide mass fingerprinting via tandem mass spectrometry (CSU, Proteomics and Metabolomics Facility).

Analysis of Human Sera for Antibodies to BbHtrA^{S226A}

BbHtrA^{S226A} (7 µg) was electrophoresed on a Criterion prep gel (BioRad), transferred to a nitrocellulose membrane (BioRad), and the membrane was

blocked overnight (Starting Block). The membrane was cut into strips which were probed with human sera (1:2000 in Starting Block) or polyclonal rabbit antibodies (1 µg/ml) for 60 min at room temperature, washed four times (TBS, 0.05% Tween 20), and incubated with alkaline phosphatase conjugated secondary antibodies diluted in Starting Block: goat anti-human (KPL), 0.1 µg/ml or goat anti-rabbit (KPL), 0.05 µg/ml. Bands were visualized with precipitating alkaline phosphatase substrate (BioRad). Commercial rabbit polyclonal antibodies: anti-HtrA1, Thermo Scientific PA5-11413; anti-HtrA2, Sigma HPA027366; anti-HtrA3, Abcam ab65911; anti-HtrA4, Sigma SAB2101111. All Lyme disease patients met clinical criteria for Lyme disease and were IgG positive by 2-tiered testing (CDC reference panel). Healthy control sera were from donors living in regions non-endemic for Lyme disease.

Proteolysis Assays

Substrates (400nM) and proteases (100nM) were diluted in assay buffer (50mM HEPES, pH 7.4, 5mM CaCl₂) and incubated for the times indicated in the text. Proteoglycans were deglycosylated as follows: reactions were boiled for 3 min to deactivate the proteases followed by the addition of 100mM sodium acetate and 0.01U chondroitinase ABC for 5h at 37°C. Reactions were stopped by the addition of SDS-PAGE sample buffer and boiled for 4 min. Proteins were electrophoretically separated in precast Tris-HCl gels (BioRad). Gels were either silver stained (Pierce, Silver Stain Kit for Mass Spectrometry) or processed for Western blotting. Commercial reagents: ADAMTS5, R&D Systems 2198-AD; native aggrecan, Sigma A1960; recombinant aggrecan, R&D Systems 1220-PG;

biglycan, Sigma B-8041; decorin, Sigma D-8428; brevican, R&D Systems 4009-BC; chondroitinase ABC, Sigma C2905; collagen, Millipore CC052; plasma fibronectin, BD Biosciences 354008; HtrA1, R&D Systems 2916-SE; MMP2, EMD Chemicals PF023, neurocan, R&D Systems 6508-NC; tenascin-C, Millipore CC065; versican, Abnova H00001462-P01.

Immunoblot Analysis of Recombinant Aggrecan Proteolytic Fragments

Recombinant aggrecan (340nM) was incubated with ADAMTS5 (10nM), MMP2 (15nM), HtrA1 (280nM) or BbHtrA (370nM) in a total reaction volume of 20µl in assay buffer (50mM HEPES, pH 7.4, 5mM CaCl₂) for 12h. Reactions were stopped by the addition of SDS-PAGE sample buffer and boiled for 4 min. Proteins were electrophoretically separated in precast Tris-HCl gels (BioRad) and transferred to nitrocellulose (BioRad). The membrane was blocked (Starting Block, Pierce) before overnight incubation with 2 µg/ml mouse anti-³⁷⁴ARGSVIL “BC-3” (Thermo Scientific, MA3-16888); in blocking buffer (Starting Block). Following 3 washes (TBS, 0.05% Tween 20), the membrane was incubated with 0.1 µg/ml goat anti-mouse (KPL) in blocking buffer for 60 min at room temperature. Signals were detected by chemiluminescence. The membrane was stripped (Restore, Pierce), blocked, and probed with 1 µg/ml mouse anti-³⁴¹DIPEN (MD Bioproducts, 1042002) for 4h.

Evaluating Inflammatory Cytokine Responses to BbHtrA Activity

Mesenchymal Stem Cell Culture

1x10⁶ human mesenchymal stem cells (passage one, Lonza, catalog #PT-2501) were plated in a T150 flask (Corning) and cultured in growth media: mesenchymal stem cell basal media (MSCBM, Lonza, #PT-3238), mesenchymal growth supplements (SingleQuots, Lonza, #PT-4105), and 5 ng/ml recombinant human fetal growth factor (Shenandoah Biotechnology). Cells were maintained at 37 °C and 5% CO₂. When confluent, cells were trypsin-released (0.5% trypsin EDTA, Gibco), expanded to two T150 flasks and fed with growth media every three days. When confluent, cells were harvested, resuspended in fresh growth media containing 5% DMSO and aliquots of 1x10⁶ cells were cryopreserved in liquid nitrogen.

Chondrogenesis and Aggregate Formation

Two vials of passage three cryopreserved stem cells were thawed, plated in growth media in two T150 flasks and then expanded to six T150 flasks as above. Cells were harvested (0.5% trypsin EDTA, Gibco), pooled, enumerated and induced to chondrogenic differentiation (244, 245) as follows. Cells were resuspended in defined chondrocyte differentiation media: high glucose DMEM (Gibco), 50 µg/ml ascorbic acid-2-phosphate (Sigma), 39.3 ng/ml dexamethasone (Sigma), 40 µg/ml L-proline (Sigma), ITS + Premix (BD Biosciences), 10 ng/ml transforming growth factor β-3 (Shenandoah Biotechnology) and 30 µg/ml gentamicin sulfate + 15 ng/ml amphotericin-B (GA-1000, Lonza, #PT-4504E). High density aggregates were obtained by plating, on

average, 3×10^5 cells per well in a conical bottom 96 well plate (Thermo Scientific), pelleting by centrifugation (5 min at 600xg), and incubating at 37 °C and 5% CO₂. Pellets formed coherent spherical aggregates by day two of culture. After seven days, wide bore tips were used to transfer aggregates to V-bottom 96 well plates (Corning). Aggregates were maintained in differentiation medium at 37°C and 5% CO₂ for 4-5 weeks and fed every two days until experimentation. Dexamethasone containing medium was removed 24 hours prior to experimentation, aggregates were rinsed with DPBS (Gibco) and dexamethasone-free differentiation medium was added.

Chondrocyte Cytokine Induction

Prior to addition to aggregates, LPS (44ng, 200EU), BbHtrA^{WT} (20µg, 27.9EU LPS) and BbHtrA^{S226A} (20µg, 1.99EU LPS) were incubated in 1 mg/ml polymyxin B sulfate (Sigma) on ice for 30 min with occasional mixing. Warmed dexamethasone-free medium was then added to each test condition to a final volume of 1ml. Control aggregates were maintained in untreated medium also containing polymyxin B sulfate. The final concentration for all test conditions was 60 µg/ml polymyxin B sulfate. For chondrocyte cytokine induction, equivalent numbers of aggregates per test condition were transferred to individual wells of 24 well plates, spent medium was removed and 1ml freshly warmed dexamethasone-free medium containing test components was added. Aggregates were incubated at 37°C and 5% CO₂ for 48 hours.

Cytokine Assays

Proteome Profiler Human Cytokine Arrays (R&D Systems, #ARY005) were used to detect 32 cytokines released in response to various conditions and were performed per product inserts. Briefly, spent medium from chondrocyte assays was immediately diluted 1:5 in assay buffer containing biotinylated cytokine detection antibodies and incubated at room temperature for 60 min. The capture antibodies are spotted in duplicate on nitrocellulose membranes which were blocked with supplied buffer for 60 min. The samples were added to the blocked membranes and incubated overnight at 4°C with mixing. After washing to remove unbound cytokines, membranes were incubated with 0.05 µg/ml phosphatase-labeled streptavidin (KPL) for 30 min. After washing to remove unbound streptavidin, precipitating phosphatase substrate (BioRad) was added. Membranes were developed simultaneously to control for development time and images were acquired with a BioRad GelDoc 2000. Pixel densities were measured with BioRad Quantity One imaging software using the same volume array tool for all membranes.

Analysis of Cytokine Pixel Density

To compare cytokine responses between the various study conditions, pixel densities were measured and compared using a statistical model developed by CDC statistician Mark J. Delorey. Before modeling, background values, defined as the mean response for four negative control spots on each membrane, were subtracted from all density values for that membrane. The data were then analyzed using a linear mixed-effects model with test condition and

cytokine, along with an interaction between the two, as fixed effects and the background-corrected Pixel Density (ODu/mm^2) as the response variable. Membrane number, established by the manufacturer, was included as a random effect. Between-membrane variance was allowed to differ by cytokine and condition. Standard diagnostics, including residual analysis and quantile-quantile plots, were performed to verify model fit and assumptions of normality for the random effects and error terms. Simultaneous, two-sided 95% confidence intervals for differences in mean background-corrected Pixel Density among the test conditions for each cytokine were computed using Sidak's method. The critical value for the joint confidence region was computed as the 97.5th quantile of a multivariate t-distribution with 272 d.f. (the number of residual d.f. from the model fit). Results of the comparisons are found in Table 6, where shaded rows indicate a statistically significant difference in mean density. Two-tailed p-values from univariate t-tests on the differences in means are also shown. Univariate $p < 0.001$ were considered statistically significant with this level of significance determined by applying Sidak's inequality to ensure an overall Type I error rate of 0.05. Analysis was performed using R software (Version 2.14.1) and Spotfire S+, v8.2 (TIBCO Software, Inc.).

Mass Spectrometry of Fibronectin Fragments

Performed by Colorado State University Proteomics and Metabolomics Core Facility: In-gel reduced, alkylated, and trypsin digested peptides were purified and concentrated using an on-line enrichment column (Agilent Zorbax C18, 5 μm , 5 x 0.3mm). Subsequent chromatographic separation was performed

on a reverse phase nanospray column (Agilent 1100 nano HPLC, Zorbax C18, 5 μ m, 75 μ m ID x 150mm column) using a 42 min linear gradient from 25%-55% buffer B (90% ACN, 0.1% formic acid) at a flow rate of 300 nanoliters/min. Peptides were eluted directly into the mass spectrometer (Thermo Scientific LTQ linear ion trap) and spectra were collected over a m/z range of 200-2000 Da using a dynamic exclusion limit of 2 MS/MS spectra of a given peptide mass for 30 s (exclusion duration of 90s). Compound lists of the resulting spectra were generated using Bioworks 3.0 software (Thermo Scientific) with an intensity threshold of 5,000 and 1 scan/group. MS/MS spectra were searched against the International Protein Index (IPI) human database (56,555 sequence entries) using the Mascot database search engine (version 2.2.1). The following parameters were employed in the database searches: peptide mass tolerance of 2 Da, fragment ion mass tolerance of 1.5 Da, fully tryptic digestion allowing for 1 missed cleavage, variable modification of methionine oxidation, and a fixed modification of cysteine carbamidomethylation. Protein identifications from all samples were combined using probabilistic protein identification algorithms implemented in Scaffold software (Proteome Software, Portland, OR). Peptide and protein probability thresholds of 95% and 95%, respectively, were applied to the results (2.2% FDR as calculated by Scaffold based on probability statistics). A minimum of 2 unique peptides were required for protein identification. Proteins containing shared peptides are grouped by Scaffold to satisfy the laws of parsimony. Manual validation of MS/MS spectra was performed for all protein identifications above these thresholds that were based on one or two peptides.

Criteria for manual validation included the following: 1) The peptide must be identified by all three search engines (Sequest, Mascot, and X! Tandem); 2) there must be a minimum of 80% coverage of theoretical y or b ions (at least 5 in consecutive order); 3) there must be an absence of prominent unassigned peaks greater than 5% of the maximum intensity; and 4) indicative residue specific fragmentation, such as intense ions N-terminal to proline and immediately C-terminal to aspartate and glutamate, were used as additional parameters of confirmation.

CHAPTER 6: Results

Characterization of the Aggrecan Used in These Studies

Commercially available aggrecan is purified from bovine articular cartilage (Sigma A1960). Although the exact method for purification is proprietary, Fig. 4A shows the general purification scheme for this proteoglycan. Proteins in cartilage are denatured and solubilized by incubation with guanidinium hydrochloride. Size exclusion chromatography (2500kD) is used as an initial purification step to separate aggrecan from the majority of the smaller proteins and proteoglycans in cartilage extracts. Next, the highly negatively charged glycosaminoglycan side chains allow for separation of aggrecan from other large proteins. Finally, the protein and uronic acid (GAG component) content of the fractions are used to pinpoint fractions containing aggrecan with the greatest amount of glycosaminoglycan (GAG). Electrophoresis and dot blot immunodetection were used to further analyze the purity of the aggrecan used in these studies (Sigma A1960, lot# 089K4071).

Sigma obtains aggrecan from an Israeli supplier who agreed to analyze this lot, as it does others, using composite gel electrophoresis (CAPAGE). Native aggrecan is too large to enter standard polyacrylamide gels and is instead analyzed on composite gels composed of 1.2% polyacrylamide and 0.7% agarose. To confirm that only one proteoglycan is isolated during the purification, gels are stained with toluidine which binds to the aggrecan GAG side chains. Aggrecan monomer mass is variable by virtue of the varying number and lengths of its GAG side chains. As a consequence, native aggrecan appears as a wide

band on CAPAGE gels (Fig. 4B). Lot #089K4071 was used for the studies described in this report and three previous lots are shown for comparison.

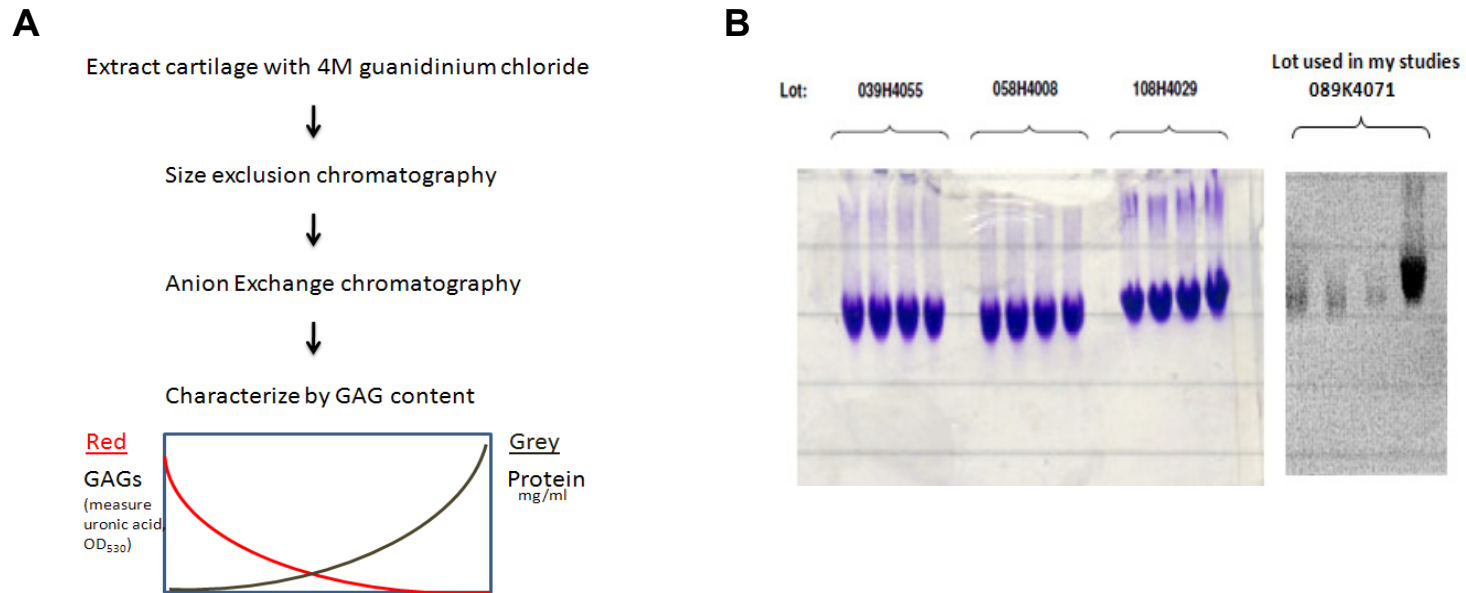


Figure 4 Purification of bovine aggrecan by Sigma supplier

A. Aggrecan purification scheme based on aggrecan's physical characteristics as a very large, negatively charged and highly glycosylated protein. Guanidinium chloride is used to extract proteins from bovine nasal cartilage. Very large proteins, including aggrecan, are isolated using size exclusion chromatography. Negatively charged proteins are then isolated using anion exchange chromatography. Lastly, because aggrecan has the largest glycosaminoglycan (GAG) to protein ratio of any proteoglycan, protein fractions are examined for GAG content. **B.** CAPAGE gels of four lots of Sigma bovine articular cartilage aggrecan (courtesy of Sigma Aldrich). Lot#089K4071 was used in the studies described herein.

I examined Sigma aggrecan for integrity and contamination with other proteoglycans by immunodetection with commercially available antibodies. The charged glycosaminoglycan side chains prevent efficient transfer of aggrecan to nitrocellulose or PVDF membranes, preventing Western blot analysis of the intact monomer. Consequently, dot blot analysis was used to probe for various proteoglycans and ECM components. Experimental details are provided in the Methods section. Figures 5A and 5B demonstrate that this lot contains intact aggrecan with all three globular domains, both types of chondroitin sulfates, and very little if any aggrecanase mediated degradation. Cartilage normally contains several small leucine-rich proteoglycans which migrate at approximately 100 kilodaltons (kD) on SDS-PAGE gels. Given that Sigma did not supply images of the complete aggrecan CAPAGE gels, aggrecan lot 089K4071 was examined for the most abundant small proteoglycans, decorin and biglycan, whose presence might not be revealed on the upper portion of the CAPAGE gel images (Fig. 5C). Finally, since this cartilage was harvested from bovine nasal cartilage, it was also probed for the presence of brain proteoglycans neurocan and brevican and the skin proteoglycan versican (Fig. 5C). The signals for these proteoglycans were not greater than that of the secondary antibody alone, indicating that none of these proteoglycans are enriched in Sigma A1960 lot089K4071.

These results demonstrate that Sigma aggrecan contains intact aggrecan monomers free from the contaminating proteoglycans versican, brevican, neurocan, biglycan or decorin. It remains possible that there are trace contaminants from ECM components not evaluated.

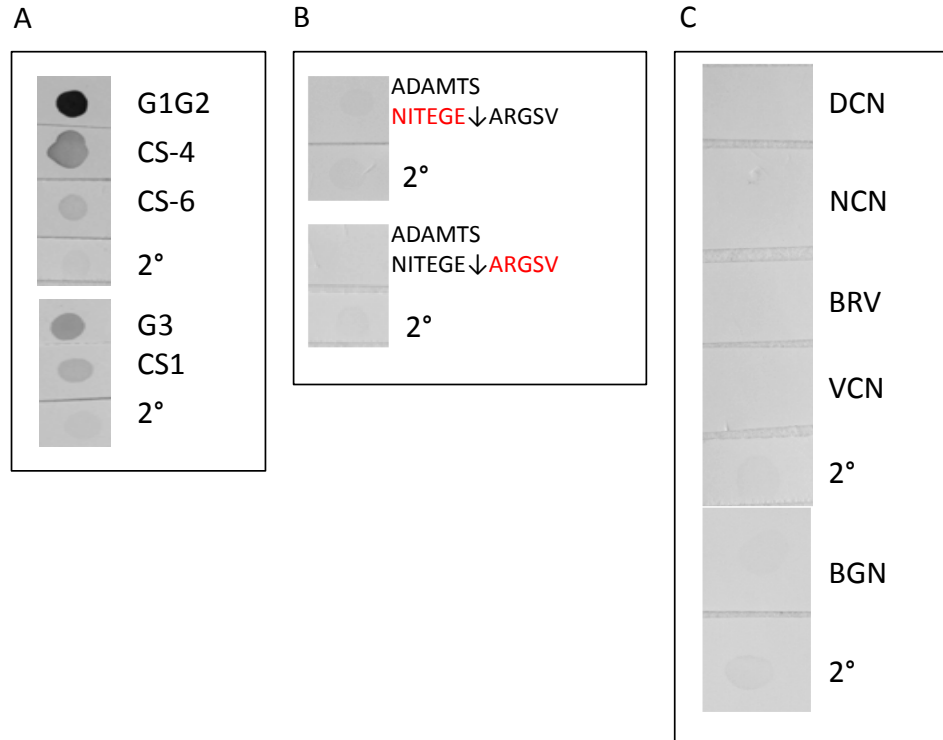


Figure 5 Dot blots of Sigma aggrecan A1960 Lot 089K4071 to assess composition, integrity, and purity.

A. Sigma A1960 contains all aggrecan domains. Detection of: G1-IGD-G2 domain, chondroitin 4-SO₄, chondroitin 6-SO₄, G3 domain, and chondroitin sulfate region 1. 2° is the secondary antibody alone (either goat anti-mouse or rabbit anti-goat, as appropriate). **B.** Sigma A1960 does not contain aggrecanase (ADAMTS) degradation products. Neo-epitope antibodies recognize the cleavage products highlighted in red. **C.** Sigma A1960 does not contain the other hyaluronan-binding proteoglycans, decorin, or biglycan. DCN, decorin; NCN, neurocan; BRV, brevican; VCN, versican; BGN, biglycan.

Examination of the Interaction of Intact *Borrelia* with Aggrecan

Physiologically relevant interactions with aggrecan would be expected to be mediated by surface exposed or secreted spirochetal proteins. Fluorescence confocal microscopy was used to examine aggrecan interactions with intact *Borrelia*. *B. burgdorferi* (strain B31) were grown to late log phase and fixed with 2% paraformaldehyde to stabilize the membranes. To identify *Borrelia* with intact membranes, the bacteria were incubated with a monoclonal antibody against a periplasmic flagellar protein (FlaB) which would only be exposed by membrane rupture (Fig. 6A, left panel and 4B, upper left panel). Spirochetes without FlaB staining are intact and relevant for examination. Auto-fluorescence in the red channel was minimal and is shown in Fig. 6A (right panel). Spirochetes were markedly labeled with fluorescent aggrecan (Fig. 6B, upper right panel). The merge of the images of FlaB and aggrecan-labeled spirochetes (Fig. 6B, lower right panel) demonstrates fluorescently labeled aggrecan bound to intact spirochetes as evidenced by aggrecan staining in the absence of flagellar protein staining.

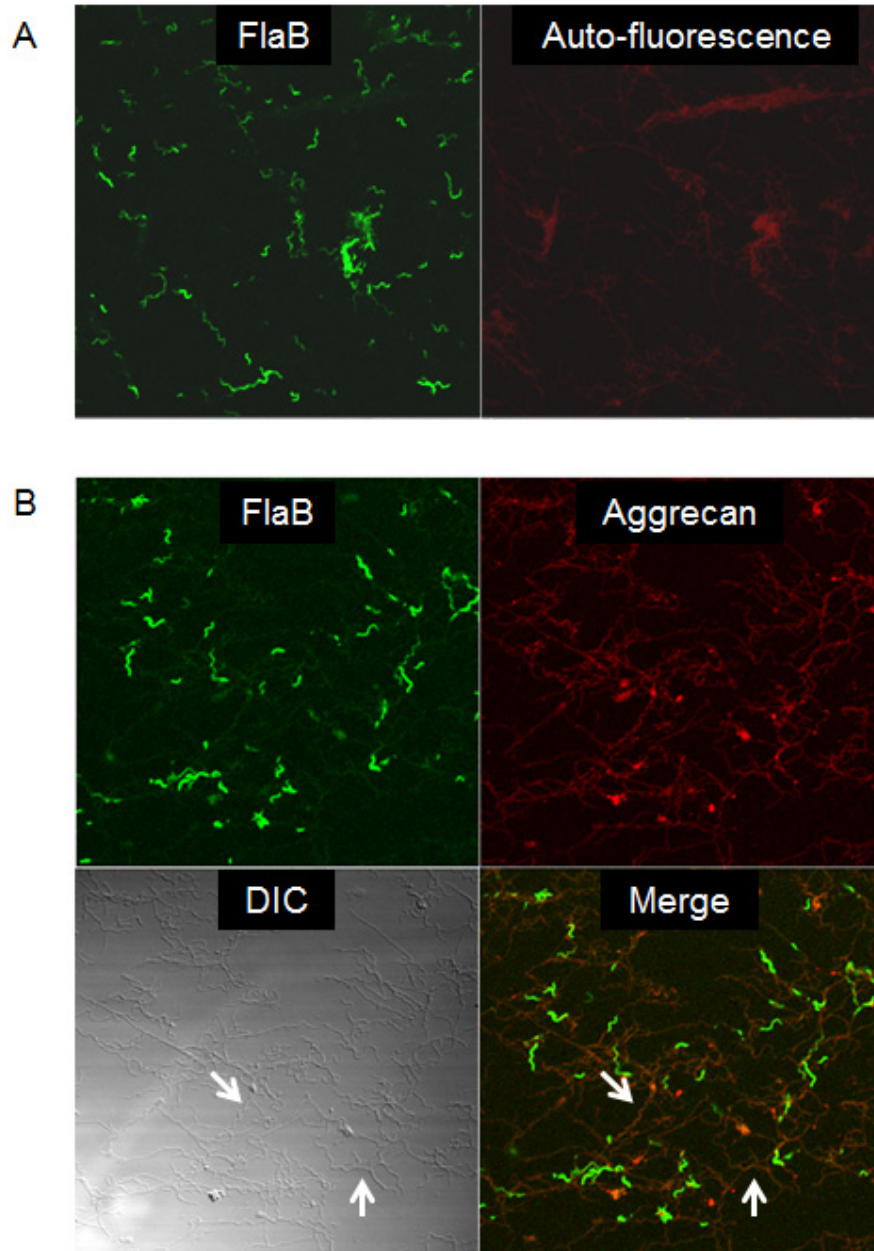


Figure 6 Confocal microscopy of intact *B. burgdorferi* with fluorescently labeled aggrecan

A. Control showing labeling of disrupted borrelial membranes (left) and minimal auto-fluorescence in the red channel (right). **B.** Double staining of *Borrelia*. FlaB staining identifies *Borrelia* with ruptured membranes (green, upper left) and labeled aggrecan binding to *Borrelia* (red, upper right). The merge of the images shown in the upper panels is shown below. Arrows highlight intact *Borrelia* with surface bound aggrecan. DIC, differential interference contrast image of *Borrelia* within the same field.

Identification of *B. burgdorferi* Aggrecan-Binding Proteins

B. burgdorferi aggrecan-binding proteins in borrelial lysates were identified using aggrecan affinity chromatography and mass spectrometry (MS) of proteins specifically enriched in the presence of aggrecan. Purified bovine articular cartilage aggrecan (Sigma) was immobilized on commercially available affinity chromatography supports. In initial experiments using agarose-based supports, it was observed that numerous proteins bound to the support itself. Given the structural similarities between agarose and the chondroitin sulfate GAGs on aggrecan, the agarose-based system was inadequate to distinguish specific interactions. Therefore, in subsequent experiments, aggrecan was immobilized on a polyacrylamide-based chromatography support.

Agarose-Based Affinity Chromatography Using *B. burgdorferi* Clonal Isolate A3

Initial experiments used an agarose-based aggrecan affinity column coupled with 1.5mg aggrecan. Borrelial lysates were incubated with the column and unbound proteins were removed by extensive washing with 1M NaCl. Interacting proteins were eluted with a pH 2.8 glycine buffer. Eluted aggrecan-binding proteins were probed with pooled sera from five Lyme disease patients with a history of Lyme arthritis to identify aggrecan-binding proteins expressed during human disease. Even after 50 column volumes of 1M NaCl, numerous proteins were eluted in these early experiments (data not shown). Given the large number of basic proteins in the borrelial genome and the acidic nature of

the aggrecan GAG chains, 5M NaCl was included as a second wash buffer for subsequent experiments to disrupt non-specific electrostatic interactions.

The immunoblot in Figure 7 demonstrates that several borrelial proteins bound to the aggrecan column with sufficient avidity to be retained through 1M and 5M NaCl washes. Proteins (90, 75, 47, 40 and 30kD) were eluted with pH 2.8 glycine buffer. The 30, 18 and 16kD proteins were absent in the final 1M NaCl wash and predominantly eluted with 5M NaCl.

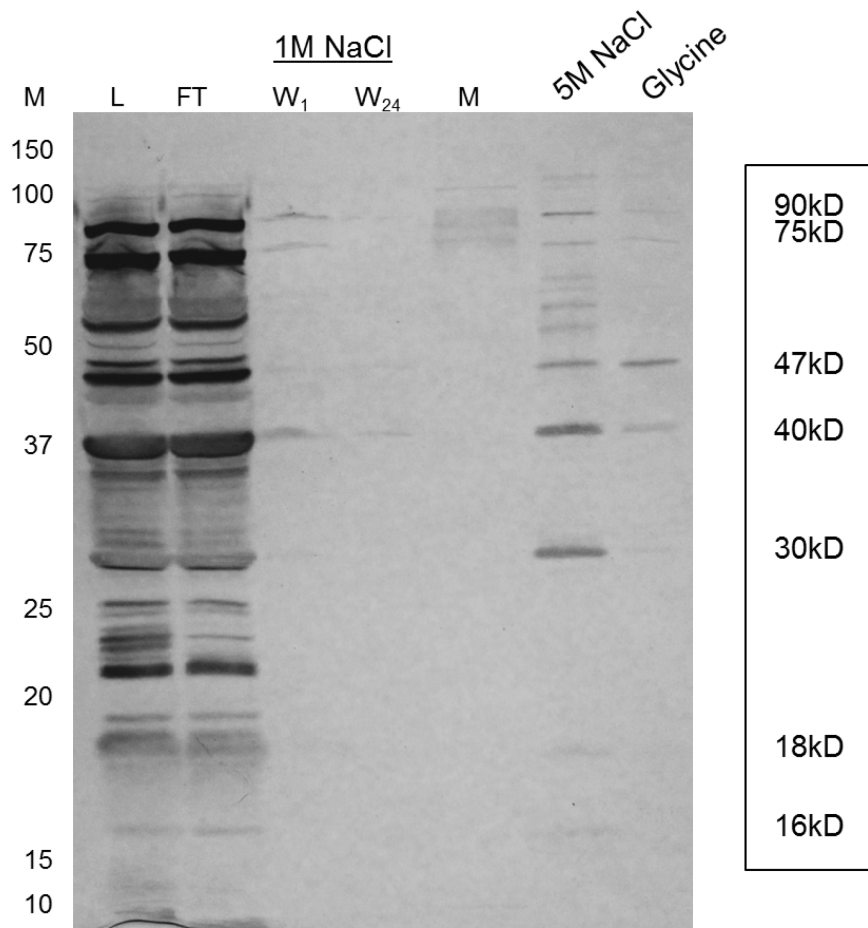


Figure 7 *B. burgdorferi* B31 A3 proteins eluted from an agarose-based aggrecan column

Immunoblot of fractions from an aggrecan affinity chromatography column incubated with borrelial lysates. Fractions were separated by SDS-PAGE electrophoresis and transferred to a nitrocellulose membrane. The membrane was probed with pooled sera from 5 Lyme disease patients identifying immunogenic aggrecan-binding proteins. L, load; FT, flow through; W₁, first wash; W₂₄, 24th column volume wash which was dialyzed and concentrated prior to loading; numbers in subscripts are fractions collected. Inset lists proteins enriched in the glycine elution.

The 1.5mg aggrecan column contained roughly 150µgs of aggrecan core protein. In an attempt to increase the yield of borrelial aggrecan-binding proteins, subsequent experiments were performed with a larger 4mg aggrecan column. Another experiment was performed using a 1.2L *B. burgdorferi* A3 culture divided evenly between the 1.5mg and 4mg columns. No additional aggrecan-binding bands were seen using the larger column; however increased yield was obtained (Fig.8). Six proteins in the 4mg elution lanes (75, 47, 40, 30, 18 and 16kD) were enriched to levels greater than what was observed in the final 1M NaCl wash and were considered significant in this experiment. Eluates were electrophoresed, the gel was stained with Coomassie blue and visible protein bands were excised. None of the proteins in the glycine elution were abundant enough to be visualized. The 30kD and 16kD protein bands were excised from the 5M NaCl sample and OspA (30kD) and truncated OspB (16kD) were identified by tryptic-peptide mass fingerprinting via tandem mass spectrometry.

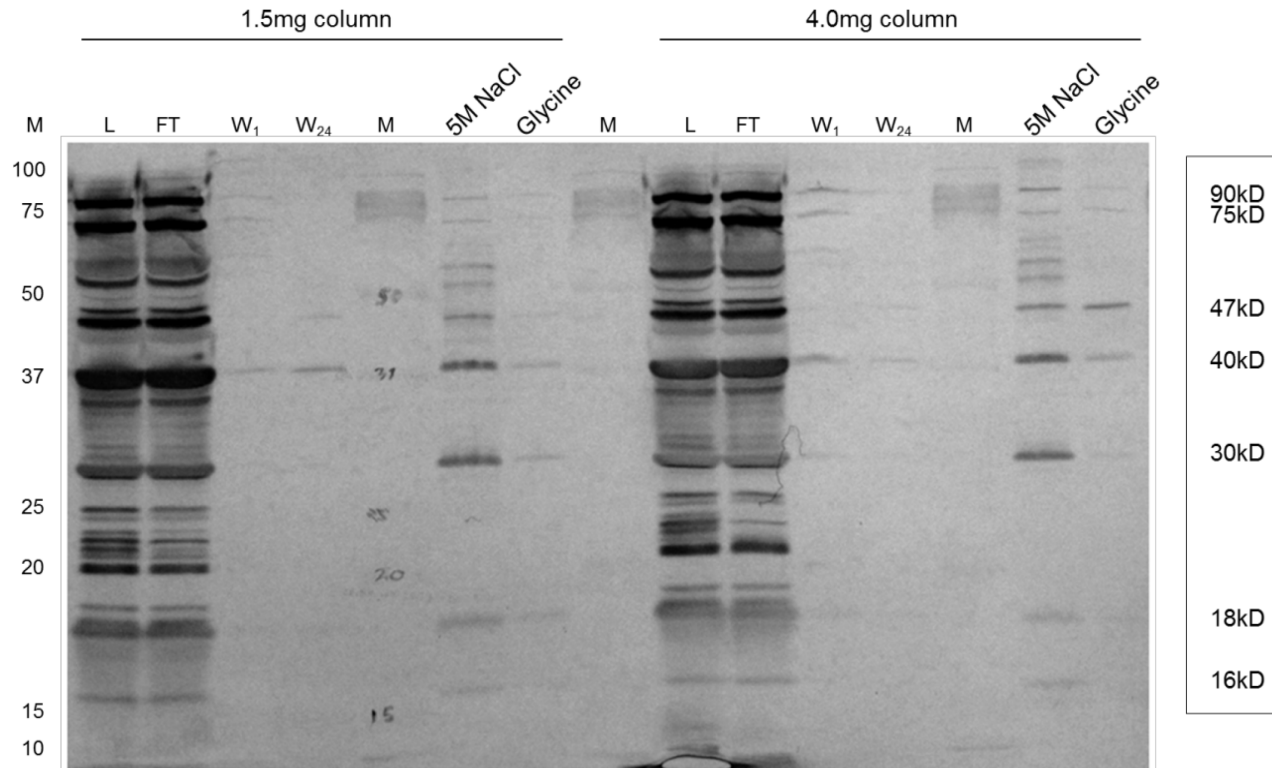


Figure 8 *B. burgdorferi* B31 A3 proteins eluted from two agarose-based aggrecan columns.

Comparison of clonal *B. burgdorferi* B31 A3 lysates divided evenly and applied to a 1.5mg and a 4.0mg aggrecan column. Immunoblot was probed with pooled sera from 5 Lyme disease patients identifying immunogenic aggrecan-binding proteins in the glycine elution lanes. M, molecular weight markers; L, load; FT, flow through; W₁, first wash; W₂₄, 24th column volume wash which was dialyzed and concentrated prior to loading; numbers in subscripts are fractions collected. Inset lists proteins enriched in the glycine elution.

Agarose-Based Affinity Chromatography Using Non-Clonal *B. burgdorferi*

Initial affinity chromatography experiments were performed with clonal *B. burgdorferi* B31 A3 derived from the parental strain of MI B31. The clonal strain differs from the parent population in some respects that could be relevant to aggrecan binding. Specifically, the A3 clone expresses a truncated OspB gene product that runs at ~18kD instead of the normal 34kD protein. A band of approximately 18kD was observed in earlier experiments. Additionally, MI-A3 is known to be missing cp9, a 9.3Mb circular plasmid containing 11 genes. This strain retains infectivity and is routinely used due to its ability to be transformed more readily than the parent strain (Elias *et al.*, 2002). However, these observations raised the concern that this clonal population and other clones within B31 might express proteins that react differently with aggrecan. Consequently, the experiment was repeated with the non-clonal parent strain. Additionally, a chondroitin sulfate elution step was added. Approximately, 90% percent of the mass of aggrecan is comprised of keratan and chondroitin sulfate (CS) glycosaminoglycans. Incubating the column with purified CS types A and C could release proteins that react with this part of aggrecan. Differential elution of proteins was observed. As seen in Figure 9, three of the interacting proteins were eluted more effectively with the CS-A/C GAGs (90, 75 and 40kD). The altered mobility of the lower molecular weight proteins in the GAG elution might be explained by GAG binding. The 5M NaCl elution released greater amounts of the 52kD, 42kD and 30kD proteins. The most intriguing finding of this experiment was the retention of the 47kD protein and, though faint, a 20kD protein through

both the GAG and 5M NaCl elutions. Retentions of these proteins through these stringent wash conditions is suggestive of strong interactions with the aggrecan protein backbone.

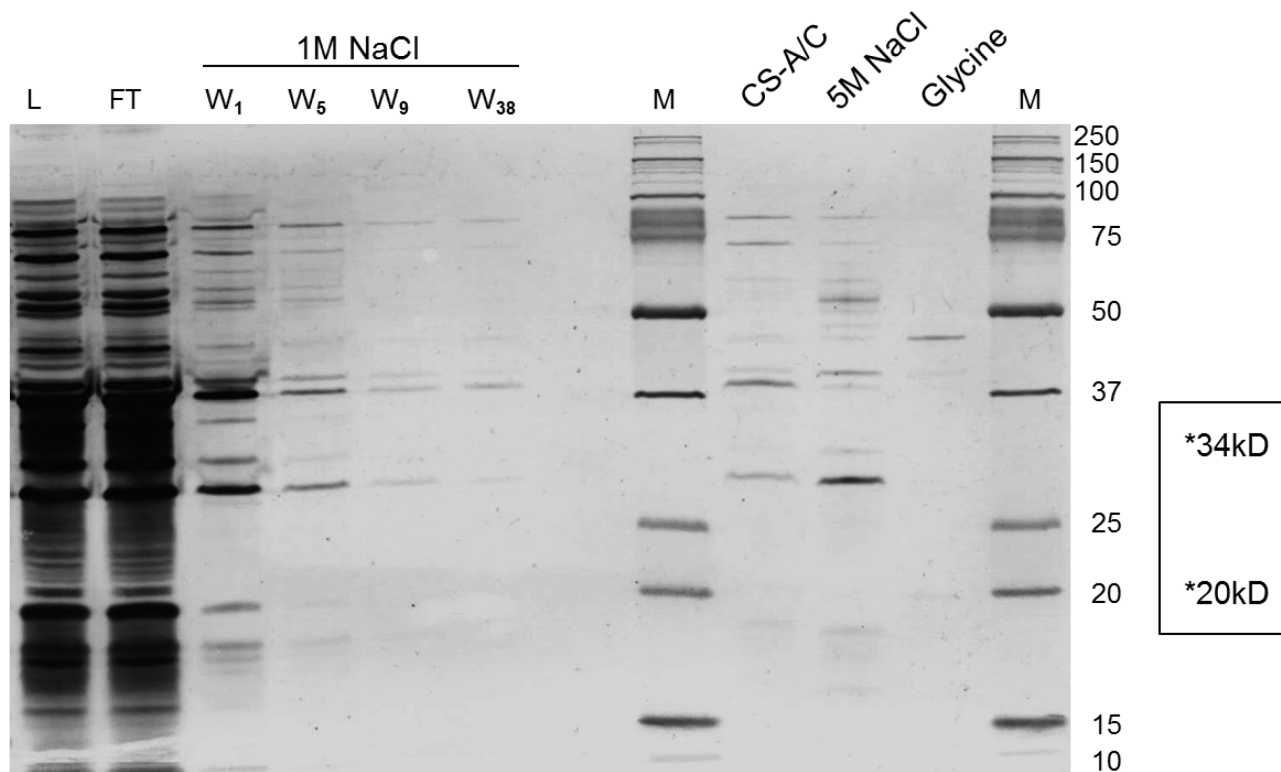


Figure 9 Immunoblot of aggrecan-binding proteins within lysates of non-clonal *B. burgdorferi* B31
 Immunoblot of proteins within lysates of non-clonal *B. burgdorferi* B31 differentially eluted from the 4mg agarose-based aggrecan column. Blot probed with pooled sera from 5 Lyme disease patients identifying immunogenic aggrecan-binding proteins. L, load; FT, flow through; W₁, first wash; W₃₈, 38th column volume wash which was dialyzed and concentrated prior to loading. CS-A/C, chondroitin sulfate A/C elution; *, proteins not previously observed in lysates of clonal *B. burgdorferi* A3.

As with earlier experiments, Fig. 9 demonstrates a characteristic pattern of proteins eluted differentially from the aggrecan column. However, twelve bands were seen in the 5M NaCl lane with the A3 clone (Fig.8) whereas 14 bands were seen in the 5M NaCl elution with the parental strain B31. The 2 additional bands had apparent molecular masses of 20kD and 34kD, the latter presumably full length 34kD OspB (Fig.9).

An additional experiment was performed with even more stringent conditions. The wash and elution conditions of the previous protocol were modified in three respects: 1) a gradient of NaCl concentrations was used as 5M NaCl may have eluted specifically bound proteins; 2) a non-ionic detergent (0.5% Triton X-100) was added to all wash buffers; and 3) the concentration of CS-A/C in the GAG elution was increased so that there were 2 soluble competitor molecules for every column GAG. As can be seen in Figure 10, many proteins were retained until the glycine elution. The final 1M NaCl/TX wash lane (W₂₁₅) is clear except for the faint trace of the 40kD band. The smeary appearance of the wash lanes may be due to Triton X-100 micelles which formed after the proteins were concentrated.

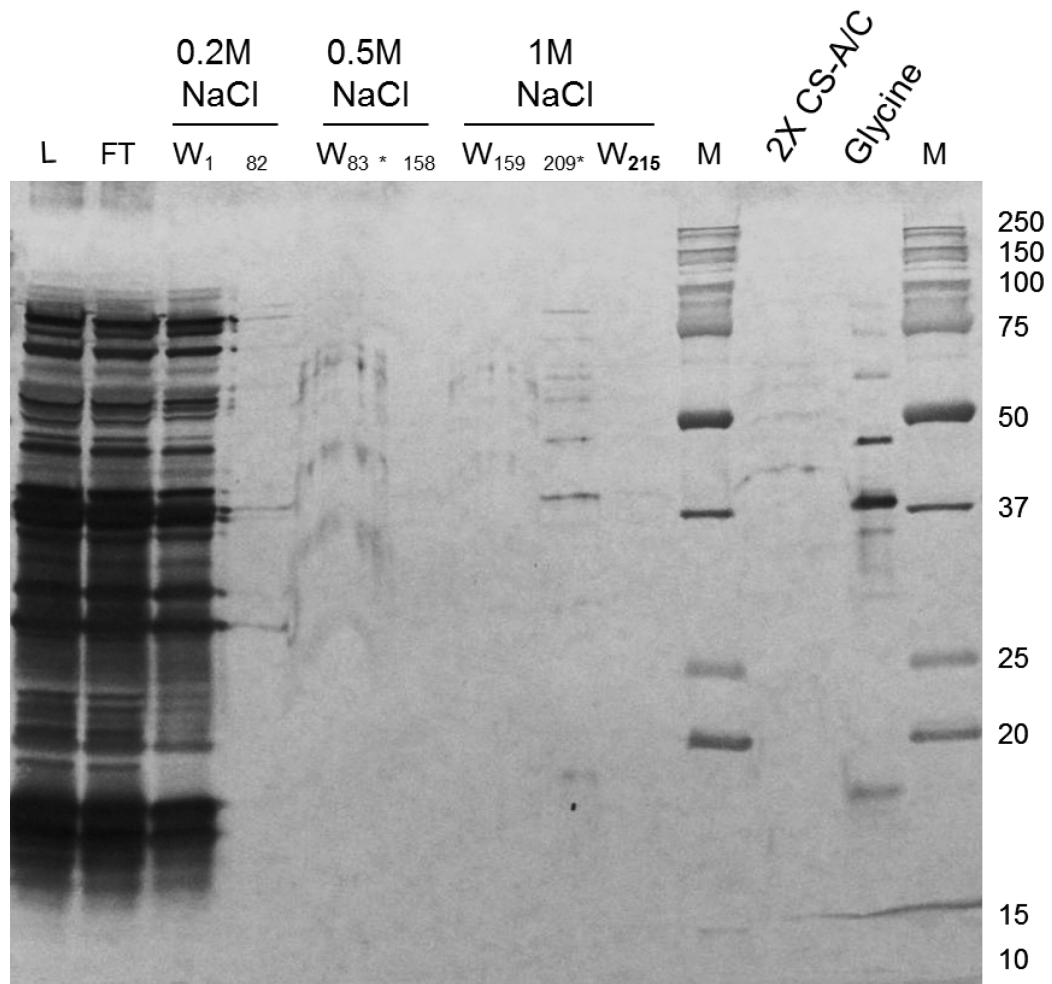


Figure 10 Immunoblot of non-clonal *B. burgdorferi* B31 aggrecan-binding proteins retained under stringent wash conditions on an agarose-based affinity column

Immunoblot demonstrating immunogenic aggrecan-binding proteins retained through high salt, Triton-X 100 and chondroitin sulfate A and C wash conditions. L, load; FT, flow through; W₁, first wash; W₂₁₅, 215th column volume wash; numbers in subscripts are fractions collected samples, samples from 0.5M and 1M NaCl washes were dialyzed against water and concentrated prior to loading; *, 30 min incubations with agitation. Blot probed with pooled sera from 5 Lyme disease patients.

Given the very characteristic and reproducible pattern of aggrecan-binding proteins observed in these experiments, proteins from the elution lanes shown in Figures 9 and 10 were electrophoretically separated and the protein bands were excised and sent for protein identification by mass spectrometry.

Parameters used for protein identification were a 2 peptide minimum and a 95% peptide identity resulting in a 99% protein identity. Eleven proteins were identified: DnaK, GroEL, OppA-II, Enolase, HtrA, FlaB, GAPDH, OspB, OspA, NapA and truncated OspB (Fig.11). Unfortunately, the 90kD band was not visible on the Coomassie gel and could not be sent for identification.

The protein-aggrecan interactions identified by affinity chromatography are potentially aggrecan specific. Aggrecan, a polyanion, reproducibly retained 6 anionic borrelial proteins with isoelectric points below the pH 7.5 used for these experiments. Thus, these proteins would have carried a net negative charge and electrostatic repulsion might have been expected. Their repeated presence may indicate hydrophobic interactions.

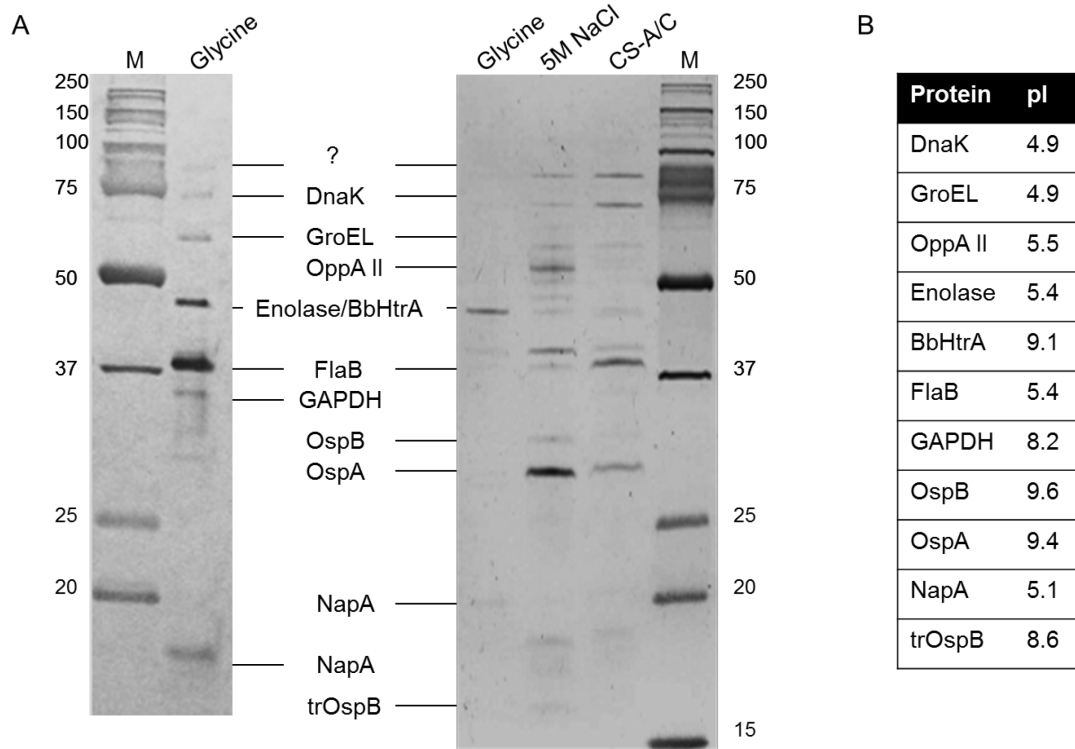


Figure 11 Aggrecan-binding proteins identified by tandem mass spectrometry
A. Immunoblots of aggrecan-binding proteins within lysates of non-clonal *B. burgdorferi* B31 which were eluted from aggrecan columns and sent for LC MS/MS analysis. Left panel, proteins present in the glycine elution after stringent wash conditions (Fig. 10). Right panel, differentially eluted proteins (Fig. 9)
B. Proteins, and their respective isoelectric points (pI), identified within the lysates.

Polyacrylamide-Based Affinity Chromatography of Non-Clonal *B. burgdorferi*

The experiments described to this point had several limitations. First, comparing the structures of agarose, chondroitin sulfate and keratin sulfate, it was conceivable that borrelial GAG-binding proteins were binding to both the agarose bead and to the aggrecan GAG side chains. Consequently, I sought to verify that the interaction was specific to aggrecan and not to the agarose chromatography matrix. A polyacrylamide chromatography support was chosen to test this hypothesis and coupled with 4mg aggrecan. Eluates were compared to those obtained with the agarose-based column. Additionally, comparisons were made between proteins binding to the supports alone and those retained only in the presence of aggrecan. Finally, the reliance on immunodetection to visualize interacting proteins excluded the detection of potential interactions between aggrecan and non-immunogenic borrelial proteins. Therefore, electrophoresed eluates were silver stained to visualize all interacting proteins.

Another large prep of *B. burgdorferi* was grown to late log phase, washed to remove media components and sonicated as before (details available in the Methods section). Half of this preparation was applied to the aggrecan column and half to a column containing the agarose support alone. The columns were processed in tandem and samples were run on duplicate gels, one of which was stained with silver and the other was transferred to nitrocellulose and probed with sera from LD patients. The results are shown in Figure 12.

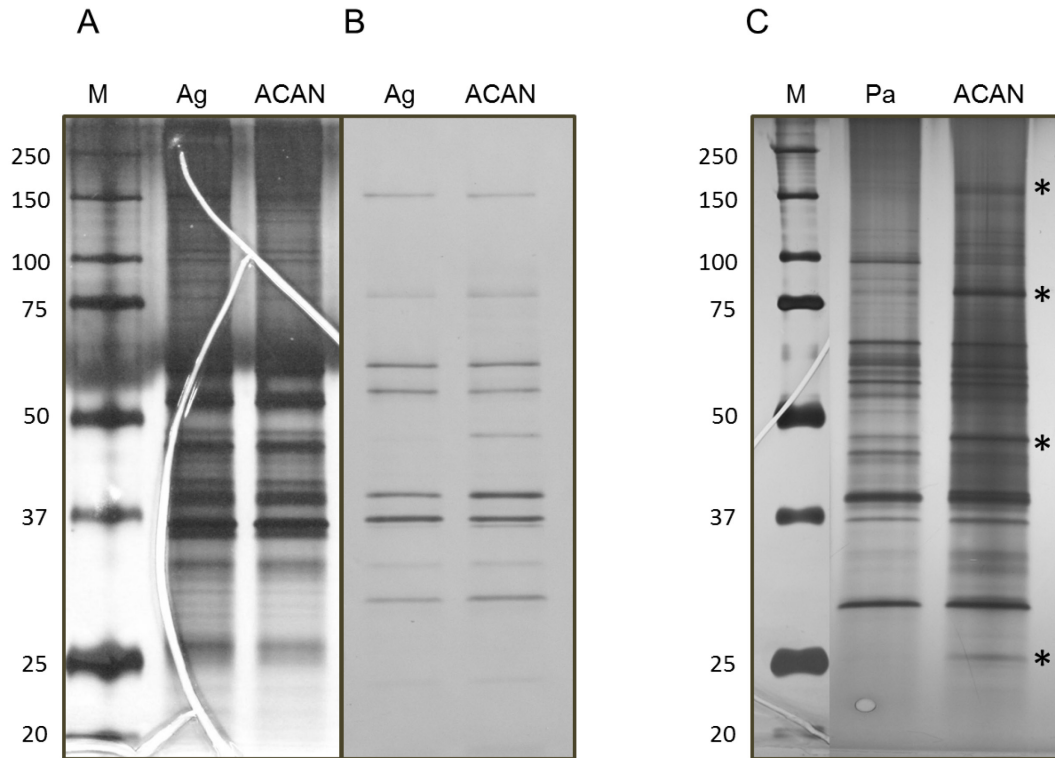


Figure 12 Affinity chromatography demonstrating *B. burgdorferi* aggrecan binding proteins

A. Comparison of silver stained borrelial lysate proteins eluted from agarose support columns with 1M NaCl. **B.** Western blot comparison of samples from A. A 47kD immunogenic protein is enriched in the presence of aggrecan. Western blot probed with pooled sera from 5 Lyme disease patients identifying immunogenic aggrecan-binding proteins. **C.** Comparison of silver stained borrelial lysate proteins eluted from polyacrylamide support columns with 1M NaCl. * Asterisks highlight four proteins eluted from aggrecan on both supports. Ag, agarose support; Pa, polyacrylamide support; ACAN, support containing aggrecan; M, molecular weight marker.

Silver stained eluates from the agarose support alone (Fig. 12A, Ag lane 2) and the support with aggrecan (Fig. 12A, ACAN lane 3) appeared to be identical. Immunodetection revealed a 47kd band that was specifically enriched in the presence of aggrecan (Fig. 12B, ACAN lane 2).

Numerous proteins also bound non-specifically to the polyacrylamide support (Fig. 12C, Pa lane 2). However, in contrast to proteins visualized by silver staining of the eluates of the agarose-based columns (Fig. 12A), several proteins were enriched only in the presence of aggrecan on the polyacrylamide-based columns (150, 75, 47, 25kD) (Fig. 12C, ACAN lane 3).

Comparison of the results of these two different chromatography supports demonstrated that these four candidate aggrecan adhesins bound to aggrecan on both types of columns (compare Fig. 12A, ACAN lane 3 with Fig. 12C, ACAN lane 3). This observation was strongly suggestive of specific interactions between aggrecan and the 150kD, 75kD, 47kD and 25kD borrelial proteins.

Mass Spectrometric Identification of *B. burgdorferi* Aggrecan-Binding Proteins

To identify proteins binding only in the presence of aggrecan, bands were excised from both types of supports and both in the presence and absence of aggrecan. As before, the proteins were electrophoretically separated and the bands excised and sent for mass spectrometric analysis. The following criteria were applied to the data set: the protein had to be enriched by interaction with aggrecan on *both* supports and at least 2 unique peptides needed to be identified with a minimum of 95% peptide identity resulting in greater than 99% protein

identity. Two proteins met those criteria, periplasmic serine protease DO (BB0104, BbHtrA) (Fig. 13 and Table 3) and pfs-2 protein (BB0588, Borrelial glycosaminoglycan binding protein, Bgp). The mass spectrometry peptide fragmentation data and protein coverage for these proteins are shown in Figure 14 (BbHtrA) and Figure 15 (Bgp). In addition to these mass spectrometry results, BbHtrA was twice before identified by MS in earlier independent experiments using the agarose-based aggrecan column.



Figure 13 Proteins with a minimum of 2 unique peptides identified in eluates from chromatography columns. Sixteen proteins were identified in eluates from agarose (AL) and polyacrylamide (UL) columns in the presence (AL/UL AC) or absence of aggrecan. Only two borrelial proteins were enriched in the presence of aggrecan on both types of chromatography support; periplasmic serine protease DO (BbHtrA) and pfs-2 protein (Bgp). Scaffold 3.0 representation of MASCOT data.

Table 3 Summary of BbHtrA and Bgp mass spectrometry data

Aggrecan-binding proteins, identified by LC-MS/MS, specifically enriched on both agarose and polyacrylamide affinity columns and only in the presence of aggrecan.

Protein Identified	kDa	Gel slice identified in	# of unique peptides	% Coverage
BbHtrA	53	Ag-ACAN-47	2	5
		Pa-ACAN-47	13	26
Bgp	29	Ag-ACAN-25	5	34
		Pa-ACAN-25	4	25

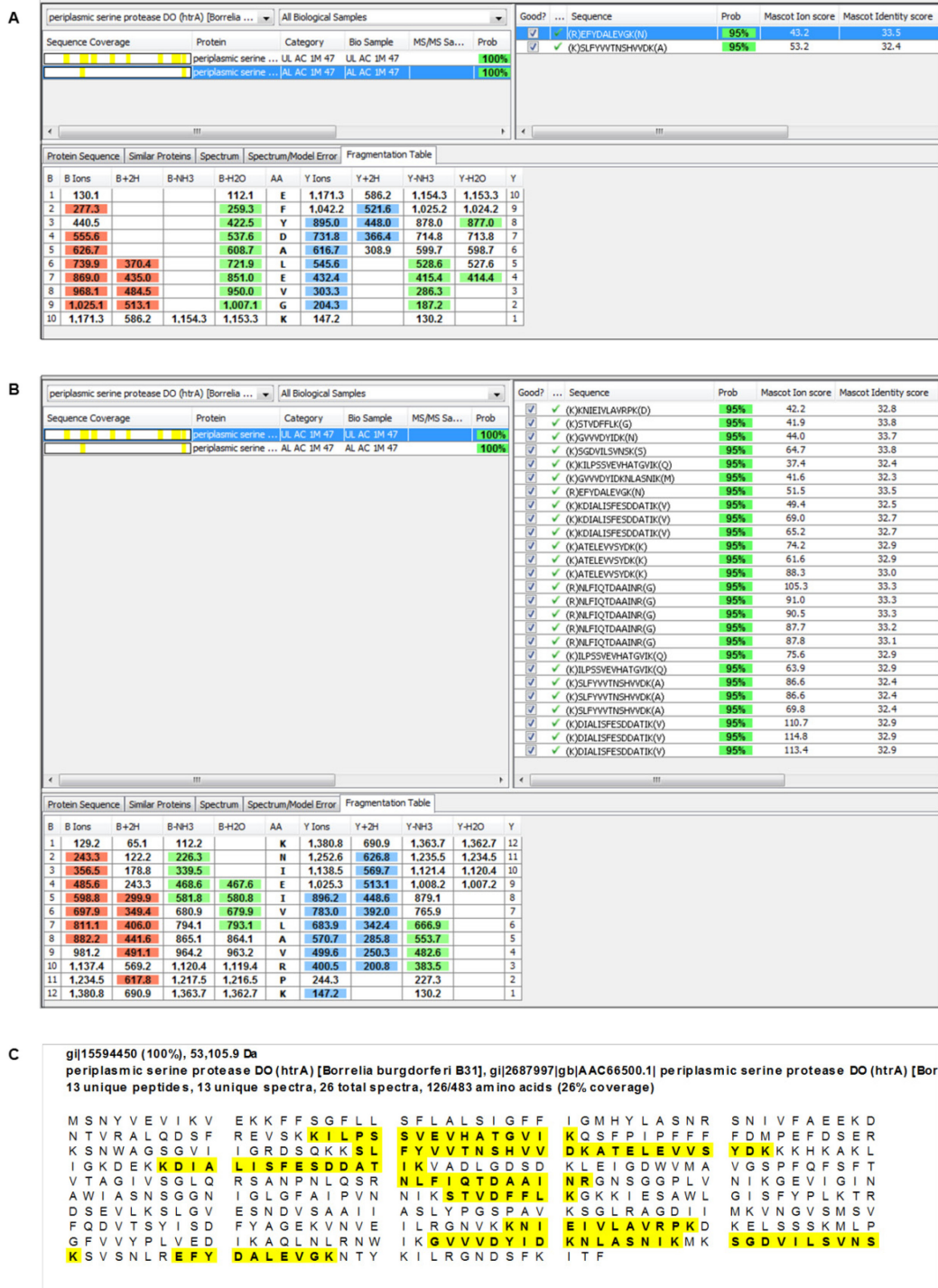


Figure 14 Mass Spectrometry data for BbHtrA identified in aggrecan affinity chromatography eluates

BbHtrA sequence coverage, sequences obtained, and fragmentation tables for peptides in the trypsin digest of the 47kD gel slices from **A.** agarose-based aggrecan column and **B.** polyacrylamide-based aggrecan column. **C.** BbHtrA sequence showing peptide coverage. Scaffold 3.0 representation of MASCOT data.

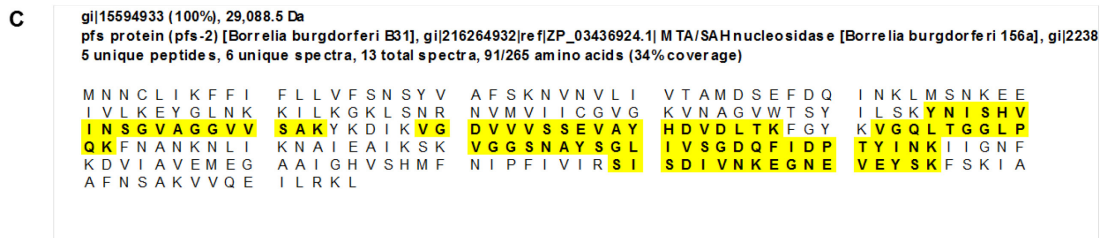
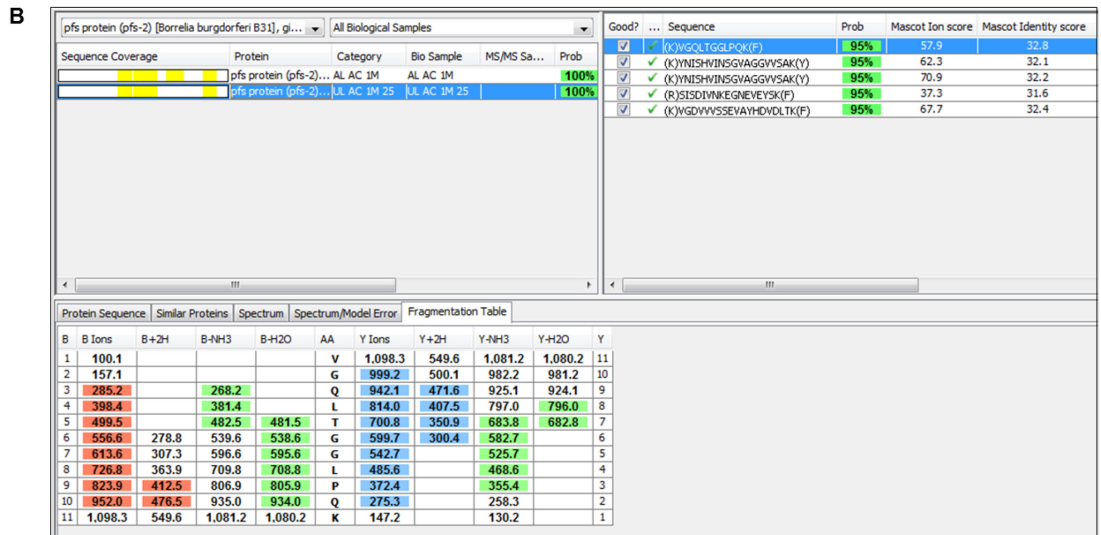
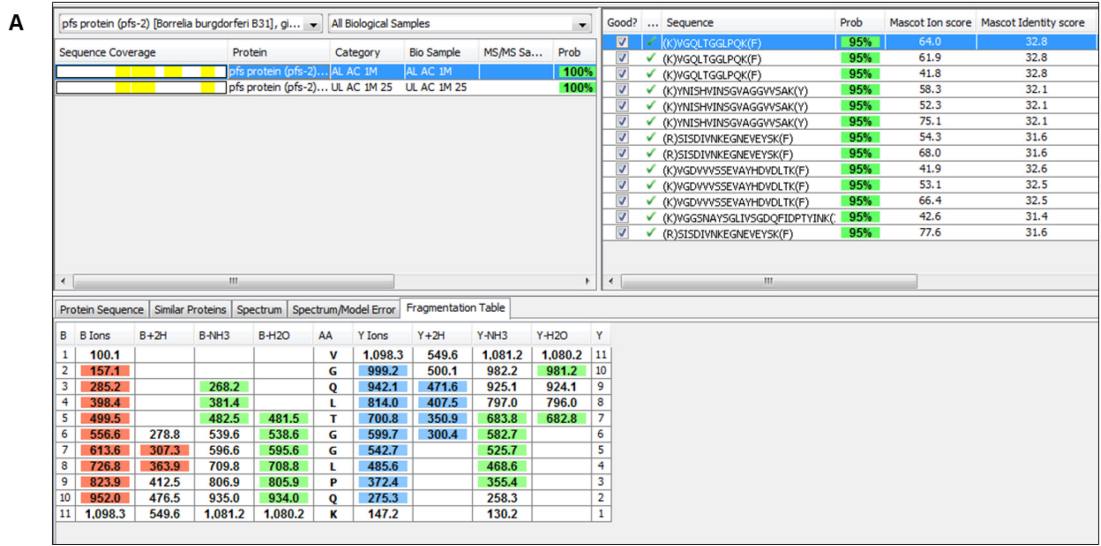


Figure 15 Mass Spectrometry data for Bgp identified in aggrecan affinity chromatography eluates

Bgp sequence coverage, sequences obtained, and fragmentation tables for peptides in the trypsin digest of the 25kD gel slices from **A.** agarose-based aggrecan column and **B.** polyacrylamide-based aggrecan column. **C.** Bgp sequence showing peptide coverage. Scaffold 3.0 representation of MASCOT data.

Bgp (BB0588)

Bgp has previously been described as a surface exposed GAG binding protein expressed during mammalian infection (246, 247). Bgp is a functional 5'-methylthioadenosine/S-adenosyl homocysteine nucleosidase (MTA/SAH or MTAN) (248). These enzymes are used by bacteria for methionine salvage and the generation of quorum sensing autoinducers. The *B. burgdorferi* genome encodes two additional MTANs: plasmid encoded MtnN and chromosomal pfs-1. These enzymes are attractive targets for antimicrobials since humans utilize two enzymes for methionine salvage which are unaffected by MTAN inhibitors. Cornell *et al.* examined the borreliacidal effects of several of these inhibitors and concluded that structure-based optimization could be used to develop new antibiotics targeting Bgp to treat Lyme disease (249). A Bgp knockout was fully infectious suggesting that, while this gene has been maintained in the borrelial genome, its dual activities are redundant (249). Saidac *et al.* later established that the Bgp knock out mutant required a larger infectious dose than wild type and that the pathogen load was reduced 10 fold in all tested mouse tissues (250). To date, Bgp is the only known secreted (251) and surface localized MTAN. Bgp, like enolase and GAPDH in other bacteria, seems to have adopted moonlighting functions as an adhesin that helps this organism persist in its mammalian host.

BbHtrA (BB0104)

B. burgdorferi HtrA has yet to be characterized. (A description of HtrA proteases is included in Chapter 4). The gene for BbHtrA (BB0104) lies on the

megabase chromosome (239). The full sequence gives a predicted molecular mass of 53kDa and cleavage at the putative signal sequence is expected to produce a 48kDa product. This is consistent with the observed mass of ~47kDa and with the protein being identified in that band by MS.

Using a heparin affinity column, BB0104 was identified as a 47kDa heparin binding protein isolated from a membrane extract of *B. burgdorferi* strain N40 (Leong *et al.*, 2000). However, membrane localization could not be confirmed using other methods. Detergent extracts of borrelial membrane proteins were eluted from a heparin column (agarose-support) and fractions were tested for their ability to agglutinate RBCs. Alternatively, borrelial detergent extracts were incubated directly with RBCs which were then washed and the bound proteins eluted with 2M NaCl. Comparison of the elution profiles of these approaches demonstrated the presence of a 47kD band which was identified as BbHtrA (BB0104). Parveen *et al.* then tried to establish surface localization by biotinylation. Borrelial surface proteins were biotinylated by incubating viable *Borrelia* with membrane impermeable sulfo-NHS-LC-biotin. Membrane proteins were then enriched by detergent extraction and incubated with RBCs. The 47kD band was not apparent in the biotinylated proteins eluted from the RBCs leading to the conclusion that BbHtrA is not surface localized in *B. burgdorferi* strain N40. An alternative interpretation is that biotinylation altered the interactions of the protein. Indeed, an altered elution profile is seen post-biotinylation which supports this hypothesis. For example, OspD, a known outer surface protein, is

missing in the biotinylated sample as is BB0366 which has been identified in both membrane and soluble protein fractions (246).

BbHtrA up-regulation has been observed in deletion mutants of two borrelial porins (P13 and P66) (252). The cargo of these porins is not currently known, however, their absence induced BbHtrA expression leading the author to conclude that deletion resulted a the stress response.

BbHtrA expression levels were down-regulated in a BosR-deficient (*Borrelia* oxidative stress regulator, BB0647) mutant strain suggesting that BB0104 transcription may be repressed by this transcription regulator (253).

During the course of these studies, Chamberland *et al.* (160) demonstrated that the human HtrA ortholog (HtrA1) degrades aggrecan. Hence, BbHtrA was the borrelial aggrecan-binding protein chosen for characterization.

Characterization of BbHtrA

In Silico Analysis of Homology between BbHtrA and Selected Orthologs

Comparative sequence analyses between *Borrelia burgdorferi* HtrA (BbHtrA), *Borrelia afzelii* HtrA (BaHtrA), and *Borrelia garinii* HtrA (BgHtrA) as well as other characterized orthologs (*E. coli* DegP, *E. coli* DegQ, *H. pylori* HpHtrA and human HtrA1) were performed by a variety of methods. Sequence comparisons obtained by utilizing the Basic Local Alignment Search tool (BLAST, protein-protein mode, http://blast.ncbi.nlm.nih.gov/Blast.cgi?CMD=Web&PAGE_TYPE=BlastHome) at the National Center for Biotechnology Information(NCBI) are shown in Table 4. Within *B. burgdorferi sensu lato*, there is over 95% sequence identity in HtrA proteases.

Multiple sequence alignment of these proteins (Fig.16 and Fig. 17, performed by Praline at <http://www.ibi.vu.nl/programs/pralinewww/>) demonstrates significant similarities within the catalytic domain.

Phyre2 (Protein Orthology/analogy Recognition Engine V 2.0, <http://www.sbg.bio.ic.ac.uk/phyre2/html/page.cgi?id=index>) was used to generate a structural model of mature BbHtrA. This model was then threaded into the monomer of the *E. coli* DegP dodecamer crystal structure (254) (Krojer, 2008; PDB code 2ZLE), also using Phyre2. The model was rendered using Polyview 3D (<http://polyview.cchmc.org/polyview3d.html>) and is shown in Figure 18.

Table 4 Homology of selected HtrA orthologs and homologs with BbHtrA determined by BLAST analysis

Ortholog	% Identity	% Similarity	E Value
BgHtrA	97	99	0
BaHtrA	95	97	0
DegP	35	53	1×10^{-67}
DegQ	33	54	5×10^{-67}
HpHtrA	32	52	1×10^{-57}
HtrA1	34	50	2×10^{-40}

Unconserved 0 1 2 3 4 5 6 7 8 9 10 Conserved

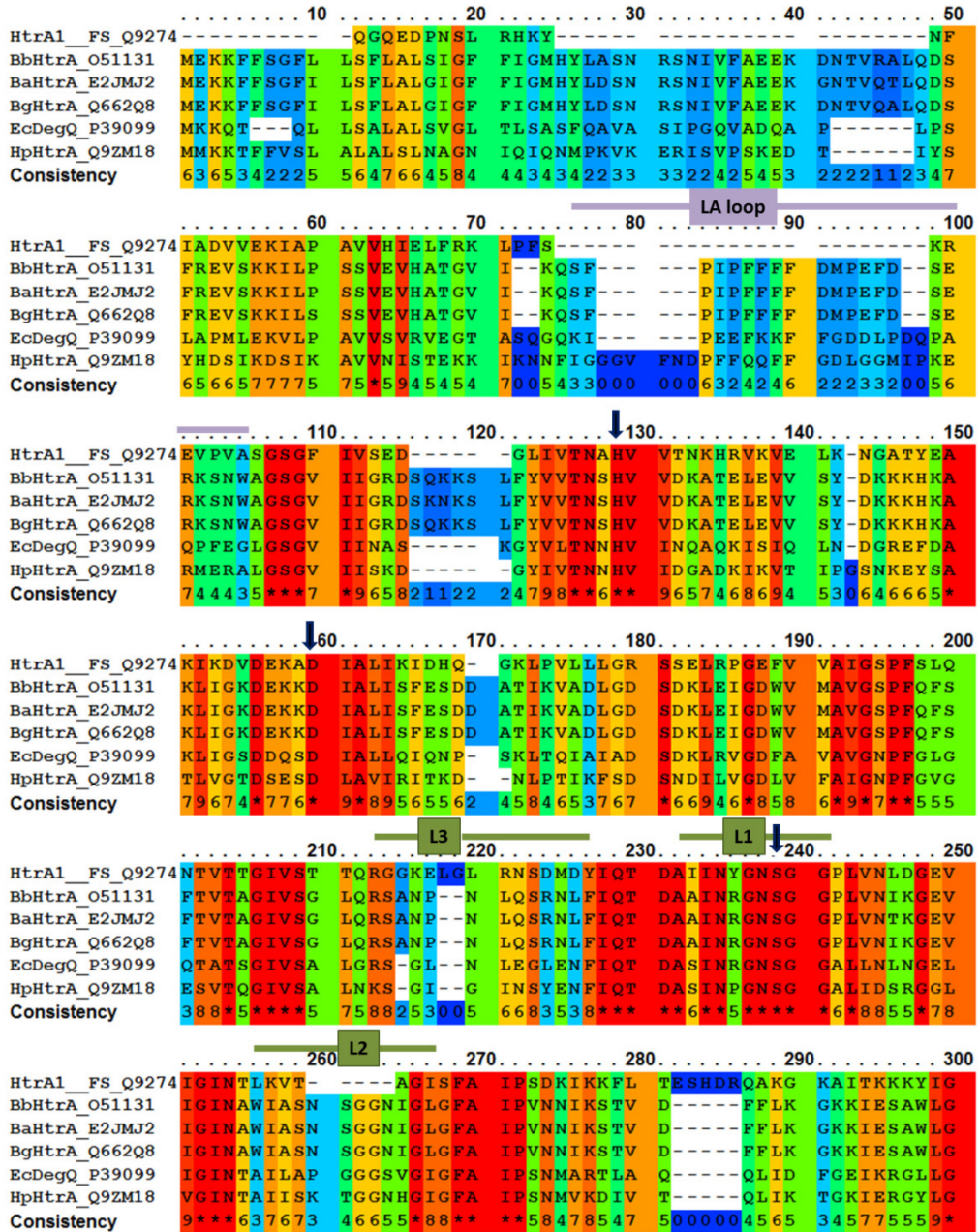


Figure 16 Protein Sequence Alignments of Amino Acids 1-300 for Selected HtrA Orthologs Demonstrating Conservation

Results are color-coded for amino acid conservation. Black arrows indicate catalytic triad residues. Unstructured loop regions (LA, L1-L3) are labeled. Protein labels include their Uniprot identifier codes. HtrA1 without the amino terminal regulatory (Follistatin, FS) domain is shown.

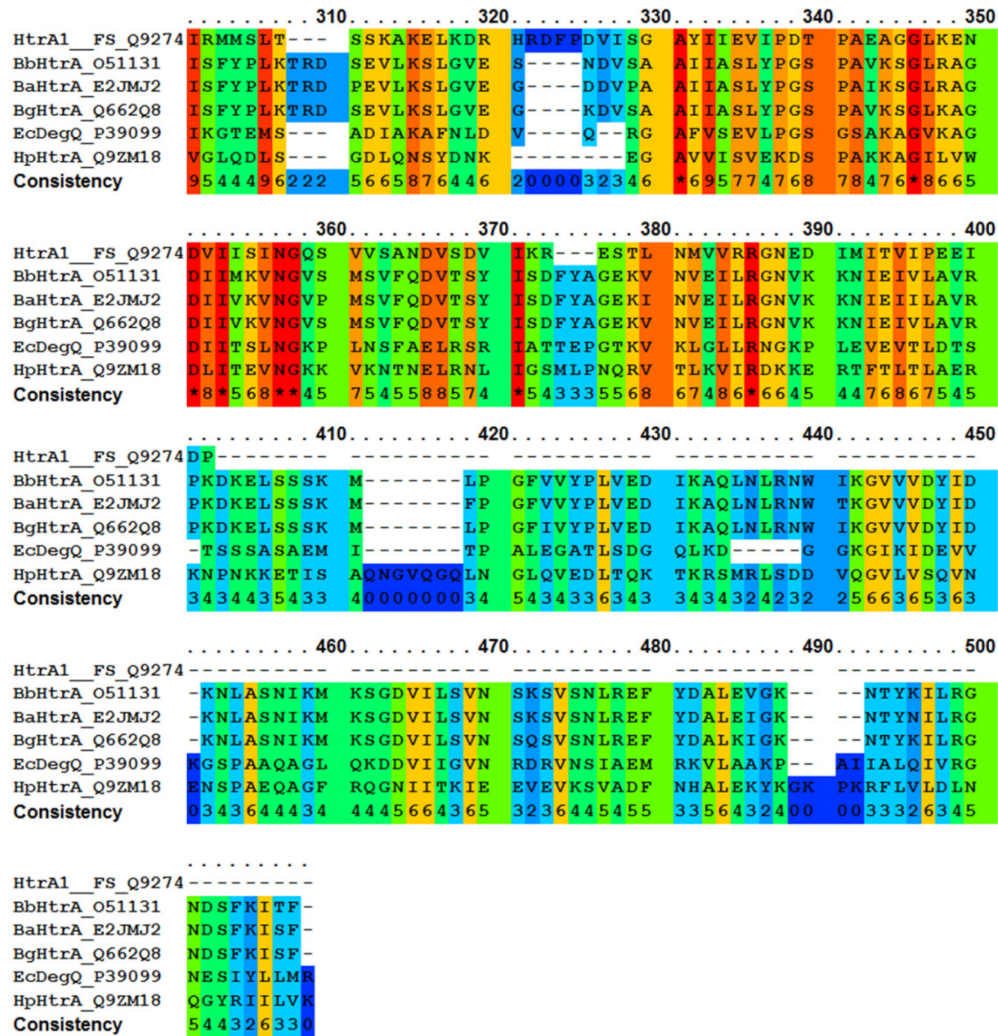


Figure 17 Protein Sequence Alignments of Amino Acid 301 to Carboxyl Terminus For Selected HtrA Orthologs Demonstrating Conservation
HtrA1 without the amino terminal regulatory (Follistatin) domains is shown. Results are color-coded for amino acid conservation.

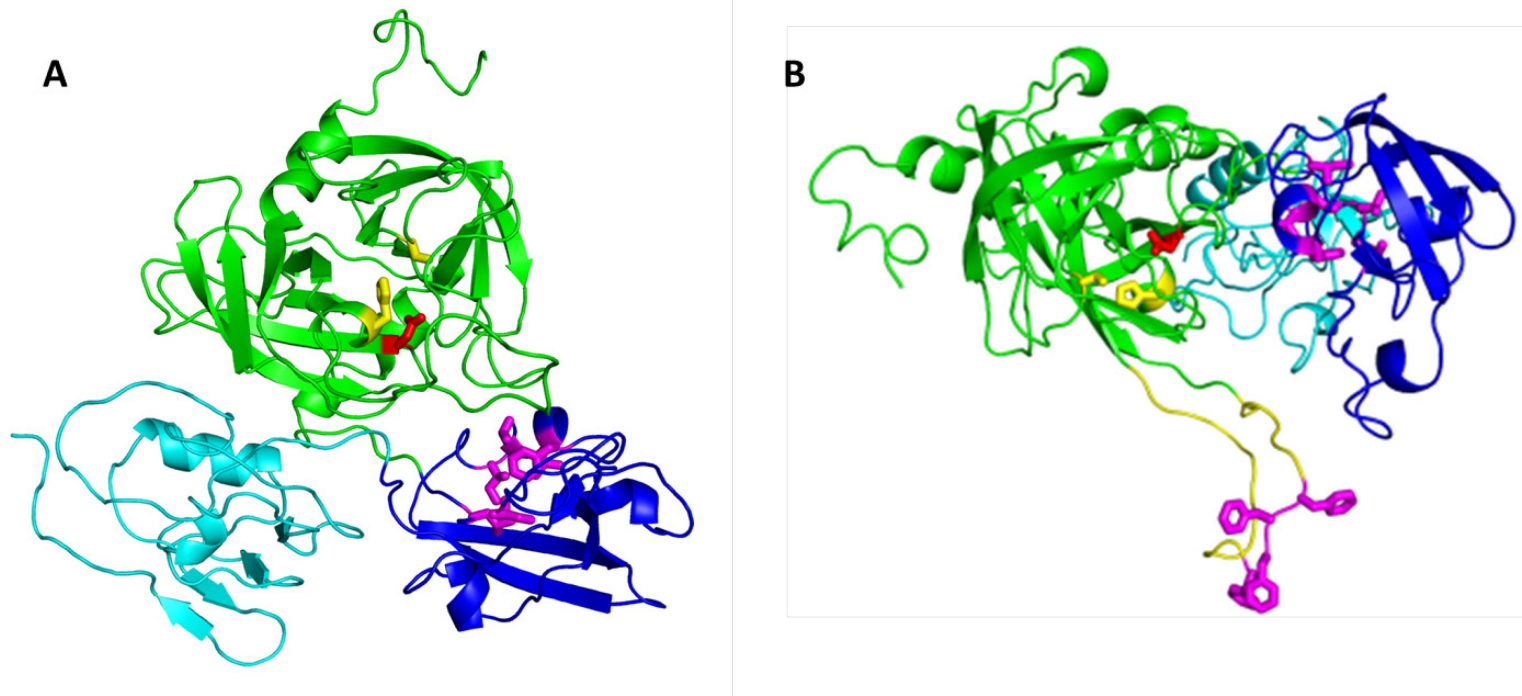


Figure 18 Structural model of BbHtrA

A. Rendering of the “underside” of BbHtrA looking into the catalytic site. Green, catalytic domain, triad His119 and Asp149 in yellow, Ser226 in red; blue, PDZ1 domain with magenta substrate binding cleft; cyan, PDZ2. **B.** Rendering of “side-view” rotated to show LA-loop. Coloring as in A with added LA-loop in yellow and self-cleavage site (Phe88-92) in magenta.

Expression and Purification of Recombinant BbHtrA and BbHtrAS226A

In silico analysis predicts that BbHtrA contains a signal peptidase signal sequence and a mature protein of 437 amino acids with an amino terminus beginning at amino acid 47 (EEKDNTVRAL; NCBI Reference Sequence: NP_212238.1, analyzed with Phobius and SignalP 3.0). Full length BbHtrA is expected to yield a protein of 53kD, while signal peptide removal reduces the expected size to 47kD. Experimental data confirms the removal of the signal peptide: Mass spectrometry analysis identified the 47kD protein in my studies as BbHtrA and Parveen *et al.* obtained an N' sequence of XEKDNTVRALQDFSR (246). Consequently, the carboxyl terminus was chosen for placement of a 6x-histidine tag to facilitate purification of recombinant BbHtrA. His-tagged wild type BbHtrA and an active site mutant (S226A) were generated using an *E. coli* system by a commercial supplier (GenScript USA, Inc.) (Fig. 19A, 19B). HtrA proteases are auto-catalytic (255, 256) yielding protein preparations with multiple bands. Recombinant wild type BbHtrA preparations also contain several bands (Fig. 19A) and Edman degradation identified these bands as BbHtrA degradation products (Fig. 19C). As expected, the catalytically inactive mutant purified as one band.

Contaminating *E. coli* lipopolysaccharide was reduced using a commercial LPS removal kit and residual LPS was measured by the Limulus Amoebocyte Lysate (LAL) method (BbHtrA, 1.4EU/ μ g, BbHtrA^{S226A} 0.099EU/ μ g; Lonza, Walkersville, MD).

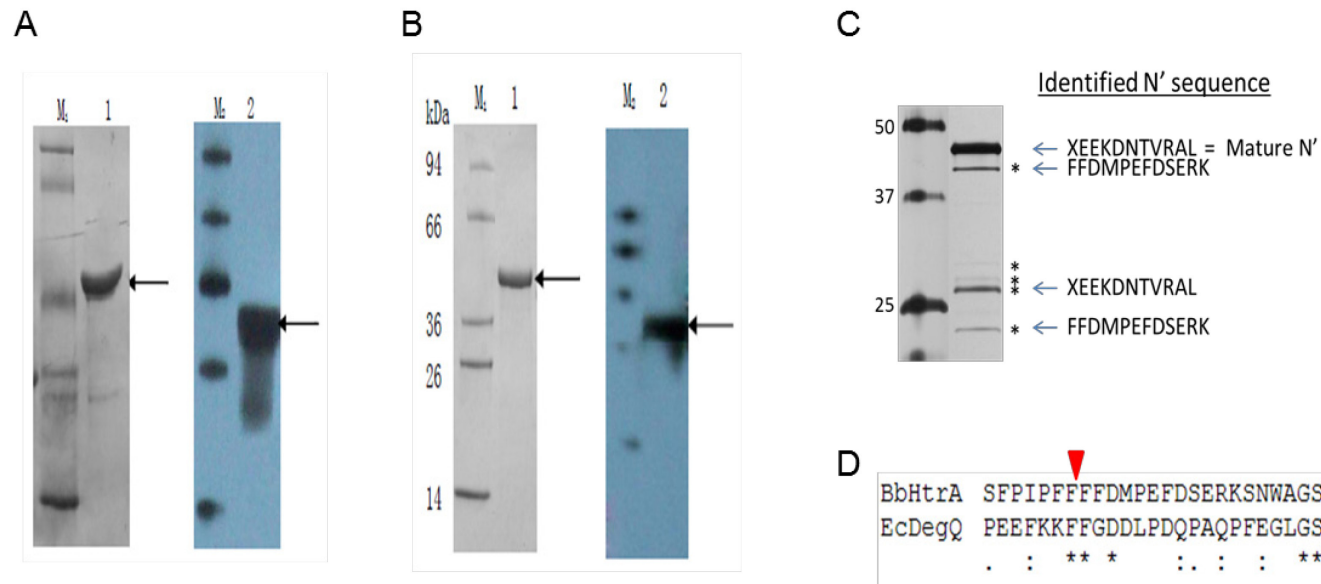


Figure 19 Purity of recombinant BbHtrA and BbHtrA^{S226A} and auto-degradation of BbHtrA
A. BbHtrA (3µg) and **B.** BbHtrA^{S265A} (2µg) as visualized by Coomassie stain of SDS-PAGE gels (left panels) and anti-his tag Western blots (right panels) (courtesy of GenScript USA, Inc.). **C.** Silver stain of SDS-PAGE gel showing the location of BbHtrA amino terminal signals obtained by Edman degradation. * BbHtrA self-cleavage products. **D.** ClustalW partial sequence alignment of BbHtrA and *E. coli* DegQ showing conserved paired phenylalanines.

BbHtrA is Auto-catalytic, Cleaving between Phe89-Phe90

To confirm the purity of recombinant BbHtrA and to identify the self-cleavage site, BbHtrA was subjected to amino terminal sequence analysis. Edman degradation of the major degradation products enabled identification of the cleavage site between Phe89 and Phe90 (Fig.19C). This cleavage removes 44 residues from the mature protein, resulting in a predicted ~5kD mass change which is consistent with the observed changes in the protein bands. It appears that the ~23 and ~28 kD bands, having the same amino terminal sequences as the full length and short forms, result from c-terminal processing at the same point in the protein. Comparison of the BbHtrA sequence aligned with that of *E. coli* DegQ demonstrates that these paired phenylalanines are conserved in the bacterial orthologs (Fig. 19D). Indeed, these residues are conserved in DegQ orthologs from many other organisms (149) suggesting their importance and the possibility that auto-degradation in DegQ orthologs generally arises from processing at this site.

Recombinant BbHtrA is Proteolytically Active

Casein was used as a model substrate to test the proteolytic activity of recombinant BbHtrA. Relative efficiency of the test conditions was determined by analysis of both the loss of the casein bands and of the full length 47kD BbHtrA band. HtrA proteases are allosterically activated by substrate peptides and degrade themselves once substrate has been exhausted (257). Thus the level of self-degradation may correlate to level of processed substrate.

Figure 20 demonstrates BbHtrA proteolysis of casein in all tested conditions. HtrA proteolytic activity in the presence of serine protease inhibitors has been described for *E. coli* (256), *H. influenza* (258) and *A. thaliana* (259) HtrA orthologs. BbHtrA activity was not inhibited by the serine protease inhibitor AEBSF (lane 4). A protease inhibitor cocktail (lane 5) containing the serine protease inhibitors AEBSF, aprotinin and leupeptin, as well as inhibitors for amino-peptidases (Bestatin), cysteine proteases (E64) and aspartic acid proteases (Pepstatin A) had minimal effect on the degradation of casein. However, BbHtrA self-degradation was decreased by the presence of the inhibitor cocktail suggesting that proteolytic activity was diminished (Fig. 20, compare protease band in lanes 3 and 5). BbHtrA, like other orthologs (256), was active in the presence of EDTA (Fig. 20, lanes 9-10) and in the presence of physiologic sodium chloride (lane 7). The addition of glycerol seemed to enhance BbHtrA activity (Fig. 20, lane 6), which can be explained either by stabilization of the protease or by prevention of casein aggregation thereby making it more accessible for processing. pH effects varied with the buffering agent; BbHtrA was more efficient at pH 8.0 in HEPES (Fig. 20, compare lanes 3 and 8) and at pH 7.5 in TBS (compare lanes 12 and 13). BbHtrA was also active in the commercial zymogram development buffer (50mM Tris pH 7.5, 200mM NaCl, 5mM Ca²⁺, 0.02% Brij-35) used for studies discussed later in this report (lane 14).

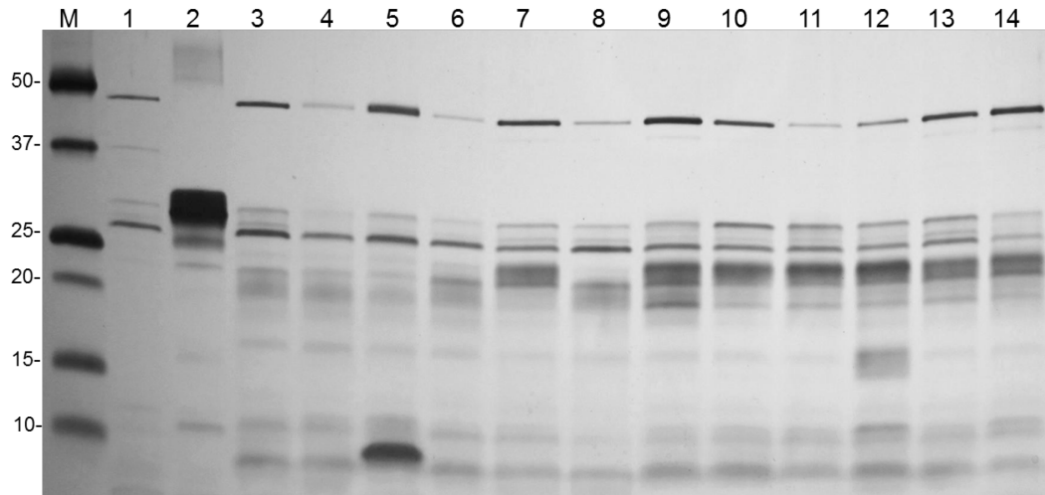


Figure 20 Analysis of BbHtrA proteolytic activity in various reaction conditions

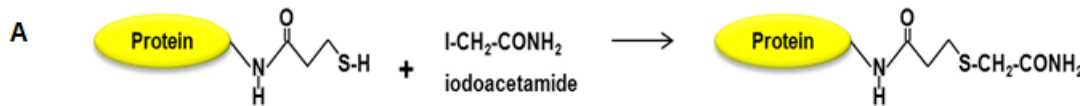
Silver stained SDS-PAGE gel of digestion products. M, marker; Buffer conditions for lanes 1-7 were 50mM HEPES, 5mM Ca^{2+} , pH 7.4.

1. Recombinant BbHtrA
2. Casein alone
3. Reaction products
4. + 1mM AEBSF
5. + 1X HALT
6. + 5% Glycerol
7. + 150mM NaCl
8. Increased to pH 8.0
9. Without Ca^{2+}
10. + 5mM EDTA
11. In PBS + 5mM Mg^{2+}
12. In TBS pH 7.5
13. In TBS pH 8.5
14. In Zymogram development buffer

Examination of Surface Exposure of BbHtrA

BbHtrA is Surface Exposed on Intact *B. burgdorferi*

Surface exposure of BbHtrA was analyzed by surface biotinylation of intact spirochetes. *Borrelia* were grown to late log phase and washed to remove media components. Washed spirochetes were incubated with a membrane impermeable, reducible and amine-reactive biotinylation reagent. Biotinylated borrelial surface proteins were separated by gel electrophoresis and the 47kD band was excised and sent for MS analysis (CSU, Proteomics Core Facility). During sample preparation for mass spectrometry, the biotin tag was removed by reduction with DTT and the proteins were alkylated with iodoacetamide. These modifications were expected to add 145.18 Daltons to amino termini and lysine residues of biotinylated sample proteins (Fig. 21A). Tryptic fragments were analyzed with this modification. BbHtrA was identified with the expected change in mass in the biotinylated samples (Fig. 21B), as were two other surface proteins that migrate at 47kD (BBK32 and VlsE). Two BbHtrA peptides were detected with peptide confidences of 76% and 73%, yielding a 92% confidence in the identification of BbHtrA in the biotinylated sample. As these peptide confidences are below what is required for complete certainty in BbHtrA surface exposure, a complementary approach was used.



Net tag = $\text{COCH}_2\text{CH}_2\text{SCH}_2\text{CONH}_2$ (1 hydrogen removed for the loss on the primary amine) = 145.18 Daltons

B

BbHtrA Biotinylated Peptide	%Peptide Identity	Amino Acids
(R)DSEVLKSLGVEGKDVSAIIASLYPGSPAVK(S)	76	290-322
(K)KNIEIVLAVRPK(D)	73	370-380
% Protein identity	92	

Figure 21 Surface biotinylation of BbHtrA

A. Expected mass change per BbHtrA primary amine. **B.** Unique BbHtrA peptides identified by mass spectrometry with the correct mass change.

BbHtrA is Diminished by Exposure to Proteinase K

Protease accessibility studies on intact spirochetes were used to examine the exposure of BbHtrA to proteinase K. *Borrelia* were grown to late log phase and incubated with either buffer alone or buffer containing proteinase K. Proteins separated by electrophoresis were transferred to a nitrocellulose membrane which was stained to reveal total protein (Fig. 22A). The membrane was then probed with antibodies for a known surface protein (OspA), a periplasmic protein (FlaB) and BbHtrA (Fig. 22B). As expected, the signal for OspA was lost and that of FlaB was retained after exposure to the protease. The BbHtrA signal was greatly diminished upon treatment, indicating that part of the cellular pool was accessible to proteinase K and part may be protected by intracellular localization.

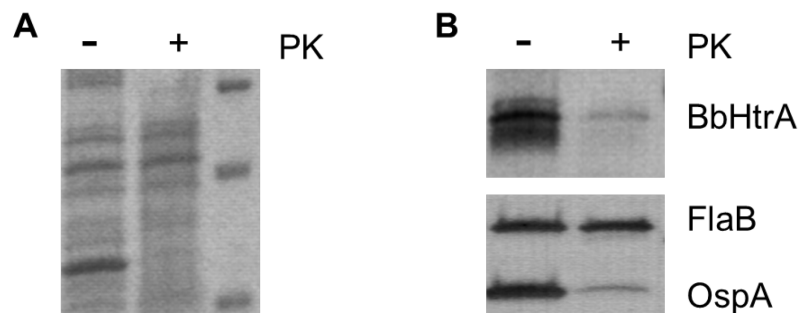


Figure 22 BbHtrA surface exposure on intact spirochetes assessed by sensitivity to proteinase K

A. Total protein stain (Ponceau) demonstrating equivalent loading levels and the efficacy of the proteinase K treatment. **B.** Western blots showing loss of surface protein signal (OspA), retention of periplasmic protein signal (FlaB) and diminished BbHtrA signal. Results representative of two independent experiments. PK; proteinase K.

BbHtrA is an Early Immunogenic Protein

BbHtrA was initially visualized in Western blots of the affinity chromatography eluates of aggrecan binding proteins. Pooled sera, from Lyme disease patients with a history of Lyme arthritis, were used to probe the eluates to highlight proteins recognized by the human immune system. To explore the specificity of the antibody response observed against BbHtrA, Western blot strips of purified recombinant BbHtrA^{226A} were probed with individual sera from IgG-seropositive Lyme disease patients and healthy controls (Fig. 23). Patients with both early and late Lyme disease symptoms were included. BbHtrA was strongly recognized by antibodies in several of the patient samples from both early and late disease. Because mammals express four HtrA proteins (HtrA1-4), potential cross-reactivity between antibodies against the mammalian orthologs and BbHtrA was examined using polyclonal antibodies specific for each of those proteins. These antibodies did not recognize BbHtrA, suggesting that the antibodies in the patient sera were specific to BbHtrA (Fig. 23).

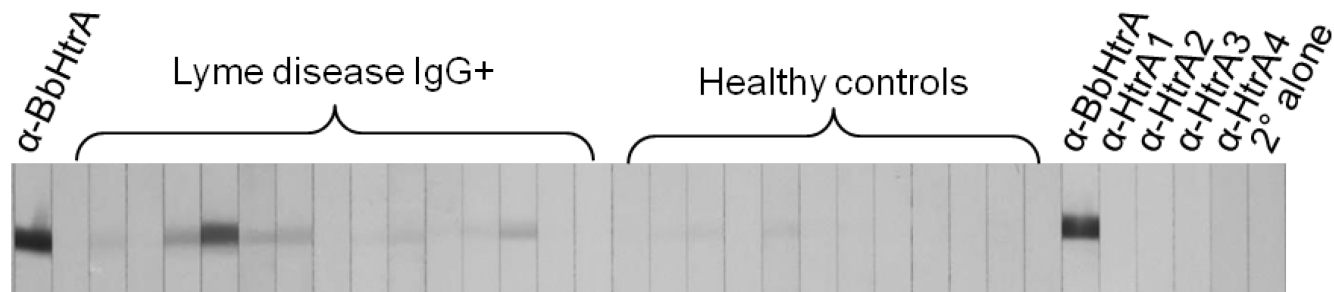


Figure 23 BbHtrA is an immunogenic protein expressed during human disease

Recombinant BbHtrA^{S226A} is recognized by IgG antibodies present in serum samples from Lyme disease patients. Antibodies against human HtrA1, HtrA2, HtrA3 or HtrA4 do not recognize BbHtrA^{S226A}.

HtrA is Conserved Among Lyme Disease Spirochetes

Sequence analysis indicated that HtrA proteases are highly conserved among the Lyme disease spirochetes (Table 4). To examine this experimentally, lysates of all of the major agents of Lyme disease - *B. afzelii* (strain ACA1), *B. garinii* (strain PKo) and *B. burgdorferi* (strain B31 MI) - were examined for the presence of HtrA.

Proteolytic activity was studied by zymography. Recombinant BbHtrA was proteolytically active against β -casein as evidenced by clearing around the protein band whereas BbHtrA^{S226A} was not (Fig. 24A, lanes 1 and 2). Within the lysates, proteases displaying caseinolytic activity migrated at similar positions to the recombinant BbHtrA bands (Fig. 24A, lanes 3-5). Proteolytic activity against gelatin was not observed for recombinant or lysate HtrAs (data not shown). All genospecies contained Western blot bands reactive with anti-BbHtrA peptide IgG antibodies (Fig. 24B), which likely represent the HtrA homologs.

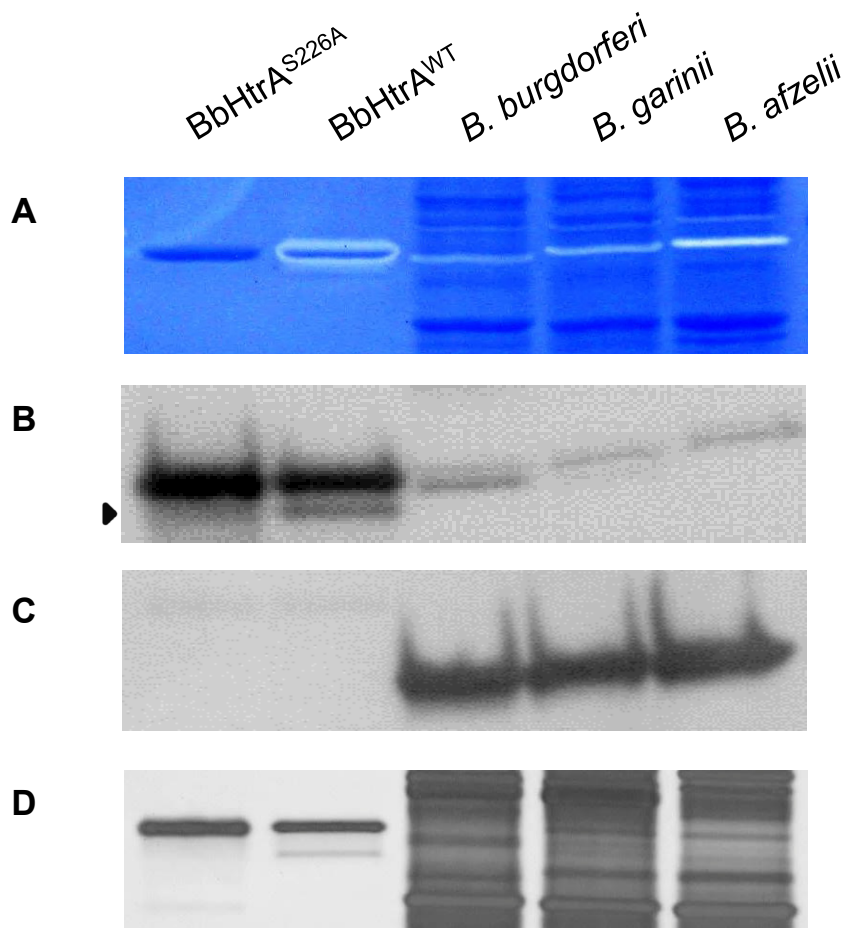


Figure 24 HtrA expression and activity is conserved among the major genospecies of Lyme disease spirochetes

Borrelial lysates (1×10^8 spirochetes) and recombinant proteins ($1 \mu\text{g}$) were electrophoresed in triplicate and examined for HtrA expression and activity. **A.** β -casein zymogram of borrelial lysates and recombinant proteins demonstrating casein degradation by catalytically active BbHtrA^{WT} and proteases within borrelial lysates. **B.** Immunoblot probed with anti-BbHtrA antibody demonstrating reactivity against recombinant BbHtrA and proteins within the borrelial lysates. Black arrowhead indicates recombinant BbHtrA^{WT} self-degradation product (Fig. 16C). **C.** Immunoblot probed with anti-flagellar protein antibody (FlaB) demonstrating relative loading of samples. **D.** Silver stain of borrelial lysates and recombinant proteins demonstrating total protein.

Characterization of the Interaction Between BbHtrA and Aggrecan

BbHtrA Degrades Recombinant and Native Aggrecan

BbHtrA has orthology with HtrA1 which is known to degrade aggrecan (160), fibronectin (215) and many other components of the extracellular matrix (161). Consequently, protease assays with BbHtrA were performed to examine the conservation of this activity. Although not required for BbHtrA proteolytic activity (Fig. 20, lane 9), the buffer chosen for these assays (50mM HEPES, pH 7.4, 5mM Ca²⁺) contained calcium for proper aggrecan folding (132).

Purified aggrecan was incubated with wild type BbHtrA, BbHtrA^{S226A}, ADAMTS-5, MMP-2 and HtrA1. BbHtrA cleavage of recombinant aggrecan generated three high molecular weight proteolytic fragments which migrated at ~85kd, ~60kd and ~50kd (Fig. 25A, lane 5). These fragments were dependent on the presence of proteolytically active BbHtrA since incubation of recombinant aggrecan (Fig. 25A, lane 1) alone or with the inactive mutant (Fig. 25A, lane 6) failed to generate these products. In an effort to determine the site of BbHtrA-mediated aggrecan cleavage, the reaction products were compared to other aggrecan degrading proteases (Fig. 25A).

BbHtrA also degraded native, fully glycosylated bovine aggrecan (Fig. 25B, lane 5). Again, this degradation required BbHtrA catalytic activity (Fig. 25B, lane 6). Interestingly, the lower molecular weight BbHtrA-generated aggrecan fragment appears to be a doublet, unlike that generated by HtrA1. Hoy *et al.* (215) also observed conserved substrate specificity yet distinct fragmentation of E-cadherin with degradation by HpHtrA and HtrA1.

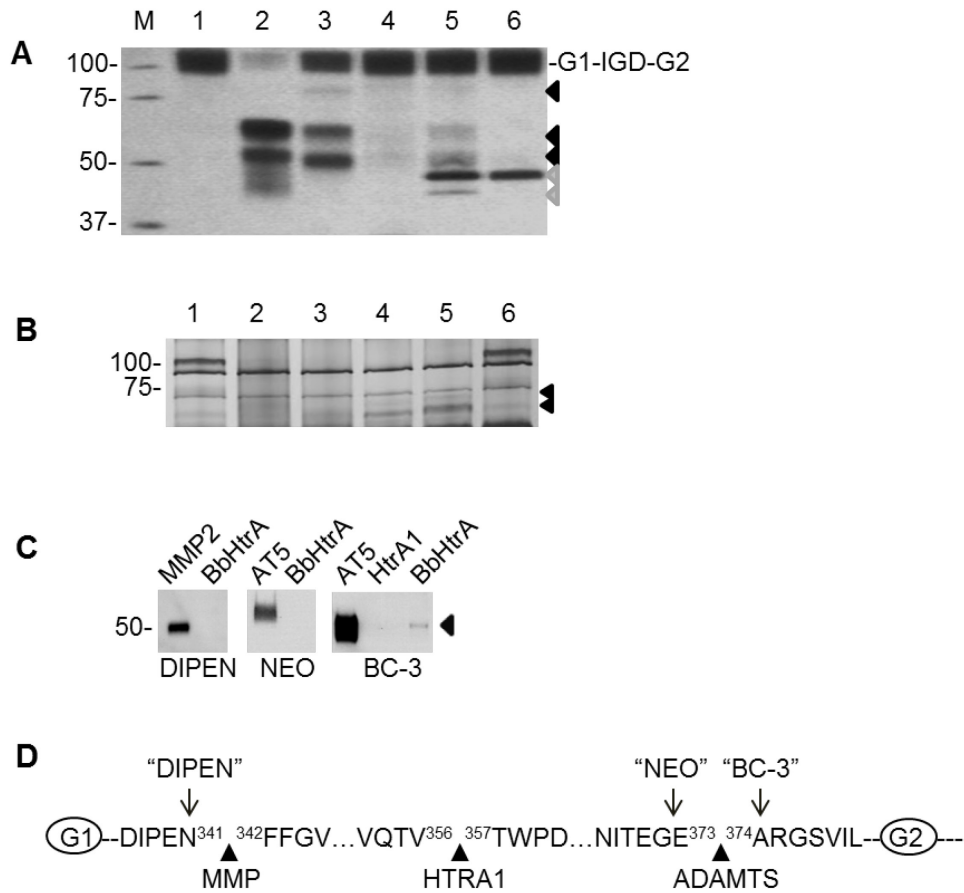


Figure 25 BbHtrA degradation of aggrecan

Aggrecan was incubated with recombinant proteases (4:1 molar ratio, as described in the Methods). **A.** Degradation of recombinant human aggrecan G1-IGD-G2. Digestion products were separated by SDS-PAGE and silver stained. 1, substrate alone; 2, ADAMTS-5; 3, MMP2; 4, HtrA1; 5, BbHtrA; 6, BbHtrA^{S226A}. Black arrows, BbHtrA cleavage products; gray arrows, protease. **B.** Degradation of native bovine aggrecan. Labels as in A. **C.** Immunoblots of recombinant aggrecan proteolytic fragments probed with neo-epitope antibodies. Arrow indicates BbHtrA-generated fragment recognized by the BC-3 antibody. **D.** Schematic of the aggrecan IGD showing the position of the pathologic cleavage sites, the proteases responsible for the scission (below) and the neo-epitope antibodies to the newly exposed termini (above).

ADAMTS-5, matrix metalloproteinase-2 and HtrA1 cleave aggrecan within the interglobular domain (IGD) between globular domains 1 and 2 (Fig. 25D). Comparison of the proteolytic fragments suggests that BbHtrA, likewise, cleaves within the IGD (Fig. 25A).

Cleavage of Aggrecan at the Aggrecanase 374ARGS Site

Cleavage within the aggrecan IGD by ADAMTS-5, MMP-2 and HtrA1 is very specific. Monoclonal antibodies to the newly exposed termini (“neo-epitopes”) have been developed to aid in the identification of the protease responsible for observed degradation. Currently, neo-epitope antibodies are commercially available to detect the activity of aggrecanases and MMPs (Fig. 25D). Given the similarity in the sizes of the aggrecan fragments generated by host proteases and BbHtrA, BbHtrA reaction products were probed with three of these antibodies. To examine cleavage at the MMP site, BbHtrA reaction products were probed with the DIPEN neo-epitope antibody. Cleavage at DIPEN³⁴² was not detected (Fig. 25C).

The “Neo” antibody, which recognizes the newly generated carboxyl terminus (³⁷³NITEGE) of aggrecanase-generated fragments, did not detect these fragments in the BbHtrA reaction products (Fig. 25C). A possible explanation for this observation is that BbHtrA, like HtrA1 (160), also cleaved at ³⁵⁶VQTV releasing the peptide fragment 357-373 containing the NITEGE neo-epitope. Unfortunately, the VQTV neo-epitope antibody is not yet commercially available to directly test this hypothesis. Quite unexpectedly, the amino terminus at the

aggrecanase site (³⁷⁴ARGS) was weakly identified by the BC-3 antibody in the BbHtrA-generated aggrecan fragments (Fig. 25C).

Amino terminal sequence analysis of the reaction products was pursued as a complementary approach. The major signals detected for all products were consistent with the amino terminus of recombinant aggrecan (²⁰VETSDHDNSLS) (Fig. 26A). The abundance of recombinant aggrecan amino terminal fragments was not completely unexpected since DegP/HtrA proteases are believed to primarily degrade substrates processively from the carboxyl terminus (203). However, the very reproducible and characteristic bands generated by BbHtrA suggest that the protease degrades aggrecan to a minimum of two distinct points within the IGD. One possible explanation is that the protease is halted by variable post-translational modifications of the aggrecan IGD. In support of this hypothesis, there are potential O-linked keratan sulfate attachment sites very near the proteolytic sites (Fig. 26B) and, at least in calf and steer aggrecan, 2/3 of these are modified with KS (260). There is 100% inter-species conservation of Asn368 at the aggrecanase site and glycosylation at Asn368 has a proposed regulatory role for aggrecanases (261).

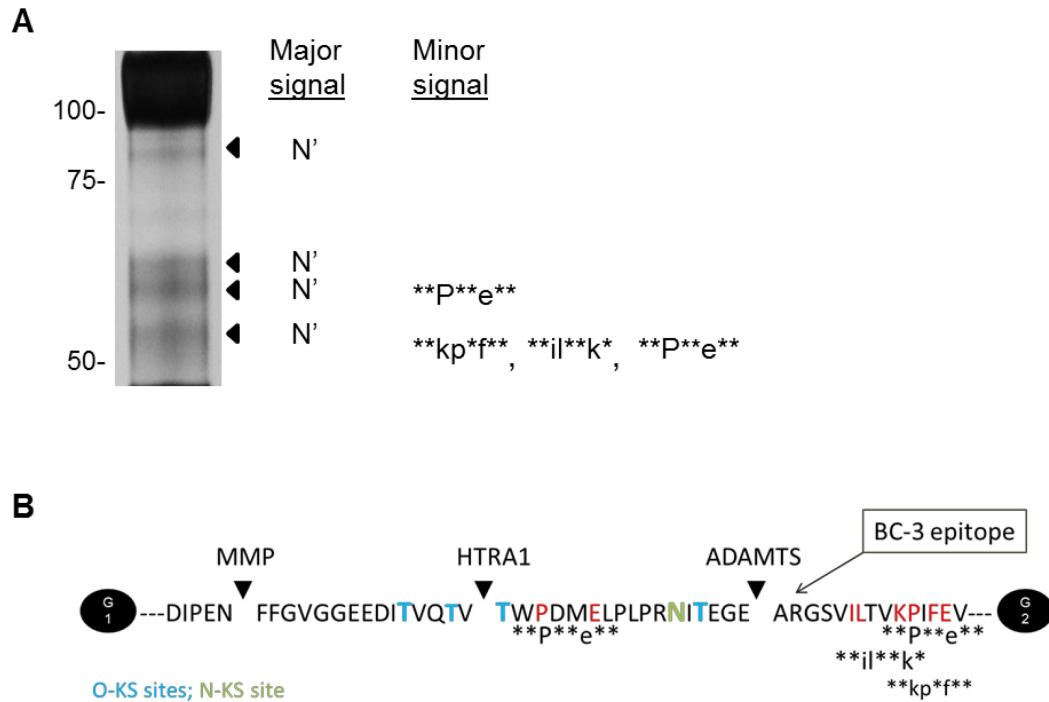


Figure 26 Amino terminal sequence analysis of BbHtrA-generated aggrecan fragments

A. Major and minor amino acid residues identified by Edman degradation of the aggrecan fragments. Black arrows indicate aggrecan fragments, * indicates that no amino acid could be assigned to that position **B.** Schematic of the pathologic proteolytic cleavage sites within the aggrecan IGD showing possible location of BbHtrA-generated minor signals. Red, residues identified by Edman degradation; blue and green, potential glycosylation sites discussed in text.

Several minor signals were identified in the BbHtrA-generated ~50kD fragment detected by the “BC-3” antibody (Fig. 25C) which is consistent with cleavage at or near the ADAMTS site (Fig. 26B). Additionally, minor signals obtained from the ~60kD fragment could be consistent with cleavage at the HtrA1 site (Fig. 26A, 26B). These minor signals could only have been generated by BbHtrA cleavage at an internal sequence. Endopeptidase activity has also been described for HtrA1 (160).

Degradation of Hyalactins, Small Leucine-Rich Proteoglycans, and Fibronectin

Aggrecan is the largest member of the family of chondroitin sulfate proteoglycans known as hyalactins. These proteoglycans play critical roles in ECM organization and stabilization. As with aggrecan, they are tethered to the ECM by interactions between their conserved amino terminal G1 domains and hyaluronic acid. Carboxyl terminal G3 domain interactions with numerous ECM proteins are equally important (262). There is considerable variability in the intervening protein backbone resulting in significant variation in the number of chondroitin sulfate GAG chains attached. For example, brevican, the most abundant hyalactin in the adult brain (263), is the smallest hyalactin with 911 amino acids and 3 GAG chains whereas aggrecan has 2403 amino acids and more than 100 GAG chains.

Using the same conditions used for aggrecan proteolysis, BbHtrA activity against several additional proteoglycans was assessed. With respect to other

members of the hyalactin family, BbHtrA cleaved recombinant, full length neurocan and thoroughly degraded brevican as well as recombinant versican (G1 domain only) (Fig. 27A). Consistent with HtrA1 reports, BbHtrA completely degraded native bovine decorin and biglycan (Fig. 27A). As expected, degradation was not observed upon incubation with proteolytically inactive BbHtrA^{S226A}.

Purified native human plasma fibronectin was also examined as a substrate (Fig. 27B). Overnight incubation of BbHtrA with fibronectin generated fragments with approximate molecular masses of 100kD, 37kD, and 33kD (Fig 27E, lane 2). With longer incubation times (up to 96 hours), loss of those species as well as the appearance of ~27kD and 29kD bands was observed (Fig. 27B, lane 3).

Degradation of collagen II and tenascin C was not observed (Fig. 27A), indicating BbHtrA substrate selectivity for proteoglycans and fibronectin.

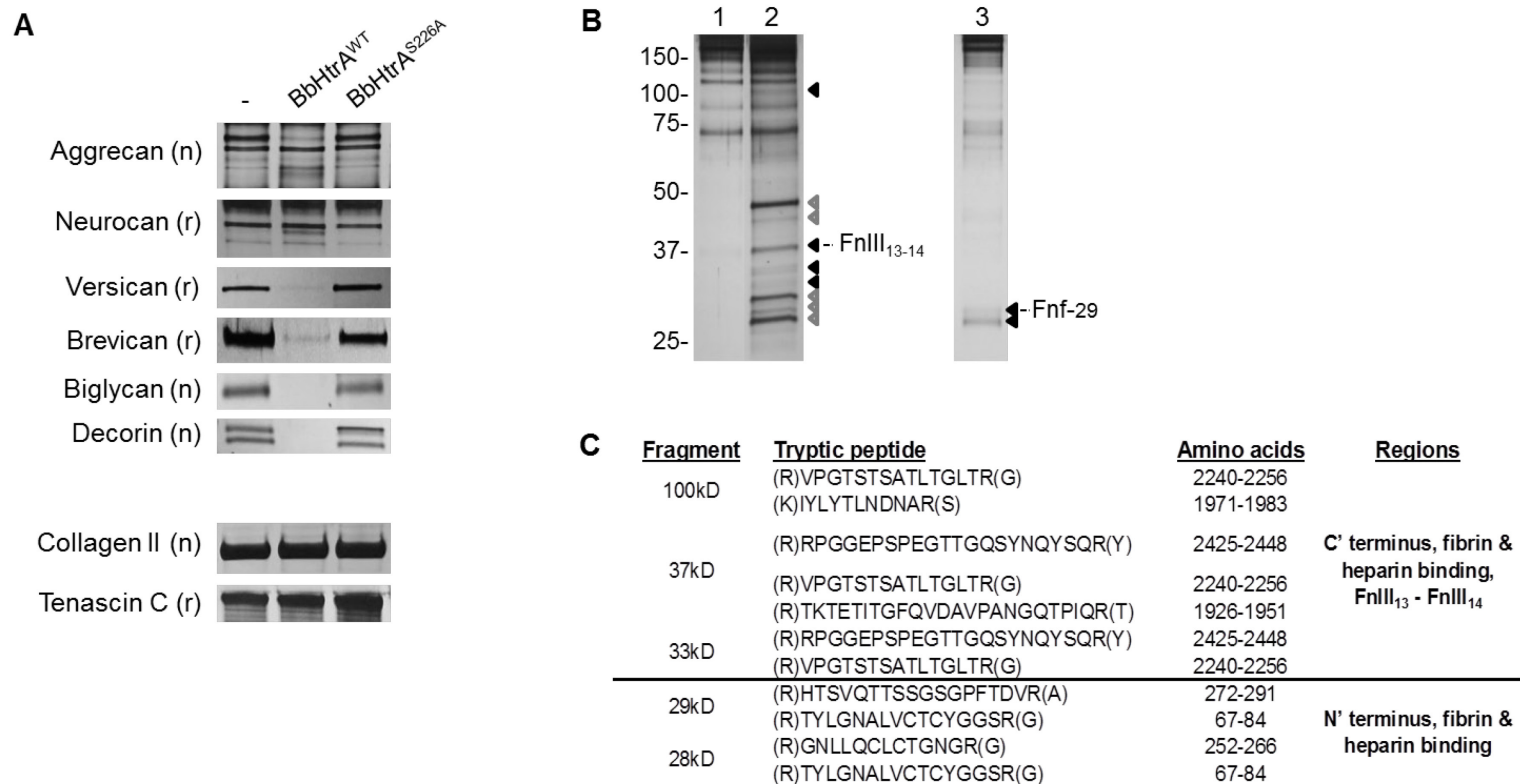


Figure 27 BbHtrA degradation of proteoglycans and fibronectin

A. Purified native (n) or recombinant (r) proteins were incubated overnight with BbHtrA or BbHtrA^{S226A}. Degradation was observed by SDS-PAGE and silver staining. **B.** SDS-PAGE and silver staining analysis of time course analysis of fibronectin (Fn) fragments generated by BbHtrA. Lane 1, Fn alone; lane 2, Fn incubated with BbHtrA 16 hours; lane 3, Fn incubated with BbHtrA 96 hours (same gel). Black arrows indicate BbHtrA-generated Fn fragments; grey arrows indicate BbHtrA and its auto-degradation products. Fn fragments are labeled. **C.** BbHtrA-generated Fn fragments identified by LC MS/MS. All peptides had peptide identity scores of greater than 95% yielding a 100% protein identity.

BbHtrA Generates Pro-inflammatory Fibronectin Fragments

The BbHtrA-generated fibronectin fragment profile is similar that obtained by digestion with HtrA1 (156). A subset of fibronectin fragments has been characterized as bioactive ECM components which stimulate inflammatory responses leading to the upregulation of host proteases and subsequent ECM damage (156, 178, 264, 265). To identify the fibronectin fragments generated by BbHtrA, reaction products were separated electrophoretically and the bands were excised and analyzed by tandem LC MS/MS (CSU Proteomics Facility) (Fig. 27C). Peptides from the early fibronectin fragments (~100kD, ~37kD, ~33kD) all mapped to the carboxyl terminal heparin- and fibrin- binding regions. The most abundant fragment (~37kD) yielded sequences within fibronectin type three repeat 13 (FnIII₁₃), a fragment with known inflammatory properties (266). As was seen with aggrecan, the observation of these carboxyl terminal fragments indicates endopeptidase activity. With prolonged incubation, amino terminal fragments (~27-29kD) were also observed (Fig. 27C). Amino terminal fibronectin fragments incite particularly strong responses *in vitro* and *in vivo* (179, 264).

In Vitro Consequences of BbHtrA Activity in a Cartilage-like System

Chondrocytes are the only resident cells within cartilage. A limited number of primary chondrocytes can be isolated from fresh tissues but the acquisition and methods made this approach both difficult and impractical. Bone marrow-derived mesenchymal stem cells are the progenitor cells for chondrocytes. Chondrogenesis and cartilage matrix production can be stimulated using a chemically defined medium which includes TGF β and ascorbic acid (267-269) In

addition to being regulated by the medium components mentioned above, chondrocytes are regulated by morphology and rapidly lose their differentiated phenotype in monolayer cultures. Three dimensional cultures are required to maintain chondrocyte phenotype and a variety of 3D culture methods exist. Chondrocyte aggregate cultures can be generated and maintained in 96-well plates allowing for the simultaneous maintenance of hundreds of cartilage-like aggregates (244, 245). Within 2-3 weeks of culture, the aggregates form an extensive extracellular matrix with components characteristic of articular cartilage including aggrecan and type II collagen (244, 270) and the expression of these chondrocytic markers continues for at least 6 weeks. The studies described in this report utilized passage four human mesenchymal stem cells differentiated to chondrocytes in an appropriate differentiation medium and in 3D aggregate cultures (experimental scheme shown in Fig. 28A).

To examine the possibility that BbHtrA-mediated ECM degradation stimulates an inflammatory response, recombinant proteins or LPS were added to culture medium and incubated with chondrocyte cartilage-like aggregate cultures (Figure 28A). LPS, the canonical TLR4 ligand (271), was chosen as the positive control for these assays. After 48 hours of incubation, spent medium was incubated with biotinylated detection antibodies for 32 inflammatory cytokines. The mixture was applied to membranes spotted in duplicate with cytokine capture antibodies (Fig. 28B). Development of the membrane with alkaline phosphatase-labeled streptavidin enabled identification of secreted cytokines present in the media (Fig. 28C).

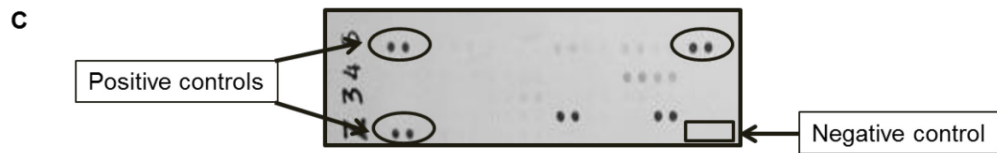
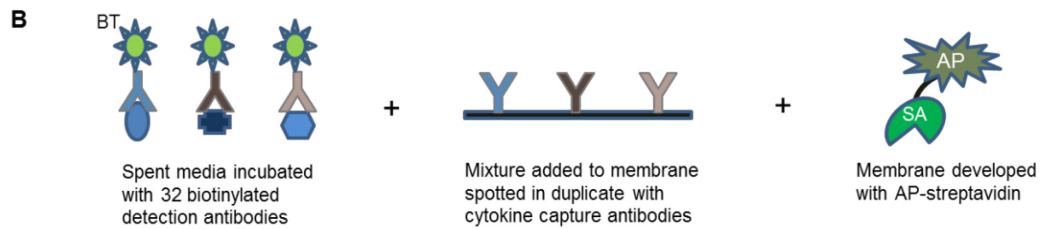
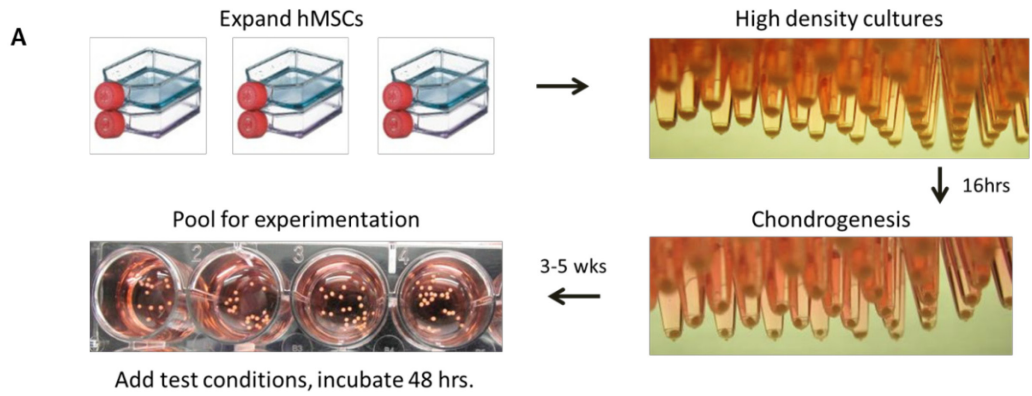


Figure 28 Identification of cytokines induced in chondrocyte cultures
A. Schematic of chondrocyte aggregate culture generation and experimental set up. **B.** Membrane-based antibody arrays detected cytokines in the spent media. **C.** Representative antibody-based cytokine array membrane showing position of control and cytokine spots.

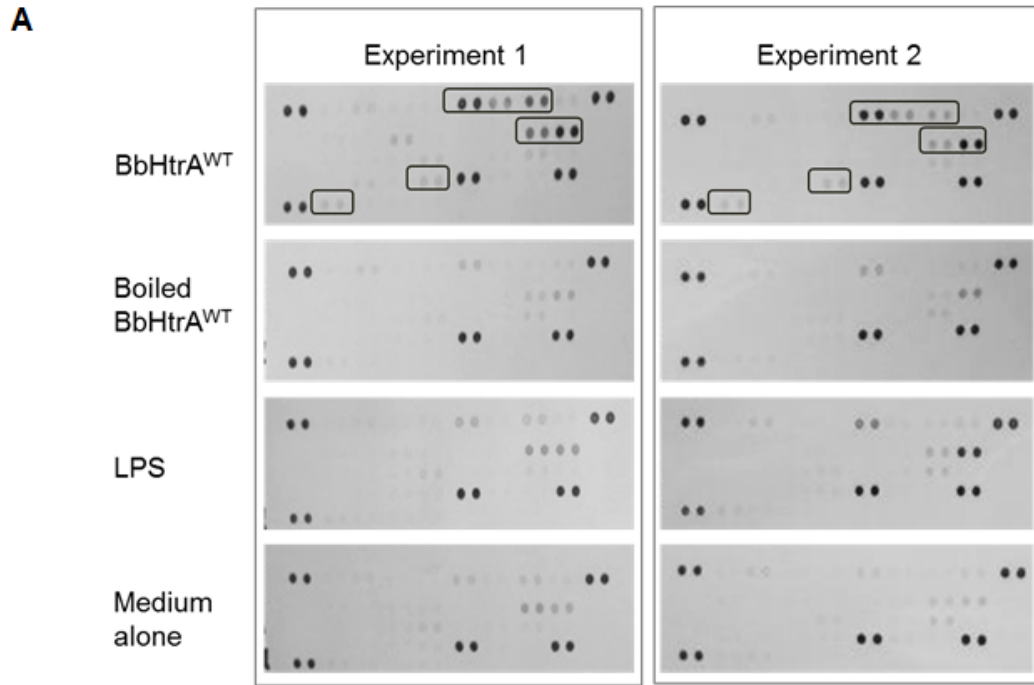
BbHtrA Stimulates Chondrocyte Release of Inflammatory Cytokines

Purified LPS, in great excess of the residual LPS in recombinant BbHtrA (LPS, 200 EU vs. BbHtrA, 28EU), was used as the positive control for these studies to allow for the identification of cytokines stimulated by TLR4 engagement. To confirm that the cytokine signals observed were due to the test conditions and not from endotoxin contaminants, potential LPS contamination of media components and residual LPS in the recombinant proteins were neutralized by pre-incubation with polymyxin B sulfate. The purified LPS control was also treated with polymyxin B to allow for the identification of “break-through” LPS-induced signaling.

Comparison of BbHtrA, Heat-denatured BbHtrA and LPS-induced Cytokine Responses

Initial experiments compared BbHtrA, heat denatured BbHtrA and LPS (Fig. 29A, and Cytokine Profiler key 29B). The medium alone condition demonstrated that chondrocytes constitutively expressed cytokines MIF and Serpin E1 and very low levels of several others. LPS induced TLR4-mediated release of the cytokines CXCL1, IL-6 and IL-8 and very low levels of CCL5 (Fig. 29A, LPS condition). BbHtrA, like LPS, stimulated release of CXCL1, IL-6, IL-8 and CCL5. Unlike LPS, however, CCL2 and sICAM-1 were also released in response to BbHtrA (Fig. 29A, BbHtrA condition). It should be noted that the level of LPS used in these experiments was 7-fold greater than the residual LPS in recombinant BbHtrA, yet many of the cytokine signals were stronger from the BbHtrA treated chondrocytes and two were unique to the response to BbHtrA.

The requirement of BbHtrA proteolytic activity for these responses was demonstrated by the near loss of all induced signals upon heat denaturation of BbHtrA (Fig. 29A, Boiled BbHtrA condition).



B

Pos Control	C5a	CD40 Ligand	G-CSF	GM-CSF	GRO α (CXCL1)	I-309 (CCL1)	siCAM-1 (CD54)	IFN-g	Pos Control
	IL-1a	IL-1 β	IL-1ra	IL-2	IL-4	IL-5	IL-6	IL-8 (CXCL8)	
	IL-10	IL-12 p70	IL-13	IL-16	IL-17	IL-17E	IL-23	IL-27	
	IL-32a	CXCL10	CXCL11	MCP-1 (CCL2)	MIF	CCL3	CCL4	Serpin E1	
Pos Control	RANTES (CCL5)	CXCL12	TNF-a	sTREM-1					Neg Control

Figure 29 Comparison of cytokine responses induced in chondrocytes by BbHtrA, heat-denatured BbHtrA and LPS

A. Chondrocyte aggregate cultures were incubated with 1ml of media containing recombinant BbHtrA or heat denatured BbHtrA (400nM, 28EU, LPS (200EU) or medium alone. Contaminating LPS was dampened in all test conditions by pre-incubation with polymyxin B sulfate. Antibody-based membrane arrays, spotted in duplicate, were used to screen spent medium for 32 cytokines. **B.** Proteome Profiler Human Cytokine Array key.

Comparison of BbHtrA, BbHtrA^{S226A} and LPS-induced Cytokine Responses

To examine the impact of BbHtrA proteolytic activity on the observed responses, additional experiments compared BbHtrA^{WT}, BbHtrA^{S226A}, LPS and medium alone (Fig. 30). Visual examination of the membranes showed very similar results to the previous experiments. Inter-assay variability was observed in the strength of the responses although the cytokines induced were consistent. Chondrocytes again released CCL5, CCL2, CXCL1, CCL1, sICAM-1, IL-6 and IL-8 in response to BbHtrA (Fig. 30, BbHtrA condition). Results with BbHtrA^{S226A} demonstrated that catalytic activity was required for most of these responses (Fig. 30, BbHtrA^{S226A} condition). Interestingly, BbHtrA^{S226A} stimulated release of IL-8 and CXCL1 which may suggest direct BbHtrA interaction with surface receptors or the displacement of a receptor agonist from the ECM (Fig. 30, BbHtrA^{S226A} condition). IL6, IL8 and low levels of CXCL1 were observed upon LPS stimulation of TLR4 (Fig. 30, LPS condition).

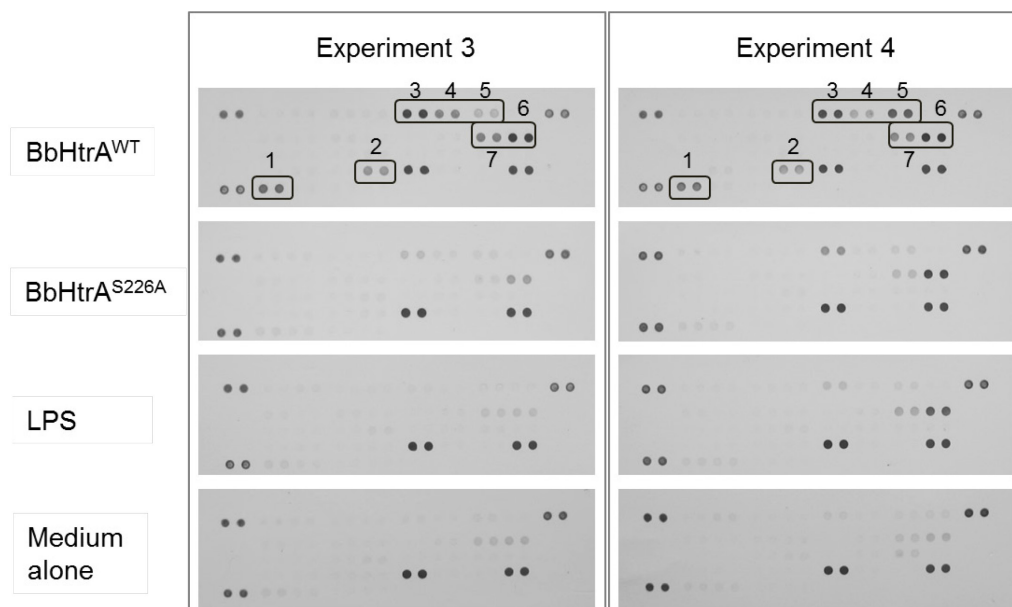


Figure 30 Comparison of cytokine responses induced in chondrocytes by wild type BbHtrA, mutant BbHtrA^{S226A} and LPS

A. Chondrocyte aggregate cultures were incubated with recombinant BbHtrA (400nM, 28EU/ml LPS), BbHtrA^{S226A} (400nM, 2EU/ml LPS), purified LPS (200EU/ml), or medium alone for 48 hours. Antibody-based membrane arrays, spotted in duplicate, were used to screen spent medium for 32 cytokines (key, Fig. 29). Numbers indicate cytokines stimulated in response to BbHtrA: P, positive controls; 1, CCL5; 2, CCL2; 3, CXCL1; 4, CCL1; 5, sICAM-1; 6, IL-8; 7, IL-6.

For evaluation of the significance of the observed differences, pixel densities were measured from experiments 2, 3 and 4. These experiments all used 60µg/ml polymyxin B sulfate pre-treatment, whereas 120µg/ml polymyxin B was used in experiment 1. Thus, experiment 1 results were not directly comparable. Pixel densities for each spot on a membrane were measured, the averaged background values from the negative controls for that membrane were subtracted and then the duplicate values for a particular cytokine were averaged. A summary of the background-corrected and averaged pixel densities are shown in (Table 5). Figure 31 shows box plot graphical representations of these data.

To compare between assays, a statistical model was developed by Mark Delorey, a statistician with the CDC. The mixed effects model made adjustments for variability among membranes arising from manufacturing processes or development time, and unequal variances due to inter-assay variability in the chondrocyte aggregate responses to a particular condition. These considerations gave rise to a scalar value which was applied to all sample data. These values were used to determine statistically significant differences in cytokine responses between the test conditions (Table 6, highlighted rows). In all cases, the cytokine responses to BbHtrA were statistically significantly different from the medium alone condition ($p \leq 0.0001$).

Table 5 Pixel densities of cytokines altered by test conditions
Background corrected and averaged data from two independent experiments are shown.

Cytokine	Condition	Mean	StdDev	N
RANTES/CCL5	Medium	0.246	0.053	6
	BbHtrA	0.736	0.393	8
	S226A	0.265	0.056	6
	LPS	0.365	0.084	6
MCP-1/CCL2	Medium	0.055	0.031	6
	BbHtrA	0.452	0.275	8
	S226A	0.050	0.041	6
	LPS	0.082	0.028	6
GRO α /CXCL1	Medium	0.174	0.044	6
	BbHtrA	1.349	0.095	8
	S226A	0.647	0.251	6
	LPS	0.631	0.431	6
I-309/CCL1	Medium	0.123	0.033	6
	BbHtrA	0.535	0.138	8
	S226A	0.163	0.017	6
	LPS	0.132	0.037	6
sICAM-1/CD54	Medium	0.173	0.035	6
	BbHtrA	0.890	0.598	8
	S226A	0.257	0.070	6
	LPS	0.166	0.022	6
IL-8	Medium	0.402	0.089	6
	BbHtrA	1.581	0.126	8
	S226A	1.187	0.422	6
	LPS	1.063	0.667	6
IL-6	Medium	0.253	0.041	6
	BbHtrA	0.627	0.310	8
	S226A	0.309	0.147	6
	LPS	0.353	0.199	6
Positive control	Medium	1.392	0.181	18
	BbHtrA	1.438	0.118	24
	S226A	1.406	0.138	18
	LPS	1.298	0.135	18

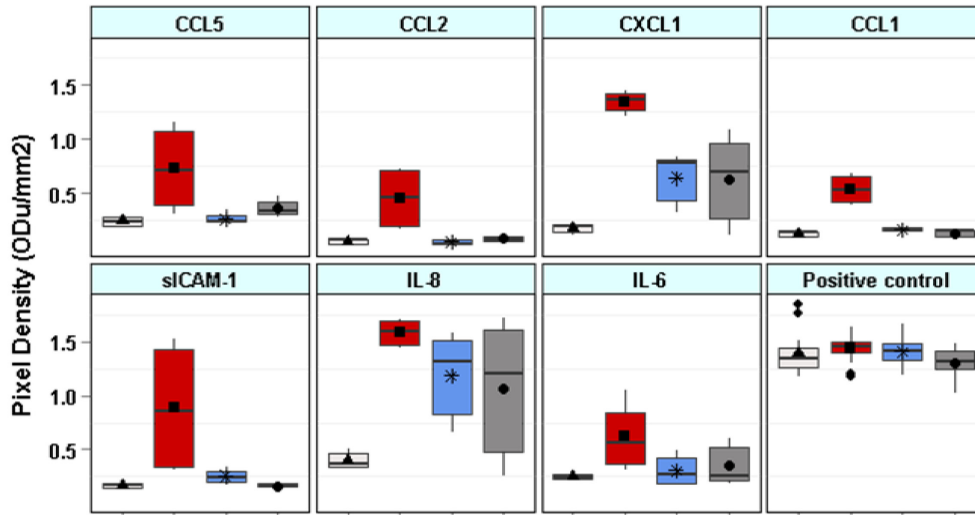


Figure 31 Box plots of pixel density data for induced cytokine responses
 Box plots of pixel densities indicating chondrocyte cytokine responses to test conditions: medium alone, ▲ and white; BbHtrA, ■ and red; BbHtrA^{S226A}, * and grey; LPS, ● and blue. Data shown in Table 5. Shapes within the box represent the mean, lines within the box represent the median, the box represents the 25th and 75th percentiles and the bars outside the box correspond to the ends of the data range. Before analysis, negative control pixel densities for each membrane were subtracted from all density values on that membrane. Data from two independent experiments are shown.

Table 6 Statistical significance of differences in cytokine expression between chondrocyte culture conditions

Density differences and 95% confidence intervals of these differences are shown for comparisons of cytokine array data. Highlighted rows indicate cytokines significantly different between the specified test conditions ($p \leq 0.001$).

Comparison	Cytokine	Difference in Means	Standard Error	Lower Bound	Upper Bound	P-value
Medium-BbHtrA	RANTES/CCL5	-0.49	0.12	-0.89	-0.0894	0.0001
	MCP-1/CCL2	-0.397	0.0862	-0.684	-0.11	<0.0001
	GRO α /CXCL1	-1.17	0.0648	-1.39	-0.959	<0.0001
	I-309/CCL1	-0.412	0.0637	-0.624	-0.2	<0.0001
	sICAM-1/CD54	-0.717	0.18	-1.32	-0.118	0.0001
	IL-8	-1.18	0.0694	-1.41	-0.948	<0.0001
	IL-6	-0.374	0.0965	-0.696	-0.0534	0.0001
Medium-LPS	RANTES/CCL5	-0.12	0.0807	-0.388	0.149	0.1403
	MCP-1/CCL2	-0.0266	0.0702	-0.26	0.207	0.7051
	GRO α /CXCL1	-0.456	0.18	-1.05	0.142	0.012
	I-309/CCL1	-0.0089	0.0667	-0.231	0.213	0.8937
	sICAM-1/CD54	0.0068	0.0668	-0.215	0.229	0.9193
	IL-8	-0.662	0.273	-1.57	0.248	0.0166
	IL-6	-0.1	0.102	-0.44	0.24	0.3277
Medium-S226A	RANTES/CCL5	-0.0187	0.0789	-0.281	0.244	0.8133
	MCP-1/CCL2	0.0051	0.0728	-0.237	0.247	0.9443
	GRO α /CXCL1	-0.473	0.119	-0.868	-0.078	0.0001
	I-309/CCL1	-0.0397	0.0665	-0.261	0.182	0.551
	sICAM-1/CD54	-0.084	0.0704	-0.318	0.15	0.234
	IL-8	-0.785	0.183	-1.39	-0.178	<0.0001
	IL-6	-0.0563	0.087	-0.346	0.233	0.5183
LPS-BbHtrA	RANTES/CCL5	-0.37	0.12	-0.769	0.0287	0.0023
	MCP-1/CCL2	-0.37	0.0839	-0.649	-0.0913	<0.0001
	GRO α /CXCL1	-0.718	0.179	-1.31	-0.122	0.0001
	I-309/CCL1	-0.403	0.0639	-0.616	-0.191	<0.0001
	sICAM-1/CD54	-0.724	0.18	-1.32	-0.125	0.0001
	IL-8	-0.517	0.271	-1.42	0.383	0.0577
	IL-6	-0.274	0.122	-0.68	0.131	0.0257
LPS-S226A	RANTES/CCL5	0.101	0.0782	-0.159	0.361	0.1988
	MCP-1/CCL2	0.0317	0.07	-0.201	0.265	0.6513
	GRO α /CXCL1	-0.0164	0.205	-0.698	0.665	0.9363
	I-309/CCL1	-0.0308	0.0667	-0.253	0.191	0.6446
	sICAM-1/CD54	-0.0908	0.0702	-0.324	0.143	0.1973
	IL-8	-0.124	0.319	-1.19	0.938	0.6987
	IL-6	0.044	0.114	-0.337	0.425	0.7011
BbHtrA-S226A	RANTES/CCL5	0.471	0.119	0.0762	0.866	0.0001
	MCP-1/CCL2	0.402	0.086	0.116	0.688	<0.0001
	GRO α /CXCL1	0.702	0.117	0.311	1.09	<0.0001
	I-309/CCL1	0.372	0.0636	0.161	0.584	<0.0001
	sICAM-1/CD54	0.633	0.181	0.0298	1.24	0.0006
	IL-8	0.393	0.178	-0.2	0.987	0.0288
	IL-6	0.318	0.109	-0.0458	0.682	0.0041

CHAPTER 7: Discussion

The foundational hypothesis of this work was that *B. burgdorferi* interact with aggrecan and that such an interaction would have implications for aggrecan function and, thereby, joint integrity. The main findings of these studies strongly support this hypothesis. At least four borrelial proteins interact specifically with aggrecan, two of which were identified as BbHtrA and Bgp.

Borrelial interactions with the extracellular matrix are important for the full pathogenic potential of this organism. The redundancy of interactions between borrelial adhesins and a widening array of ECM molecules make evident the importance of adhesion for colonization and persistence. The interactions between *Borrelia* and aggrecan described in this report could provide the spirochete with an additional means of adherence. Bgp, and the other as-yet-identified aggrecan-binding proteins, could contribute to this process.

Bgp is a well-characterized member of the family of borrelial GAG-binding proteins (246). Enrichment of this protein on the aggrecan columns, then, was consistent with previously described activities of Bgp.

The function and activity of BbHtrA had not yet been described. As discussed in Chapter 4, the human ortholog, HtrA1, is an aggrecan-degrading protease up-regulated in inflammatory arthritis and implicated in the degradation of numerous ECM components in several diseases. This knowledge prompted characterization of BbHtrA.

Examination of the genomes of the Lyme disease spirochetes demonstrated that HtrA is highly conserved. *B. burgdorferi sensu lato* HtrA amino

acid sequences have greater than 95% amino acid identity. BbHtrA was shown to be expressed during human disease caused by *B. burgdorferi* as evidenced by interaction of antibodies in serum from Lyme disease patients with recombinant BbHtrA^{S226A}. Therefore, if BbHtrA contributes to the pathology of Lyme disease, this role might also be expected from BaHtrA and BgHtrA.

A caseinolytic protease was observed within the lysates of *B. afzelii* ACA-1, *B. garinii* PKo and *B. burgdorferi* which migrated at the same position as a protein identified by an anti-BbHtrA antibody. These results are in contrast to the observations made by Guyard *et al.* (2006) in their study of a *B. hermsii* 60kD HtrA-like protease (BhpA) conserved within the relapsing fever group of spirochetes (272). *B. hermsii* also possesses an HtrA homolog (BH0104), although only BhpA showed caseinolytic activity by zymography. Additionally, in that study, casein zymography was also negative for several members of the Lyme disease group, including *B. burgdorferi* and *B. garinii*. Methodological differences are likely the cause of the discrepancy, particularly in the development times of the zymograms. Caseinolytic activity within the lysates of the Lyme disease spirochetes was enhanced by renaturation times of 60-90 minutes and development times of greater than 24hrs.

Other investigators have explored the caseinolytic activity of intact *Borrelia* using plaque zymography (229, 273) and observed no such activity. In the assays performed in this report, BbHtrA caseinolytic activity was demonstrated by assays with purified proteins in solution and by β -casein zymography. While the β -casein zymograms were positive, the amount of clearing observed was

minimal relative to the amount of recombinant protease in the gel (1 μ g) and activity within the lysates was only seen after prolonged incubation. Catalytic activity of HtrA proteases follows substrate-induced multimer formation (204). Efficiency of renaturation of monomers and higher order structures, then, strongly impacts zymogram results. Additionally, BbHtrA proteolysis assays using casein solubilized from a commercial powder showed very little activity, whereas complete casein degradation was observed using a commercially prepared casein solution. Thus, the treatment of casein affects its suitability as a substrate for BbHtrA and may be the source of the discrepancies between my results and those previously described.

As with other bacterial HtrA orthologs, at least part of the cellular pool of BbHtrA was found to be surface-exposed in *B. burgdorferi*. This observation is consistent with a recent report identifying BbHtrA in an outer membrane complex with surface proteins P66 and RevA (274). Furthermore, another recent investigation used multiple approaches to define the borrelial membrane proteome (274). In agreement with the studies in this report, biotinylated BbHtrA and BaHtrA, the homologous protease in *B. afzelii*, were identified by mass spectrometric analysis following surface biotinylation of intact spirochetes. Fragments of BaHtrA and BgHtrA were also released from intact spirochetes during controlled proteolysis (275).

It is suspected that, as in other bacteria, BbHtrA performs critical periplasmic protease/chaperone functions required for protein quality control (150, 201). *Borrelia* possess other periplasmic chaperones capable of assisting

protein folding (276), yet BbHtrA activity appears to provide a function which may be required for viability. BbHtrA transposon mutants were not recovered in a transposon mutant library which contained an average of 2.69 unique insertion sites per kb DNA in the borrelial genome resulting in 4,479 mutants (*B. burgdorferi* infectious strain B31 5A18NP1) (277) (Tao Lin, personal communication). These results suggest that insertional inactivation of the BbHtrA gene is lethal for *B. burgdorferi*.

HtrA protease chaperones are regulated at the protein level, in part, by self-degradation after substrate exhaustion (255, 257, 278). In *E. coli* DegP this process begins by cleavage at Cys⁵⁷, Cys⁶⁹ or Gln⁸² in the unstructured “LA-loop” and gives rise to a short form (s-HtrA, ~43kD) that has reduced catalytic activity (279). The LA-loop is 21 residues shorter in *E. coli* DegQ and the residues mentioned above are not conserved, yet DegQ also undergoes self-degradation (280). The DegQ self-cleavage site has not yet been reported. Like DegQ, BbHtrA also contains a shortened LA loop and readily degrades itself. Amino terminal sequence analysis identified the self-cleavage site between paired phenylalanines in the LA loop. These residues are conserved in DegQ orthologs from many other organisms (149) underscoring their importance and suggesting the possibility that auto-degradation in DegQ orthologs generally arises from processing at this site.

Potential BbHtrA degradation of aggrecan and several other known HtrA1 substrates was examined in proteolysis assays with purified proteins. Incubation of BbHtrA with recombinant and native aggrecan established that, like HtrA1,

BbHtrA is able to cleave aggrecan in the IGD. Degradation at this region is considered pathologic as it removes from aggrecan the ability to attract and retain water and to stabilize the ECM through protein-protein interactions. Further analysis demonstrated that at least some of the recombinant aggrecan fragments arose from cleavage at the “aggrecanase site” at ³⁷⁴ARGS. Comparison of aggrecan degradation products generated by BbHtrA and HtrA1 highlighted differences in the fragment profile and suggests that BbHtrA may cleave aggrecan at a unique site. As mentioned above, proteases which cleave aggrecan within the IGD do so at very specific sites. Thus, the proteolytic fragments are characteristic and those generated by BbHtrA may have diagnostic value.

BbHtrA-mediated degradation of all of the hyalactins (aggrecan, versican, neurocan and brevican) was observed. These chondroitin sulfate proteoglycans bind hyaluronic acid, participate in numerous stabilizing protein-protein interactions within the ECM and mediate cell-ECM contacts (281). All hyalactins are important in the composition and function of the ECM within the brain and CNS (282). As mentioned, aggrecan is expressed in cartilage, tendons, brain and CNS. Versican is widely distributed in the soft tissues of the body, whereas neurocan and brevican are almost exclusively CNS proteoglycans.

Decorin and biglycan were completely degraded by BbHtrA. These proteoglycans are members of the small leucine-rich proteoglycans. Decorin and biglycan are important not only in ECM architecture but also in the regulation of tissue homeostasis (283, 284) through their interaction with TGF β .

Fibronectin fragmentation was also observed upon incubation with BbHtrA. Fibronectin is a ubiquitous ECM glycoprotein with a wide variety of physiologic roles largely mediated by interaction with at least 10 different cell surface receptors. Via attachment to cell surface integrins, fibronectin is involved in tethering cells to the ECM and also coordinating matrix assembly through numerous protein-protein interactions (285).

The degradation of such a large number of ECM components suggests that this activity is important for *B. burgdorferi*. The ECM is a significant barrier that must be overcome for borrelial dissemination from primary sites of infection, entrance and exit of the vasculature during hematogenous spreading, and establishment of infection at distal sites. The mechanism of borrelial ECM degradation most frequently discussed is the coordination of host acquired plasmin to the spirochetal surface. Plasmin degrades a wide range of ECM substrates and would be expected to aid in borrelial dissemination. Reduced spirochetaemia was observed in plasminogen-deficient mice, demonstrating that plasmin does play a role in the spread of the bacteria. However, systemic infection was unimpeded demonstrating that, while plasmin is of use to *B. burgdorferi*, it is not required for dissemination or colonization of secondary sites (27). The activity of additional host proteases released during the inflammatory response likely contributes to ECM degradation. MMPs and ADAMTS-4, with the combined ability to degrade collagens, aggrecan, decorin, and fibronectin among others, are up-regulated during borrelial infection. However, incubation of cartilage with live *Borrelia* resulted in degradation of aggrecan that was not

prevented by the inhibition of these host proteases (221, 242). Studies in this report have established that *Borrelia* possess a surface-exposed HtrA protease capable of degrading vital constituents in the connective tissues through which *Borrelia* must traverse and their degradation could greatly facilitate borrelial dissemination.

In vitro and *in vivo*, borrelial migration across endothelial cell barriers occurs at cell junctions (216, 217, 286), a process which requires the ability to disrupt the adhesive interactions of junctional cadherin proteins. The mechanism of this paracellular migration has not been addressed. A recent study compared E-cadherin degradation by recombinant HtrAs from the gram-negative pathogens *Helicobacter pylori*, *Shigella flexneri*, Enteropathogenic *Escherichia coli* (EPEC), *Campylobacter jejuni* and *Neisseria gonorrhoeae*. With the exception of *N. gonorrhoeae*, recombinant HtrA from these pathogens were able to cleave E-cadherin (213). Additionally, E-cadherin degradation products were observed in culture supernatants from cells incubated with these bacteria. Although BbHtrA degradation of E-cadherin has not yet been evaluated, Hoy *et al.* (2012) suggested that the conserved ability to degrade an adhesive junctional protein might be a general mechanism for dissemination in bacteria which migrate through junctional spaces (213).

Beyond the immediate destabilizing effects of damage to host ECM molecules, degradation of many ECM components results in soluble bioactive fragments. Fibronectin fragments, and those of other ECM molecules such as biglycan, are danger-associated molecular pattern molecules (DAMPs) which

stimulate inflammatory responses by engaging cell surface receptors including TLR2, TLR4 and RAGE (receptor for advanced glycation end products) (167-170, 284, 287). With specific regard to HtrA1, HtrA1-generated Fn-fs increased production of MMPs 1, 3, 9 and 13 (156, 179, 265), the aggrecanase ADAMTS-4 (265), cytokines IL-1 β (265), IL-6 and IL-8 (265, 288) and chemokines CCL2 (179, 288) and CXCL1 (288) *in vitro*.

Examination of the BbHtrA-generated fibronectin fragments identified several carboxyl terminal fragments containing fibronectin type three repeats 13 and 14 (FnIII₁₃₋₁₄). FnIII₁₃₋₁₄ fragments stimulate cartilage destruction *in vivo* through interaction with toll like receptor 4 (TLR4) and induction of MMPs and aggrecanases (266). The strongly pro-inflammatory 29kD amino-terminal fibronectin fragment (Fn-f 29) was also identified as a product of BbHtrA proteolysis. Fn-f 29 contains the fibrin and heparin binding domains and is released by several proteases including plasmin, thermolysin and trypsin (289). Fn-f 29 is strongly pro-inflammatory and, when injected into rabbit knee joints, induced rapid proteoglycan loss within a matter of days (264). Fn-f 29 has been shown to induce TLR2 (290), to interact α 5 β 1 integrins (264) and also to induce integrin-independent proteoglycan release from cartilage (174). In agreement with these results, a very recent report has established that 27-29kD amino terminal and several carboxyl terminal Fn-fs are released upon HtrA1 digestion of fibronectin and greatly increased in the supernatants of cells treated with HtrA1 (265).

To examine possible inflammatory responses to BbHtrA-generated ECM fragments, cartilage-like chondrocyte aggregate cultures were incubated with BbHtrA and the spent media was probed for the presence of 32 inflammatory cytokines and chemokines. The requirement for BbHtrA was assessed by incubation with BbHtrA^{S226A} and LPS was used to identify cytokines released by TLR4 engagement. BbHtrA stimulated statistically significant increases in the inflammatory cytokines (IL-6, sICAM-1) and chemokines (CXCL1, CCL1, CCL2, CCL5, IL-8). Chemokines are secondary inflammatory responses induced by primary cytokines (291). Though not observed at the 48 hour time point of these experiments, earlier expression of the primary cytokines IFN γ , IL1- β or TNF α is thus implied.

In comparing the BbHtrA and LPS cytokine profiles, two of the cytokines signals were similar (CXCL1 and IL-8), potentially indicating that their release in response to BbHtrA was mediated through activation of TLR4. It should be noted that the level of LPS used in these experiments was 7-fold greater than the residual LPS in recombinant BbHtrA before polymyxin B sulfate treatment, yet the cytokine signals were stronger from the BbHtrA-treated chondrocytes and four were unique to the response to BbHtrA. These results strongly support a direct effect of BbHtrA on cytokine release.

Fibronectin fragments also signal via TLR4 and recent studies documented TLR4-mediated IL-6 and CCL2 release in response to fibronectin fragments containing FnIII₁₂₋₁₄ (179) and IL-6 and IL-8 release from cells cultured with HtrA1-generated fibronectin fragments (265). Surprisingly, BbHtrA^{S226A} also

increased chemokines CXCL1 and IL-8, which may suggest direct BbHtrA interaction with a surface receptor or the displacement of a receptor agonist from the ECM. Given the observation that CXCL1 and IL-8 were released in response to BbHtrA, BbHtrA^{S226A} and LPS, it seems plausible that TLR4 is involved in both protease-dependent and protease-independent responses to BbHtrA. Consistent with this hypothesis, Tiaden *et al.* (2012) recently reported protease-independent activity of HtrA1(265).

CCL1, CCL2, CCL5, sICAM-1 and IL-6 expression in response to BbHtrA is likely mediated by surface receptors other than TLR4. For example, aggrecan and fibronectin both bind to CD44 and it is conceivable that cleavage of these proteins would perturb their interactions with the receptor, resulting in signal transduction (292). Additionally, BbHtrA has been identified in a large complex with P66, a well characterized *B. burgdorferi* integrin-binding protein. Incubation of chondrocytes with purified P66 stimulated IL-1 β , IL-6, IL-8, CCL5 and MMP-1 release, suggesting possible integrin involvement (293).

The BbHtrA-stimulated chemokines (CXCL1, CCL1, CCL2, IL-8 and CCL5) recruit and activate monocytes, T-cells and neutrophils into sites of injury and inflammation. These cells are abundant in the joint tissue and fluid of Lyme arthritis patients and in erythema migrans lesions. Among other activities, these cells release aggrecanases and MMPs to facilitate tissue repair. However, an inflammatory response in excess of the actual need is injurious to the tissues and contributes to the pathogenesis of Lyme disease (294, 295).

The cytokines elicited by BbHtrA have been described as elevated in various samples from Lyme disease patients. CXCL1, CCL2, IL-6 and IL-8 among others were found to be elevated in skin samples from patients with erythema migrans and acrodermatitis chronicum atrophicum compared to healthy controls (296-298). CCL2 and IL-6 elevation have also been detected in serum of patients with Lyme disease (297, 298). CCL2 and IL-8 are also significantly elevated over controls in cerebrospinal fluid of neuroborreliosis patients and borderline in LA patients (299). Lastly, levels of IL-6, IL-8 and CCL2 were significantly higher in the synovial fluid of patients with antibiotic-refractory LA than in those with arthritis responsive to antibiotic therapy (300).

A New Model for Borrelial Pathogenesis

BbHtrA is a surface-exposed protease expressed during human disease and conserved within the Lyme disease spirochetes. Large and small chondroitin sulfate proteoglycans and fibronectin were degraded by BbHtrA *in vitro*. Aggrecan degradation occurred within the pathologic IGD with some BbHtrA-generated fragments arising from cleavage at the aggrecanase site. Analysis of the resultant fibronectin fragments identified previously characterized ligands of TLR2 and TLR4 which stimulate up-regulation of those receptors and of several matrix proteases and cause the release of inflammatory signaling molecules. Indeed, protease-dependent and independent inflammatory cytokine and chemokine responses were observed upon BbHtrA treatment of cartilage-like chondrocyte aggregate cultures. Thus, BbHtrA activity has implications for both

the integrity of the ECM and the homeostasis of tissues colonized by *Borrelia burgdorferi*.

Though a great many questions remain unanswered regarding BbHtrA, the observations described herein may suggest a new model of pathogenesis in Lyme disease (Fig. 32). BbHtrA activity may allow for destabilization of the host extracellular matrix and aid in borrelial dissemination. Besides impacting the survival of the spirochete, BbHtrA activity could contribute to the observed pathologies of Lyme disease, particularly Lyme arthritis. Degradation of the proteoglycans studied here results in disrupted cartilage homeostasis and altered biomechanical properties (133, 135, 137, 147). Responses to fibronectin fragments such as those generated by BbHtrA include increased activity of matrix proteases *in vitro* and *in vivo* (179, 265, 266, 301).

The inflammatory response to BbHtrA degradation products significantly extends the immediate consequences of BbHtrA activity by potentially intensifying inflammatory signaling cascades. BbHtrA could exacerbate inflammatory cytokine and chemokine responses to the spirochete itself leading to the enhanced recruitment of immune cells. The heightened inflammatory milieu could also alter the regulation of resident cells. Proteases released by resident and responding immune cells would contribute to the tissue damage, thereby releasing more ECM fragments and amplifying the inflammatory response.

Activity of BbHtrA could contribute to the various pathologies observed in Lyme disease, most especially the inflammatory response that is inexplicably out of proportion to the bacterial load.

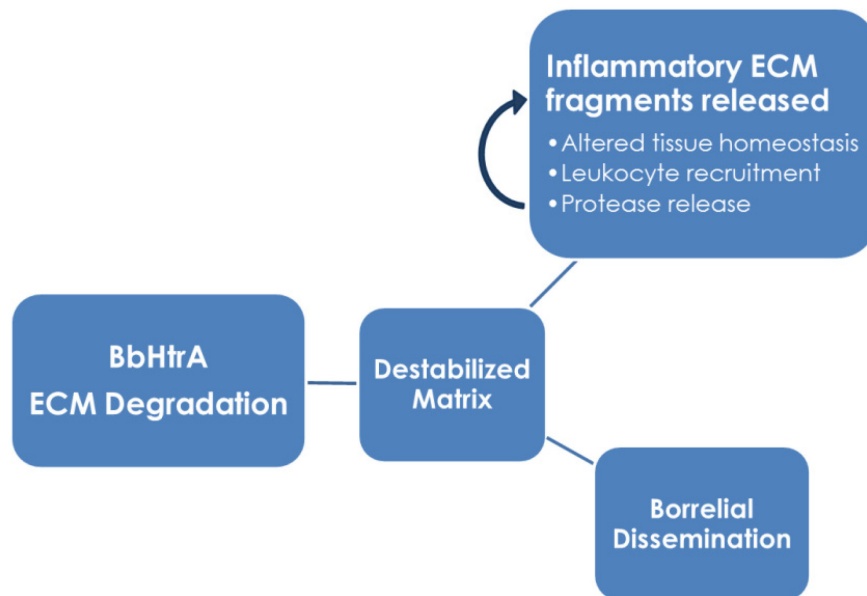


Figure 32 Model of potential consequences of BbHtrA-mediated ECM degradation.

CHAPTER 8: Future Directions

Detailed Characterization of BbHtrA

The studies in this dissertation are the first to describe BbHtrA and, while they have begun to elucidate the activities of this protease, many important questions remain unanswered. *In vivo* studies are required to determine whether, and to what extent, BbHtrA ECM degradation contributes to the pathologies observed in Lyme disease. Examination of BbHtrA expression, regulation, and the identification of endogenous substrates will shed light on the role of BbHtrA in borrelial physiology. Investigation of the association of BbHtrA with borrelial porins could provide important functional information. Additionally, the mechanism of surface exposure of BbHtrA remains unknown.

Diagnostic Potential of BbHtrA-Generated ECM Fragments

Currently, all laboratory tests cleared by the U.S. Food and Drug Administration for the diagnosis of Lyme disease rely on detecting antibodies to borrelial antigens (302). These serologic tests have a number of limitations: they are insensitive in early disease (303), they cannot distinguish a current infection from a previous one because antibody responses are long-lived (13), and they cannot determine whether infection persists in a patient after antibiotic therapy. Therefore, there is a need for a non-serologic test with the ability to identify products of active borrelial infection.

BbHtrA-generated ECM fragments would only be produced in appreciable amounts by viable organisms. Studies with aggrecan demonstrated differences in the fragment profile of HtrA1 and BbHtrA-generated aggrecan fragments (Fig.

25B) and similar differences may also exist for other ECM targets. Identification of unique BbHtrA degradation products will allow for the generation of antibodies raised against the BbHtrA-generated neoepitopes. These antibodies would be the basis for an antigen capture test for use in early Lyme disease, as a complement to current diagnostic tests, or as a tool to assess response to therapy. Studies are underway to identify unique BbHtrA-generated ECM fragments, to raise antibodies against the most promising candidate(s), and to explore the diagnostic potential of these antibodies in the murine model of Lyme disease.

REFERENCES

1. A. Rizzoli, H. Hauffe, G. Carpi, H. G. Vourc, M. Neteler *et al.*, Lyme borreliosis in Europe. *Euro Surveill* **16**, (2011).
2. S. K. Sood, S. O'Connell, K. S. Weber, in *Lyme borreliosis in Europe and North America: Epidemiology and Clinical Practice*, S. K. Sood, Ed. (Wiley, Hoboken, New Jersey, 2011), pp. 1-35.
3. S. Narasimhan, M. J. Caimano, F. T. Liang, F. Santiago, M. Laskowski *et al.*, *Borrelia burgdorferi* transcriptome in the central nervous system of non-human primates. *Proc Natl Acad Sci U S A* **100**, 15953 (Dec 23, 2003).
4. J. D. Radolf, M. J. Caimano, B. Stevenson, L. T. Hu, Of ticks, mice and men: understanding the dual-host lifestyle of Lyme disease spirochaetes. *Nat Rev Microbiol* **10**, 87 (Feb, 2012).
5. A. C. Steere, S. E. Malawista, D. R. Snyderman, R. E. Shope, W. A. Andiman *et al.*, Lyme arthritis: an epidemic of oligoarticular arthritis in children and adults in three connecticut communities. *Arthritis Rheum* **20**, 7 (Jan-Feb, 1977).
6. W. Burgdorfer, A. G. Barbour, S. F. Hayes, J. L. Benach, E. Grunwaldt *et al.*, Lyme disease—a tick-borne spirochetosis? *Science* **216**, 1317 (Jun 18, 1982).
7. J. L. Benach, E. M. Bosler, J. P. Hanrahan, J. L. Coleman, G. S. Habicht *et al.*, Spirochetes isolated from the blood of two patients with Lyme disease. *N Engl J Med* **308**, 740 (Mar 31, 1983).
8. CDC, (2012), *Reported Lyme disease cases by state, 2000-2010*. Centers for Disease Control and Prevention, Retrieved April 4, 2012. http://www.cdc.gov/lyme/stats/chartstables/reportedcases_statelocality.html
9. J. D. Radolf, J. C. Salazar, R. J. Dattwyler, in *Borrelia: Molecular Biology, Host Interactions and Pathogenesis*, J. S. Samuels, Radolf, J.D., Ed. (Caister Academic Press, Norfolk, UK, 2010), pp. 487-533.
10. U. Pal, E. Fikrig, in *Borrelia: Molecular Biology, Host Interactions and Pathogenesis*, J. S. Samuels, Radolf, J.D., Ed. (Caister Academic Press, Norfolk, UK, 2010).
11. T. G. Schwan, J. Piesman, Vector interactions and molecular adaptations of lyme disease and relapsing fever spirochetes associated with transmission by ticks. *Emerg Infect Dis* **8**, 115 (Feb, 2002).

12. CDC, (2012), *Reported Clinical Findings Among Lyme Disease Patients, 1992-2004*. Centers for Disease Control and Prevention, Retrieved April 4, 2012. <http://www.cdc.gov/lyme/stats/chartstables/casesbysymptom.html>
13. B. J. B. Johnson, in *Lyme Disease: An Evidence-based Approach*, J. J. Halperin, Ed. (CAB International, Oxfordshire, UK, 2011), vol. 20, pp. 73-88.
14. B. J. B. Johnson, in *Manual of Molecular and Clinical Laboratory Immunology* B. Detrick, R. G. Hamilton, J. D. Folds, Eds. (ASM Press, Washington, D.C. , 2006).
15. G. P. Wormser, R. J. Dattwyler, E. D. Shapiro, J. J. Halperin, A. C. Steere *et al.*, The clinical assessment, treatment, and prevention of Lyme disease, human granulocytic anaplasmosis, and babesiosis: clinical practice guidelines by the Infectious Diseases Society of America. *Clin Infect Dis* **43**, 1089 (Nov 1, 2006).
16. CDC, (2012), *Post-Treatment Lyme Disease Syndrome*. Centers for Disease Control and Prevention, Retrieved April 13, 2012. <http://www.cdc.gov/lyme/postLDS/index.html>
17. H. M. Feder, Jr., B. J. Johnson, S. O'Connell, E. D. Shapiro, A. C. Steere *et al.*, A critical appraisal of "chronic Lyme disease". *N Engl J Med* **357**, 1422 (Oct 4, 2007).
18. M. S. Klempner, Controlled trials of antibiotic treatment in patients with post-treatment chronic Lyme disease. *Vector Borne Zoonotic Dis* **2**, 255 (Winter, 2002).
19. N. Rudenko, M. Golovchenko, L. Grubhoffer, J. H. Oliver, Jr., Updates on *Borrelia burgdorferi sensu lato* complex with respect to public health. *Ticks Tick Borne Dis* **2**, 123 (Sep, 2011).
20. G. Stanek, G. P. Wormser, J. Gray, F. Strle, Lyme borreliosis. *Lancet* **379**, 461 (Feb 4, 2012).
21. M. A. Cimmino, Relative frequency of Lyme borreliosis and of its clinical manifestations in Europe. European Community Concerted Action on Risk Assessment in Lyme Borreliosis. *Infection* **26**, 298 (Sep-Oct, 1998).
22. D. Liveris, A. Gazumyan, I. Schwartz, Molecular typing of *Borrelia burgdorferi sensu lato* by PCR-restriction fragment length polymorphism analysis. *J Clin Microbiol* **33**, 589 (Mar, 1995).

23. G. Wang, C. Ojaimi, H. Wu, V. Saksenberg, R. Iyer *et al.*, Disease severity in a murine model of lyme borreliosis is associated with the genotype of the infecting *Borrelia burgdorferi sensu stricto* strain. *J Infect Dis* **186**, 782 (Sep 15, 2002).
24. G. Wang, C. Ojaimi, R. Iyer, V. Saksenberg, S. A. McClain *et al.*, Impact of genotypic variation of *Borrelia burgdorferi sensu stricto* on kinetics of dissemination and severity of disease in C3H/HeJ mice. *Infect Immun* **69**, 4303 (Jul, 2001).
25. V. Lagal, D. Portnoi, G. Faure, D. Postic, G. Baranton, *Borrelia burgdorferi sensu stricto* invasiveness is correlated with OspC-plasminogen affinity. *Microbes Infect* **8**, 645 (Mar, 2006).
26. C. G. Earnhart, E. L. Buckles, J. S. Dumler, R. T. Marconi, Demonstration of OspC type diversity in invasive human lyme disease isolates and identification of previously uncharacterized epitopes that define the specificity of the OspC murine antibody response. *Infect Immun* **73**, 7869 (Dec, 2005).
27. J. L. Coleman, J. A. Gebbia, J. Piesman, J. L. Degen, T. H. Bugge *et al.*, Plasminogen is required for efficient dissemination of *B. burgdorferi* in ticks and for enhancement of spirochetemia in mice. *Cell* **89**, 1111 (Jun 27, 1997).
28. R. Iyer, O. Kalu, J. Purser, S. Norris, B. Stevenson *et al.*, Linear and circular plasmid content in *Borrelia burgdorferi* clinical isolates. *Infect Immun* **71**, 3699 (Jul, 2003).
29. M. Labandeira-Rey, J. Seshu, J. T. Skare, The absence of linear plasmid 25 or 28-1 of *Borrelia burgdorferi* dramatically alters the kinetics of experimental infection via distinct mechanisms. *Infect Immun* **71**, 4608 (Aug, 2003).
30. J. E. Purser, S. J. Norris, Correlation between plasmid content and infectivity in *Borrelia burgdorferi*. *Proc Natl Acad Sci U S A* **97**, 13865 (Dec 5, 2000).
31. J. E. Purser, M. B. Lawrenz, M. J. Caimano, J. K. Howell, J. D. Radolf *et al.*, A plasmid-encoded nicotinamidase (PncA) is essential for infectivity of *Borrelia burgdorferi* in a mammalian host. *Mol Microbiol* **48**, 753 (May, 2003).
32. K. O. Strother, A. de Silva, Role of *Borrelia burgdorferi* linear plasmid 25 in infection of *Ixodes scapularis* ticks. *J Bacteriol* **187**, 5776 (Aug, 2005).
33. D. Grimm, K. Tilly, D. M. Bueschel, M. A. Fisher, P. F. Policastro *et al.*, Defining plasmids required by *Borrelia burgdorferi* for colonization of tick vector *Ixodes scapularis* (Acari: Ixodidae). *J Med Entomol* **42**, 676 (Jul, 2005).

34. J. Seshu, M. D. Esteve-Gassent, M. Labandeira-Rey, J. H. Kim, J. P. Trzeciakowski *et al.*, Inactivation of the fibronectin-binding adhesin gene *bbk32* significantly attenuates the infectivity potential of *Borrelia burgdorferi*. *Mol Microbiol* **59**, 1591 (Mar, 2006).
35. Q. Xu, S. V. Seemanapli, K. McShan, F. T. Liang, Increasing the interaction of *Borrelia burgdorferi* with decorin significantly reduces the 50 percent infectious dose and severely impairs dissemination. *Infect Immun* **75**, 4272 (Sep, 2007).
36. J. Anguita, M. N. Hedrick, E. Fikrig, Adaptation of *Borrelia burgdorferi* in the tick and the mammalian host. *FEMS Microbiol Rev* **27**, 493 (Oct, 2003).
37. M. E. Embers, R. Ramamoorthy, M. T. Philipp, Survival strategies of *Borrelia burgdorferi*, the etiologic agent of Lyme disease. *Microbes and Infection* **6**, 312 (2004).
38. J. Pietikainen, T. Meri, A. M. Blom, S. Meri, Binding of the complement inhibitor C4b-binding protein to Lyme disease *Borreliae*. *Mol Immunol* **47**, 1299 (Mar, 2010).
39. S. J. Norris, J. Coburn, J. M. Leong, L. T. Hu, M. Hook, in *Borrelia: Molecular Biology, Host Interaction and Pathogenesis*, J. S. Samuels, Radolf, J.D., Ed. (Caister Academic Press, Norfolk, UK, 2010), pp. 299-332.
40. T. J. LaRocca, D. J. Holthausen, C. Hsieh, C. Renken, C. A. Mannella *et al.*, The bactericidal effect of a complement-independent antibody is osmolytic and specific to *Borrelia*. *Proceedings of the National Academy of Sciences* **106**, 10752 (2009).
41. J. T. Skare, J. A. Carroll, F. X. Yang, D. S. Samuels, D. R. Akins, in *Borrelia: Molecular Biology, Host Interactions and Pathogenesis*, J. S. Samuels, Radolf, J.D., Ed. (Caister Academic Press, Norfolk, UK, 2010), pp. 67-101.
42. S. W. Barthold, D. Cadavid, M. T. Philipp, in *Borrelia: Molecular Biology, Host Interactions and Pathogenesis*, J. S. Samuels, Radolf, J.D., Ed. (Caister Academic Press, Norfolk, UK, 2010), pp. 359-411.
43. A. C. Steere, L. Glickstein, Elucidation of Lyme arthritis. *Nat Rev Immunol* **4**, 143 (Feb, 2004).
44. P. H. Duray, A. C. Steere, Clinical pathologic correlations of Lyme disease by stage. *Ann N Y Acad Sci* **539**, 65 (1988).

45. B. P. Iliopoulou, B. T. Huber, Infectious arthritis and immune dysregulation: lessons from Lyme disease. *Curr Opin Rheumatol* **22**, 451 (Jul, 2010).
46. A. L. Bernardino, T. A. Myers, X. Alvarez, A. Hasegawa, M. T. Philipp, Toll-like receptors: insights into their possible role in the pathogenesis of lyme neuroborreliosis. *Infect Immun* **76**, 4385 (Oct, 2008).
47. T. A. Myers, D. Kaushal, M. T. Philipp, Microglia are mediators of *Borrelia burgdorferi*-induced apoptosis in SH-SY5Y neuronal cells. *PLoS Pathog* **5**, e1000659 (Nov, 2009).
48. M. Hirschfeld, C. J. Kirschning, R. Schwandner, H. Wesche, J. H. Weis *et al.*, Cutting edge: inflammatory signaling by *Borrelia burgdorferi* lipoproteins is mediated by toll-like receptor 2. *J Immunol* **163**, 2382 (Sep 1, 1999).
49. Y. Ma, K. P. Seiler, K. F. Tai, L. Yang, M. Woods *et al.*, Outer surface lipoproteins of *Borrelia burgdorferi* stimulate nitric oxide production by the cytokine-inducible pathway. *Infect Immun* **62**, 3663 (Sep, 1994).
50. J. C. Miller, H. Maylor-Hagen, Y. Ma, J. H. Weis, J. J. Weis, The Lyme disease spirochete *Borrelia burgdorferi* utilizes multiple ligands, including RNA, for interferon regulatory factor 3-dependent induction of type I interferon-responsive genes. *Infect Immun* **78**, 3144 (Jul, 2010).
51. L. J. Glickstein, J. L. Coburn, Short report: Association of macrophage inflammatory response and cell death after *in vitro* *Borrelia burgdorferi* infection with arthritis resistance. *Am J Trop Med Hyg* **75**, 964 (Nov, 2006).
52. R. M. Wooten, Y. Ma, R. A. Yoder, J. P. Brown, J. H. Weis *et al.*, Toll-like receptor 2 is required for innate, but not acquired, host defense to *Borrelia burgdorferi*. *J Immunol* **168**, 348 (Jan 1, 2002).
53. X. Wang, Y. Ma, A. Yoder, H. Crandall, J. F. Zachary *et al.*, T cell infiltration is associated with increased Lyme arthritis in TLR2^{-/-} mice. *FEMS Immunol Med Microbiol* **52**, 124 (Jan, 2008).
54. D. D. Bolz, R. S. Sundsbak, Y. Ma, S. Akira, C. J. Kirschning *et al.*, MyD88 plays a unique role in host defense but not arthritis development in Lyme disease. *J Immunol* **173**, 2003 (Aug 1, 2004).
55. N. Liu, R. R. Montgomery, S. W. Barthold, L. K. Bockenstedt, Myeloid differentiation antigen 88 deficiency impairs pathogen clearance but does not alter inflammation in *Borrelia burgdorferi*-infected mice. *Infect Immun* **72**, 3195 (Jun, 2004).

56. A. K. Behera, E. Hildebrand, R. T. Bronson, G. Perides, S. Uematsu *et al.*, MyD88 deficiency results in tissue-specific changes in cytokine induction and inflammation in interleukin-18-independent mice infected with *Borrelia burgdorferi*. *Infect Immun* **74**, 1462 (Mar, 2006).
57. G. H. Giambartolomei, V. A. Dennis, M. T. Philipp, *Borrelia burgdorferi* stimulates the production of interleukin-10 in peripheral blood mononuclear cells from uninfected humans and rhesus monkeys. *Infect Immun* **66**, 2691 (Jun, 1998).
58. J. P. Brown, J. F. Zachary, C. Teuscher, J. J. Weis, R. M. Wooten, Dual role of interleukin-10 in murine Lyme disease: regulation of arthritis severity and host defense. *Infect Immun* **67**, 5142 (Oct, 1999).
59. J. J. Lazarus, M. J. Meadows, R. E. Lintner, R. M. Wooten, IL-10 deficiency promotes increased *Borrelia burgdorferi* clearance predominantly through enhanced innate immune responses. *J Immunol* **177**, 7076 (Nov 15, 2006).
60. H. Crandall, D. M. Dunn, Y. Ma, R. M. Wooten, J. F. Zachary *et al.*, Gene expression profiling reveals unique pathways associated with differential severity of lyme arthritis. *J Immunol* **177**, 7930 (Dec 1, 2006).
61. F. L. Sonderegger, Y. Ma, H. Maylor-Hagan, J. Brewster, X. Huang *et al.*, Localized production of IL-10 suppresses early inflammatory cell infiltration and subsequent development of IFN-gamma-mediated Lyme arthritis. *J Immunol* **188**, 1381 (Feb 1, 2012).
62. J. C. Miller, Y. Ma, J. Bian, K. C. Sheehan, J. F. Zachary *et al.*, A critical role for type I IFN in arthritis development following *Borrelia burgdorferi* infection of mice. *J Immunol* **181**, 8492 (Dec 15, 2008).
63. I. Kang, S. W. Barthold, D. H. Persing, L. K. Bockenstedt, T-helper-cell cytokines in the early evolution of murine Lyme arthritis. *Infect Immun* **65**, 3107 (Aug, 1997).
64. D. H. Margulies, J. McCluskey, in *Fundamental Immunology*, M. D. William E. Paul, Ed. (Lippincott Williams & Wilkins, Philadelphia, PA, USA, 2003), pp. 571-612.
65. A. C. Steere, E. Dwyer, R. Winchester, Association of chronic Lyme arthritis with HLA-DR4 and HLA-DR2 alleles. *N Engl J Med* **323**, 219 (Jul 26, 1990).
66. C. D. Reimers, U. Neubert, W. Kristoferitsch, K. H. Pfluger, W. R. Mayr, *Borrelia burgdorferi* infection in Europe: an HLA-related disease? *Infection* **20**, 197 (Jul-Aug, 1992).

67. A. C. Steere, S. M. Angelis, Therapy for Lyme arthritis: strategies for the treatment of antibiotic-refractory arthritis. *Arthritis Rheum* **54**, 3079 (Oct, 2006).
68. R. A. Kalish, J. M. Leong, A. C. Steere, Association of treatment-resistant chronic Lyme arthritis with HLA-DR4 and antibody reactivity to OspA and OspB of *Borrelia burgdorferi*. *Infect Immun* **61**, 2774 (Jul, 1993).
69. CDC, (2012), *Clinical Manifestations of Confirmed Lyme Disease Cases--United States, 2001-2010*. Centers for Disease Control and Prevention, Retrieved April 12, 2012.
<http://www.cdc.gov/lyme/stats/chartstables/casesbysymptom.html>
70. A. C. Steere, R. T. Schoen, E. Taylor, The clinical evolution of Lyme arthritis. *Ann Intern Med* **107**, 725 (Nov, 1987).
71. A. C. Steere, R. E. Levin, P. J. Molloy, R. A. Kalish, J. H. Abraham, 3rd *et al.*, Treatment of Lyme arthritis. *Arthritis Rheum* **37**, 878 (Jun, 1994).
72. A. R. Marques, Lyme disease: a review. *Curr Allergy Asthma Rep* **10**, 13 (Jan, 2010).
73. A. C. Steere, A. Gibofsky, M. E. Patarroyo, R. J. Winchester, J. A. Hardin *et al.*, Chronic Lyme arthritis. Clinical and immunogenetic differentiation from rheumatoid arthritis. *Ann Intern Med* **90**, 896 (Jun, 1979).
74. B. Wilske, V. Fingerle, U. Schulte-Spechtel, Microbiological and serological diagnosis of Lyme borreliosis. *FEMS Immunol Med Microbiol* **49**, 13 (Feb, 2007).
75. C. J. Mathews, V. C. Weston, A. Jones, M. Field, G. Coakley, Bacterial septic arthritis in adults. *Lancet* **375**, 846 (Mar 6, 2010).
76. E. Marker-Hermann, in *Rheumatology*, M. C. Hochberb, A. J. Silman, J. S. Smolen, M. E. Weinblatt, M. H. Weisman, Eds. (Mosby Elsevier, Philadelphia, PA; USA, 2008), vol. 2, pp. 1013-1028.
77. Y. E. Johnston, P. H. Duray, A. C. Steere, M. Kashgarian, J. Buza *et al.*, Lyme arthritis. Spirochetes found in synovial microangiopathic lesions. *Am J Pathol* **118**, 26 (Jan, 1985).
78. A. C. Steere, P. H. Duray, E. C. Butcher, Spirochetal antigens and lymphoid cell surface markers in Lyme synovitis. Comparison with rheumatoid synovium and tonsillar lymphoid tissue. *Arthritis Rheum* **31**, 487 (Apr, 1988).

79. P. H. Duray, Histopathology of clinical phases of human Lyme disease. *Rheum Dis Clin North Am* **15**, 691 (Nov, 1989).
80. J. J. Weis, L. K. Bockenstedt, in *Borrelia: Molecular Biology, Host Interaction and Pathogenesis*, J. S. Samuels, Radolf, J.D., Ed. (Caister Academic press, Norfolk, UK, 2010), pp. 413-441.
81. P. H. Duray, Clinical pathologic correlations of Lyme disease. *Rev Infect Dis* **11 Suppl 6**, S1487 (Sep-Oct, 1989).
82. J. P. Lawson, A. C. Steere, Lyme arthritis: radiologic findings. *Radiology* **154**, 37 (Jan, 1985).
83. R. K. Straubinger, B. A. Summers, Y. F. Chang, M. J. Appel, Persistence of *Borrelia burgdorferi* in experimentally infected dogs after antibiotic treatment. *J Clin Microbiol* **35**, 111 (Jan, 1997).
84. L. K. Bockenstedt, J. Mao, E. Hodzic, S. W. Barthold, D. Fish, Detection of attenuated, noninfectious spirochetes in *Borrelia burgdorferi*-infected mice after antibiotic treatment. *J Infect Dis* **186**, 1430 (Nov 15, 2002).
85. S. W. Barthold, E. Hodzic, D. M. Imai, S. Feng, X. Yang *et al.*, Ineffectiveness of tigecycline against persistent *Borrelia burgdorferi*. *Antimicrob Agents Chemother* **54**, 643 (Feb, 2010).
86. X. Li, G. A. McHugh, N. Damle, V. K. Sikand, L. Glickstein *et al.*, Burden and viability of *Borrelia burgdorferi* in skin and joints of patients with erythema migrans or Lyme arthritis. *Arthritis & Rheumatism* **63**, 2238 (2011).
87. J. W. Hovius, G. P. Wormser, in *Lyme Disease: An Evidence-based Approach*, J. J. Halperin, Ed. (CAB International, Oxfordshire, UK, 2011), vol. 20, pp. 89-99.
88. A. C. Steere, B. Falk, E. E. Drouin, L. A. Baxter-Lowe, J. Hammer *et al.*, Binding of outer surface protein A and human lymphocyte function-associated antigen 1 peptides to HLA-DR molecules associated with antibiotic treatment-resistant Lyme arthritis. *Arthritis Rheum* **48**, 534 (Feb, 2003).
89. E. E. Drouin, L. Glickstein, W. W. Kwok, G. T. Nepom, A. C. Steere, Searching for borrelial T cell epitopes associated with antibiotic-refractory Lyme arthritis. *Mol Immunol* **45**, 2323 (Apr, 2008).
90. Z. Haile, S. Khatua, Beyond Osteoarthritis: Recognizing and Treating Infectious and Other Inflammatory Arthropathies in Your Practice. *Primary Care: Clinics in Office Practice* **37**, 713 (2010).

91. A. J. Heilpern, W. Wertheim, J. He, G. Perides, R. T. Bronson *et al.*, Matrix metalloproteinase 9 plays a key role in lyme arthritis but not in dissemination of *Borrelia burgdorferi*. *Infect Immun* **77**, 2643 (Jul, 2009).
92. J. Bertrand, C. Cromme, D. Umlauf, S. Frank, T. Pap, Molecular mechanisms of cartilage remodelling in osteoarthritis. *Int J Biochem Cell Biol* **42**, 1594 (Oct, 2010).
93. D. Heinegard, T. Saxne, The role of the cartilage matrix in osteoarthritis. *Nat Rev Rheumatol* **7**, 50 (Jan, 2011).
94. J. P. Pelletier, J. Martel-Pelletier, S. B. Abramson, Osteoarthritis, an inflammatory disease: potential implication for the selection of new therapeutic targets. *Arthritis Rheum* **44**, 1237 (Jun, 2001).
95. M. B. Goldring, S. R. Goldring, Osteoarthritis. *J Cell Physiol* **213**, 626 (Dec, 2007).
96. A. D. Pearle, R. F. Warren, S. A. Rodeo, Basic science of articular cartilage and osteoarthritis. *Clin Sports Med* **24**, 1 (Jan, 2005).
97. Y. T. Konttinen, T. Sillat, G. Barreto, M. Ainola, D. C. Nordstrom, Osteoarthritis as an autoinflammatory disease caused by chondrocyte-mediated inflammatory responses. *Arthritis Rheum* **64**, 613 (Mar, 2012).
98. A. Opolka, R. H. Straub, A. Pasoldt, J. Grifka, S. Grassel, Substance P and norepinephrine modulate murine chondrocyte proliferation and apoptosis. *Arthritis Rheum* **64**, 729 (Mar, 2012).
99. Q. Wang, A. L. Rozelle, C. M. Lepus, C. R. Scanzello, J. J. Song *et al.*, Identification of a central role for complement in osteoarthritis. *Nat Med* **17**, 1674 (Dec, 2011).
100. F. De Ceuninck, L. Dassencourt, P. Anract, The inflammatory side of human chondrocytes unveiled by antibody microarrays. *Biochemical and Biophysical Research Communications* **323**, 960 (2004).
101. L. C. Tetlow, D. J. Adlam, D. E. Woolley, Matrix metalloproteinase and proinflammatory cytokine production by chondrocytes of human osteoarthritic cartilage: associations with degenerative changes. *Arthritis Rheum* **44**, 585 (Mar, 2001).
102. M. G. Von Herrath, D. Homann, in *Fundamental Immunology*, M. D. William E. Paul, Ed. (Lippincott Williams & Wilkins, Philadelphia, USA, 2003), pp. 1401-1438.

103. I. B. McInnes, G. Schett, Cytokines in the pathogenesis of rheumatoid arthritis. *Nature Reviews Immunology* **7**, 429 (2007).
104. S. Shiozawa, K. Tsumiyama, K. Yoshida, A. Hashiramoto, Pathogenesis of joint destruction in rheumatoid arthritis. *Arch Immunol Ther Exp (Warsz)* **59**, 89 (Apr, 2011).
105. S. Lefevre, A. Knedla, C. Tennie, A. Kampmann, C. Wunrau *et al.*, Synovial fibroblasts spread rheumatoid arthritis to unaffected joints. *Nat Med* **15**, 1414 (Dec, 2009).
106. J. Furuzawa-Carballeda, P. M. Macip-Rodriguez, A. R. Cabral, Osteoarthritis and rheumatoid arthritis pannus have similar qualitative metabolic characteristics and pro-inflammatory cytokine response. *Clin Exp Rheumatol* **26**, 554 (Jul-Aug, 2008).
107. P. A. Duc, K. Yudoh, K. Masuko, T. Kato, K. Nishioka *et al.*, Development and characteristics of pannus-like soft tissue in osteoarthritic articular surface in rat osteoarthritis model. *Clin Exp Rheumatol* **26**, 589 (Jul-Aug, 2008).
108. R. J. Reece, J. D. Canete, W. J. Parsons, P. Emery, D. J. Veale, Distinct vascular patterns of early synovitis in psoriatic, reactive, and rheumatoid arthritis. *Arthritis Rheum* **42**, 1481 (Jul, 1999).
109. E. M. Gravalles, P. A. Monach, in *Rheumatology*, M. C. Hochberb, A. J. Silman, J. S. Smolen, M. E. Weinblatt, M. H. Weisman, Eds. (Mosby Elsevier, Philadelphia, PA; USA, 2008), vol. 1, pp. 841-865.
110. M. Garcia-Arias, A. Balsa, E. M. Mola, Septic arthritis. *Best Pract Res Clin Rheumatol* **25**, 407 (Jun, 2011).
111. M. E. Shirliff, J. T. Mader, Acute septic arthritis. *Clin Microbiol Rev* **15**, 527 (Oct, 2002).
112. A. Keat, A. Toivanen, Reactive arthritis: clinical features and treatment. *Rheumatology*, M. C. Hochberb, A. J. Silman, J. S. Smolen, M. E. Weinblatt, M. H. Weisman, Eds. (Mosby Elsevier, Philadelphia, PA; USA, 2008), vol. 2, pp. 1089-1096.
113. I. Colmegna, L. R. Espinoza, Recent advances in reactive arthritis. *Curr Rheumatol Rep* **7**, 201 (Jun, 2005).
114. J. Sieper, Pathogenesis of reactive arthritis. *Curr Rheumatol Rep* **3**, 412 (Oct, 2001).

115. E. Gracey, R. D. Inman, Chlamydia-induced ReA: immune imbalances and persistent pathogens. *Nat Rev Rheumatol* **8**, 55 (Jan, 2012).
116. T. Hannu, R. Inman, K. Granfors, M. Leirisalo-Repo, Reactive arthritis or post-infectious arthritis? *Best Pract Res Clin Rheumatol* **20**, 419 (Jun, 2006).
117. T. Hannu, Reactive arthritis. *Best Pract Res Clin Rheumatol* **25**, 347 (Jun, 2011).
118. M. Leirisalo-Repo, P. Helenius, T. Hannu, A. Lehtinen, J. Kreula *et al.*, Long-term prognosis of reactive salmonella arthritis. *Ann Rheum Dis* **56**, 516 (Sep, 1997).
119. W. B. van den Berg, Articular cartilage: cause or victim in arthritis. *Scand J Rheumatol Suppl* **101**, 31 (1995).
120. P. Toivanen, A. Toivanen, Role of micro-organisms in the pathogenesis of arthritis: lessons from reactive and Lyme arthritis. *Scand J Rheumatol Suppl* **101**, 191 (1995).
121. M. S. Di Genaro, D. E. Cargnelutti, D. O. Castro, R. J. Elicabe, J. V. Gutierrez *et al.*, Yersinia-triggered arthritis in IL-12p40-deficient mice: relevant antigens and local expression of Toll-like receptor mRNA. *Scand J Rheumatol* **36**, 28 (Jan-Feb, 2007).
122. J. D. Carter, R. D. Inman, J. Whittum-Hudson, A. P. Hudson, Chlamydia and chronic arthritis. *Annals of Medicine*, 1 (2011).
123. A. Rizzo, M. D. Domenico, C. R. Carratelli, R. Paolillo, The role of Chlamydia and Chlamydophila infections in reactive arthritis. *Intern Med* **51**, 113 (2012).
124. J. D. Carter, L. R. Espinoza, R. D. Inman, K. B. Sneed, L. R. Ricca *et al.*, Combination antibiotics as a treatment for chronic Chlamydia-induced reactive arthritis: a double-blind, placebo-controlled, prospective trial. *Arthritis Rheum* **62**, 1298 (May, 2010).
125. J. D. Carter, H. C. Gerard, L. R. Espinoza, L. R. Ricca, J. Valeriano *et al.*, Chlamydiae as etiologic agents in chronic undifferentiated spondylarthritis. *Arthritis Rheum* **60**, 1311 (May, 2009).
126. D. R. Snyderman, D. P. Schenkein, V. P. Berardi, C. C. Lastavica, K. M. Pariser, *Borrelia burgdorferi* in joint fluid in chronic Lyme arthritis. *Ann Intern Med* **104**, 798 (Jun, 1986).

127. J. J. Nocton, F. Dressler, B. J. Rutledge, P. N. Rys, D. H. Persing *et al.*, Detection of *Borrelia burgdorferi* DNA by polymerase chain reaction in synovial fluid from patients with Lyme arthritis. *N Engl J Med* **330**, 229 (Jan 27, 1994).
128. J. de Koning, J. A. Hoogkamp-Korstanje, Diagnosis of Lyme disease by demonstration of spirochetes in tissue biopsies. *Zentralbl Bakteriol Mikrobiol Hyg A* **263**, 179 (Dec, 1986).
129. M. Morawski, G. Bruckner, T. Arendt, R. T. Matthews, Aggrecan: Beyond cartilage and into the brain. *Int J Biochem Cell Biol* **44**, 690 (May, 2012).
130. J. B. McGinty, S. S. Burkhart, *Operative Arthroscopy*. (Lippincott Williams & Wilkins, 2003).
131. J. A. Buckwalter, Articular cartilage. *Instr Course Lect* **32**, 349 (1983).
132. C. Kiani, L. Chen, Y. J. Wu, A. J. Yee, B. B. Yang, Structure and function of aggrecan. *Cell Res* **12**, 19 (Mar, 2002).
133. H. Watanabe, Y. Yamada, K. Kimata, Roles of aggrecan, a large chondroitin sulfate proteoglycan, in cartilage structure and function. *J Biochem* **124**, 687 (Oct, 1998).
134. J. Bondeson, S. Wainwright, C. Hughes, B. Caterson, The regulation of the ADAMTS4 and ADAMTS5 aggrecanases in osteoarthritis: a review. *Clin Exp Rheumatol* **26**, 139 (Jan-Feb, 2008).
135. L. Troeberg, H. Nagase, Proteases involved in cartilage matrix degradation in osteoarthritis. *Biochim Biophys Acta* **1824**, 133 (Jan, 2012).
136. H. Stanton, S. B. Golub, F. M. Rogerson, K. Last, C. B. Little *et al.*, Investigating ADAMTS-mediated aggrecanolysis in mouse cartilage. *Nature Protocols* **6**, 388 (2011).
137. P. Verma, K. Dalal, ADAMTS-4 and ADAMTS-5: key enzymes in osteoarthritis. *J Cell Biochem* **112**, 3507 (Dec, 2011).
138. S. Porter, I. M. Clark, L. Kevorkian, D. R. Edwards, The ADAMTS metalloproteinases. *Biochem J* **386**, 15 (Feb 15, 2005).
139. A. J. Fosang, C. B. Little, Drug insight: aggrecanases as therapeutic targets for osteoarthritis. *Nat Clin Pract Rheumatol* **4**, 420 (Aug, 2008).

140. P. J. Roughley, J. Barnett, F. Zuo, J. S. Mort, Variations in aggrecan structure modulate its susceptibility to aggrecanases. *Biochem J* **375**, 183 (Oct 1, 2003).
141. A. J. Fosang, K. Last, H. Stanton, S. B. Golub, C. B. Little *et al.*, Neopeptide antibodies against MMP-cleaved and aggrecanase-cleaved aggrecan. *Methods Mol Biol* **622**, 312 (2010).
142. J. D. Sandy, V. Thompson, K. Doege, C. Verscharen, The intermediates of aggrecanase-dependent cleavage of aggrecan in rat chondrosarcoma cells treated with interleukin-1. *Biochem J* **351**, 161 (Oct 1, 2000).
143. M. D. Tortorella, M. Pratta, R. Q. Liu, J. Austin, O. H. Ross *et al.*, Sites of aggrecan cleavage by recombinant human aggrecanase-1 (ADAMTS-4). *J Biol Chem* **275**, 18566 (Jun 16, 2000).
144. H. E. Miwa, T. A. Gerken, T. M. Hering, Effects of covalently attached chondroitin sulfate on aggrecan cleavage by ADAMTS-4 and MMP-13. *Matrix Biology* **25**, 534 (2006).
145. G. J. Wayne, S. J. Deng, A. Amour, S. Borman, R. Matico *et al.*, TIMP-3 inhibition of ADAMTS-4 (Aggrecanase-1) is modulated by interactions between aggrecan and the C-terminal domain of ADAMTS-4. *J Biol Chem* **282**, 20991 (Jul 20, 2007).
146. G. Murphy, H. Nagase, Localizing matrix metalloproteinase activities in the pericellular environment. *FEBS J* **278**, 2 (Jan, 2011).
147. T. E. Cawston, D. A. Young, Proteinases involved in matrix turnover during cartilage and bone breakdown. *Cell Tissue Res* **339**, 221 (Jan, 2010).
148. A. M. Manicone, J. K. McGuire, Matrix metalloproteinases as modulators of inflammation. *Semin Cell Dev Biol* **19**, 34 (Feb, 2008).
149. D. Y. Kim, K. K. Kim, Structure and function of HtrA family proteins, the key players in protein quality control. *J Biochem Mol Biol* **38**, 266 (May 31, 2005).
150. T. Clausen, C. Southan, M. Ehrmann, The HtrA family of proteases: implications for protein composition and cell fate. *Mol Cell* **10**, 443 (Sep, 2002).

151. K. D. Hadfield, C. F. Rock, C. A. Inkson, S. L. Dallas, L. Sudre *et al.*, HtrA1 inhibits mineral deposition by osteoblasts: requirement for the protease and PDZ domains. *J Biol Chem* **283**, 5928 (Feb 29, 2008).
152. M. Campioni, A. Severino, L. Manente, I. L. Tuduce, S. Toldo *et al.*, The serine protease HtrA1 specifically interacts and degrades the tuberous sclerosis complex 2 protein. *Mol Cancer Res* **8**, 1248 (Sep, 2010).
153. L. Zhang, S. L. Lim, H. Du, M. Zhang, I. Kozak *et al.*, High temperature requirement factor A1 (HTRA1) gene regulates angiogenesis through transforming growth factor-beta family member growth differentiation factor 6. *J Biol Chem* **287**, 1520 (Jan 6, 2012).
154. A. De Luca, M. De Falco, A. Severino, M. Campioni, D. Santini *et al.*, Distribution of the Serine Protease HtrA1 in Normal Human Tissues. *Journal of Histochemistry & Cytochemistry* **51**, 1279 (2003).
155. J. Chien, M. Campioni, V. Shridhar, A. Baldi, HtrA serine proteases as potential therapeutic targets in cancer. *Current cancer drug targets* **9**, 451 (2009).
156. S. Grau, P. J. Richards, B. Kerr, C. Hughes, B. Caterson *et al.*, The role of human HtrA1 in arthritic disease. *J Biol Chem* **281**, 6124 (Mar 10, 2006).
157. C. Oka, R. Tsujimoto, M. Kajikawa, K. Koshiba-Takeuchi, J. Ina *et al.*, HtrA1 serine protease inhibits signaling mediated by Tgfbeta family proteins. *Development* **131**, 1041 (Mar, 2004).
158. A. Tsuchiya, M. Yano, J. Tocharus, H. Kojima, M. Fukumoto *et al.*, Expression of mouse HtrA1 serine protease in normal bone and cartilage and its upregulation in joint cartilage damaged by experimental arthritis. *Bone* **37**, 323 (Sep, 2005).
159. A. E. Canfield, K. D. Hadfield, C. F. Rock, E. C. Wylie, F. L. Wilkinson, HtrA1: a novel regulator of physiological and pathological matrix mineralization? *Biochem Soc Trans* **35**, 669 (Aug, 2007).
160. A. Chamberland, E. Wang, A. R. Jones, L. A. Collins-Racie, E. R. LaVallie *et al.*, Identification of a novel HtrA1-susceptible cleavage site in human aggrecan: evidence for the involvement of HtrA1 in aggrecan proteolysis in vivo. *J Biol Chem* **284**, 27352 (Oct 2, 2009).
161. S. Vierkotten, P. S. Muether, S. Fauser, Overexpression of HTRA1 leads to ultrastructural changes in the elastic layer of Bruch's membrane via cleavage of extracellular matrix components. *PLoS One* **6**, e22959 (2011).

162. J. Mauney, B. R. Olsen, V. Volloch, Matrix remodeling as stem cell recruitment event: a novel in vitro model for homing of human bone marrow stromal cells to the site of injury shows crucial role of extracellular collagen matrix. *Matrix Biol* **29**, 657 (Oct, 2010).
163. I. Polur, P. L. Lee, J. M. Servais, L. Xu, Y. Li, Role of HTRA1, a serine protease, in the progression of articular cartilage degeneration. *Histol Histopathol* **25**, 599 (May).
164. J. M. Milner, A. Patel, A. D. Rowan, Emerging roles of serine proteinases in tissue turnover in arthritis. *Arthritis Rheum* **58**, 3644 (Dec, 2008).
165. A. K. Lemke, J. D. Sandy, H. Voigt, R. Dreier, J. H. Lee *et al.*, Interleukin-1alpha treatment of meniscal explants stimulates the production and release of aggrecanase-generated, GAG-substituted aggrecan products and also the release of pre-formed, aggrecanase-generated G1 and m-calpain-generated G1-G2. *Cell Tissue Res* **340**, 179 (Apr, 2010).
166. A. Gilicze, B. Kohalmi, P. Pocza, M. Keszei, J. Jaeger *et al.*, HtrA1 is a novel mast cell serine protease of mice and men. *Mol Immunol* **44**, 2961 (Apr, 2007).
167. N. Sofat, Analysing the role of endogenous matrix molecules in the development of osteoarthritis. *International Journal of Experimental Pathology* **90**, 463 (2009).
168. D. Foell, H. Wittkowski, J. Roth, Mechanisms of disease: a 'DAMP' view of inflammatory arthritis. *Nat Clin Pract Rheumatol* **3**, 382 (Jul, 2007).
169. T. L. Adair-Kirk, R. M. Senior, Fragments of extracellular matrix as mediators of inflammation. *Int J Biochem Cell Biol* **40**, 1101 (2008).
170. T. Yasuda, Cartilage destruction by matrix degradation products. *Modern Rheumatology* **16**, 197 (2006).
171. T. Yasuda, Activation of Akt leading to NF-kappaB up-regulation in chondrocytes stimulated with fibronectin fragment. *Biomed Res* **32**, 209 (2011).
172. M. B. Goldring, M. Otero, Inflammation in osteoarthritis. *Curr Opin Rheumatol* **23**, 471 (Sep, 2011).
173. M. D. Zack, E. C. Arner, C. P. Anglin, J. T. Alston, A. M. Malfait *et al.*, Identification of fibronectin neoepitopes present in human osteoarthritic cartilage. *Arthritis Rheum* **54**, 2912 (Sep, 2006).

174. M. L. Barilla, S. E. Carsons, Fibronectin fragments and their role in inflammatory arthritis. *Semin Arthritis Rheum* **29**, 252 (Feb, 2000).
175. G. A. Homandberg, F. Hui, C. Wen, C. Purple, K. Bewsey *et al.*, Fibronectin-fragment-induced cartilage chondrolysis is associated with release of catabolic cytokines. *Biochem J* **321 (Pt 3)**, 751 (Feb 1, 1997).
176. D. Long, S. Blake, X.-Y. Song, M. Lark, R. F. Loeser, Human articular chondrocytes produce IL-7 and respond to IL-7 with increased production of matrix metalloproteinase-13. *Arthritis Research & Therapy* **10**, R23 (2008).
177. T. Yasuda, A. R. Poole, A fibronectin fragment induces type II collagen degradation by collagenase through an interleukin-1-mediated pathway. *Arthritis Rheum* **46**, 138 (Jan, 2002).
178. H. Stanton, L. Ung, A. J. Fosang, The 45 kDa collagen-binding fragment of fibronectin induces matrix metalloproteinase-13 synthesis by chondrocytes and aggrecan degradation by aggrecanases. *Biochem J* **364**, 181 (May 15, 2002).
179. B. A. Austin, B. Liu, Z. Li, R. B. Nussenblatt, Biologically active fibronectin fragments stimulate release of MCP-1 and catabolic cytokines from murine retinal pigment epithelium. *Invest Ophthalmol Vis Sci* **50**, 2896 (Jun, 2009).
180. J. Chien, X. He, V. Shridhar, Identification of tubulins as substrates of serine protease HtrA1 by mixture-based oriented peptide library screening. *J Cell Biochem* **107**, 253 (May 15, 2009).
181. E. An, S. Sen, S. K. Park, H. Gordish-Dressman, Y. Hathout, Identification of novel substrates for the serine protease HTRA1 in the human RPE secretome. *Invest Ophthalmol Vis Sci* **51**, 3379 (Jul, 2010).
182. A. Sjoberg, P. Onnerfjord, M. Morgelin, D. Heinegard, A. M. Blom, The extracellular matrix and inflammation: fibromodulin activates the classical pathway of complement by directly binding C1q. *J Biol Chem* **280**, 32301 (Sep 16, 2005).
183. T. W. Groeneveld, M. Oroszlan, R. T. Owens, M. C. Faber-Krol, A. C. Bakker *et al.*, Interactions of the extracellular matrix proteoglycans decorin and biglycan with C1q and collectins. *J Immunol* **175**, 4715 (Oct 1, 2005).
184. J. Sorvillo, I. Gigli, E. Pearlstein, Fibronectin binding to complement subcomponent C1q. Localization of their respective binding sites. *Biochem J* **226**, 207 (Feb 15, 1985).

185. J. Chien, J. Staub, S. I. Hu, M. R. Erickson-Johnson, F. J. Couch *et al.*, A candidate tumor suppressor HtrA1 is downregulated in ovarian cancer. *Oncogene* **23**, 1636 (Feb 26, 2004).
186. A. Shiga, H. Nozaki, A. Yokoseki, M. Nihonmatsu, H. Kawata *et al.*, Cerebral small-vessel disease protein HTRA1 controls the amount of TGF-beta1 via cleavage of proTGF-beta1. *Hum Mol Genet* **20**, 1800 (May 1, 2011).
187. J. M. Lin, L. Wan, Y. Y. Tsai, H. J. Lin, Y. Tsai *et al.*, HTRA1 polymorphism in dry and wet age-related macular degeneration. *Retina* **28**, 309 (Feb, 2008).
188. T. Urano, K. Narusawa, S. Kobayashi, M. Shiraki, K. Horie-Inoue *et al.*, Association of HTRA1 promoter polymorphism with spinal disc degeneration in Japanese women. *J Bone Miner Metab* **28**, 220 (Mar, 2010).
189. D. Zurawa-Janicka, J. Skorko-Glonek, B. Lipinska, HtrA proteins as targets in therapy of cancer and other diseases. *Expert Opinion on Therapeutic Targets* **14**, 665 (Jul, 2010).
190. D. W. Holt, M. L. Henderson, C. E. Stockdale, J. T. Farrell, D. L. Kooyman *et al.*, Osteoarthritis-like changes in the heterozygous sedc mouse associated with the HtrA1-Ddr2-Mmp-13 degradative pathway: a new model of osteoarthritis. *Osteoarthritis Cartilage* **20**, 430 (May, 2012).
191. P. T. Elkington, C. M. O'Kane, J. S. Friedland, The paradox of matrix metalloproteinases in infectious disease. *Clin Exp Immunol* **142**, 12 (Oct, 2005).
192. D. Miao, J. C. Fenno, J. C. Timm, N. E. Joo, Y. L. Kapila, The *Treponema denticola* chymotrypsin-like protease dentilisin induces matrix metalloproteinase-2-dependent fibronectin fragmentation in periodontal ligament cells. *Infect Immun* **79**, 806 (Feb, 2011).
193. M. Hernandez, N. Dutzan, J. Garcia-Sesnich, L. Abusleme, A. Dezerega *et al.*, Host-pathogen interactions in progressive chronic periodontitis. *J Dent Res* **90**, 1164 (Oct, 2011).
194. J. R. Frederick, J. Sarkar, J. V. McDowell, R. T. Marconi, Molecular signaling mechanisms of the periopathogen, *Treponema denticola*. *J Dent Res* **90**, 1155 (Oct, 2011).
195. J. C. Fenno, *Treponema denticola* interactions with host proteins. *J Oral Microbiol* **4**, (2012).

196. B. Chi, M. Qi, H. K. Kuramitsu, Role of dentilisin in *Treponema denticola* epithelial cell layer penetration. *Res Microbiol* **154**, 637 (Nov, 2003).
197. C. A. Brissette, T. T. Pham, S. R. Coats, R. P. Darveau, S. A. Lukehart, *Treponema denticola* does not induce production of common innate immune mediators from primary gingival epithelial cells. *Oral Microbiol Immunol* **23**, 474 (Dec, 2008).
198. M. B. Visser, R. P. Ellen, New insights into the emerging role of oral spirochaetes in periodontal disease. *Clin Microbiol Infect* **17**, 502 (Apr, 2011).
199. L. Shaw, E. Golonka, J. Potempa, S. J. Foster, The role and regulation of the extracellular proteases of *Staphylococcus aureus*. *Microbiology* **150**, 217 (Jan, 2004).
200. M. J. McGavin, C. Zahradka, K. Rice, J. E. Scott, Modification of the *Staphylococcus aureus* fibronectin binding phenotype by V8 protease. *Infect Immun* **65**, 2621 (Jul, 1997).
201. T. Clausen, M. Kaiser, R. Huber, M. Ehrmann, HTRA proteases: regulated proteolysis in protein quality control. *Nat Rev Mol Cell Biol* **12**, 152 (Mar, 2011).
202. C. Spiess, A. Beil, M. Ehrmann, A temperature-dependent switch from chaperone to protease in a widely conserved heat shock protein. *Cell* **97**, 339 (Apr 30, 1999).
203. T. Krojer, K. Pangerl, J. Kurt, J. Sawa, C. Stingl *et al.*, Interplay of PDZ and protease domain of DegP ensures efficient elimination of misfolded proteins. *Proc Natl Acad Sci U S A* **105**, 7702 (Jun 3, 2008).
204. T. Krojer, J. Sawa, R. Huber, T. Clausen, HtrA proteases have a conserved activation mechanism that can be triggered by distinct molecular cues. *Nature Structural & Molecular Biology* **17**, 844 (2010).
205. H. Ingmer, L. Brondsted, Proteases in bacterial pathogenesis. *Res Microbiol* **160**, 704 (Nov, 2009).
206. K. Gibson, Y. Kumagai, Y. Rikihisa, Proteomic analysis of *Neorickettsia sennetsu* surface-exposed proteins and porin activity of the major surface protein P51. *J Bacteriol* **192**, 5898 (Nov, 2010).
207. Y. Kumagai, J. Matsuo, Y. Hayakawa, Y. Rikihisa, Cyclic di-GMP signaling regulates invasion by *Ehrlichia chaffeensis* of human monocytes. *J Bacteriol* **192**, 4122 (Aug, 2010).

208. N. Sabarth, S. Lamer, U. Zimny-Arndt, P. R. Jungblut, T. F. Meyer *et al.*, Identification of surface proteins of *Helicobacter pylori* by selective biotinylation, affinity purification, and two-dimensional gel electrophoresis. *J Biol Chem* **277**, 27896 (Aug 2, 2002).
209. X. Wu, L. Lei, S. Gong, D. Chen, R. Flores *et al.*, The chlamydial periplasmic stress response serine protease cHtrA is secreted into host cell cytosol. *BMC Microbiol* **11**, 87 (2011).
210. M. Boehm, B. Hoy, M. Rohde, N. Tegtmeyer, K. T. Baek *et al.*, Rapid paracellular transmigration of *Campylobacter jejuni* across polarized epithelial cells without affecting TER: role of proteolytic-active HtrA cleaving E-cadherin but not fibronectin. *Gut Pathog* **4**, 3 (Apr 25, 2012).
211. N. O. Kaakoush, S. M. Man, S. Lamb, M. J. Raftery, M. R. Wilkins *et al.*, The secretome of *Campylobacter concisus*. *FEBS J* **277**, 1606 (Apr, 2010).
212. D. Bumann, S. Aksu, M. Wendland, K. Janek, U. Zimny-Arndt *et al.*, Proteome analysis of secreted proteins of the gastric pathogen *Helicobacter pylori*. *Infection and immunity* **70**, 3396 (2002).
213. B. Hoy, T. Geppert, M. Boehm, F. Reisen, P. Plattner *et al.*, Distinct roles of secreted HtrA proteases from gram-negative pathogens in cleaving the junctional protein and tumor suppressor E-cadherin. *J Biol Chem* **287**, 10115 (Mar 23, 2012).
214. M. Lower, C. Weydig, D. Metzler, A. Reuter, A. Starzinski-Powitz *et al.*, Prediction of extracellular proteases of the human pathogen *Helicobacter pylori* reveals proteolytic activity of the Hp1018/19 protein HtrA. *PLoS One* **3**, e3510 (2008).
215. B. Hoy, M. Lower, C. Weydig, G. Carra, N. Tegtmeyer *et al.*, *Helicobacter pylori* HtrA is a new secreted virulence factor that cleaves E-cadherin to disrupt intercellular adhesion. *EMBO Rep* **11**, 798 (Oct, 2010).
216. L. E. Comstock, D. D. Thomas, Characterization of *Borrelia burgdorferi* invasion of cultured endothelial cells. *Microb Pathog* **10**, 137 (Feb, 1991).
217. L. E. Comstock, D. D. Thomas, Penetration of endothelial cell monolayers by *Borrelia burgdorferi*. *Infect Immun* **57**, 1626 (May, 1989).
218. Y. Ma, A. Sturrock, J. J. Weis, Intracellular localization of *Borrelia burgdorferi* within human endothelial cells. *Infect Immun* **59**, 671 (Feb, 1991).

219. A. Szczepanski, M. B. Furie, J. L. Benach, B. P. Lane, H. B. Fleit, Interaction between *Borrelia burgdorferi* and endothelium in vitro. *J Clin Invest* **85**, 1637 (May, 1990).
220. D. D. Thomas, L. E. Comstock, Interaction of Lyme disease spirochetes with cultured eucaryotic cells. *Infect Immun* **57**, 1324 (Apr, 1989).
221. L. T. Hu, M. A. Eskildsen, C. Masgala, A. C. Steere, E. C. Arner *et al.*, Host metalloproteinases in Lyme arthritis. *Arthritis Rheum* **44**, 1401 (Jun, 2001).
222. A. K. Behera, E. Hildebrand, S. Uematsu, S. Akira, J. Coburn *et al.*, Identification of a TLR-independent pathway for *Borrelia burgdorferi*-induced expression of matrix metalloproteinases and inflammatory mediators through binding to integrin alpha 3 beta 1. *J Immunol* **177**, 657 (Jul 1, 2006).
223. A. Kirchner, U. Koedel, V. Fingerle, R. Paul, B. Wilske *et al.*, Upregulation of matrix metalloproteinase-9 in the cerebrospinal fluid of patients with acute Lyme neuroborreliosis. *J Neurol Neurosurg Psychiatry* **68**, 368 (Mar, 2000).
224. J. A. Gebbia, J. L. Coleman, J. L. Benach, *Borrelia* spirochetes upregulate release and activation of matrix metalloproteinase gelatinase B (MMP-9) and collagenase 1 (MMP-1) in human cells. *Infect Immun* **69**, 456 (Jan, 2001).
225. B. Lin, J. M. Kidder, R. Noring, A. C. Steere, M. S. Klempner *et al.*, Differences in synovial fluid levels of matrix metalloproteinases suggest separate mechanisms of pathogenesis in Lyme arthritis before and after antibiotic treatment. *J Infect Dis* **184**, 174 (Jul 15, 2001).
226. A. K. Behera, E. Hildebrand, J. Scagliotti, A. C. Steere, L. T. Hu, Induction of host matrix metalloproteinases by *Borrelia burgdorferi* differs in human and murine lyme arthritis. *Infect Immun* **73**, 126 (Jan, 2005).
227. P. E. Van den Steen, P. Proost, A. Wuyts, J. Van Damme, G. Opdenakker, Neutrophil gelatinase B potentiates interleukin-8 tenfold by aminoterminal processing, whereas it degrades CTAP-III, PF-4, and GRO-alpha and leaves RANTES and MCP-2 intact. *Blood* **96**, 2673 (Oct 15, 2000).
228. A. Gautam, S. Dixit, M. T. Philipp, S. R. Singh, L. A. Morici *et al.*, Interleukin-10 alters effector functions of multiple genes induced by *Borrelia burgdorferi* in macrophages to regulate Lyme disease inflammation. *Infect Immun* **79**, 4876 (Dec, 2011).

229. M. S. Klempner, R. Noring, M. P. Epstein, B. McCloud, R. Hu *et al.*, Binding of human plasminogen and urokinase-type plasminogen activator to the Lyme disease spirochete, *Borrelia burgdorferi*. *J Infect Dis* **171**, 1258 (May, 1995).
230. J. L. Coleman, T. J. Sellati, J. E. Testa, R. R. Kew, M. B. Furie *et al.*, *Borrelia burgdorferi* binds plasminogen, resulting in enhanced penetration of endothelial monolayers. *Infect Immun* **63**, 2478 (Jul, 1995).
231. O. Onder, P. T. Humphrey, B. McOmber, F. Korobova, N. Francella *et al.*, OspC is a potent plasminogen-receptor on the surface of *Borrelia burgdorferi*. *J Biol Chem*, (Mar 20, 2012).
232. A. Toledo, J. L. Coleman, C. J. Kuhlow, J. T. Crowley, J. L. Benach, The enolase of *Borrelia burgdorferi* is a plasminogen receptor released in outer membrane vesicles. *Infect Immun* **80**, 359 (Jan, 2012).
233. A. M. Floden, J. A. Watt, C. A. Brissette, *Borrelia burgdorferi* enolase is a surface-exposed plasminogen binding protein. *PLoS One* **6**, e27502 (2011).
234. C. A. Brissette, K. Haupt, D. Barthel, A. E. Cooley, A. Bowman *et al.*, *Borrelia burgdorferi* infection-associated surface proteins ErpP, ErpA, and ErpC bind human plasminogen. *Infect Immun* **77**, 300 (Jan, 2009).
235. W. B. Haile, J. L. Coleman, J. L. Benach, Reciprocal upregulation of urokinase plasminogen activator and its inhibitor, PAI-2, by *Borrelia burgdorferi* affects bacterial penetration and host-inflammatory response. *Cell Microbiol* **8**, 1349 (Aug, 2006).
236. D. J. Grab, G. Perides, J. S. Dumler, K. J. Kim, J. Park *et al.*, *Borrelia burgdorferi*, host-derived proteases, and the blood-brain barrier. *Infect Immun* **73**, 1014 (Feb, 2005).
237. J. L. Coleman, E. J. Roemer, J. L. Benach, Plasmin-coated *Borrelia burgdorferi* degrades soluble and insoluble components of the mammalian extracellular matrix. *Infect Immun* **67**, 3929 (Aug, 1999).
238. J. L. Coleman, J. L. Benach, The Generation of Enzymatically Active Plasmin on the Surface of Spirochetes. *Methods* **21**, 133 (2000).
239. C. M. Fraser, S. Casjens, W. M. Huang, G. G. Sutton, R. Clayton *et al.*, Genomic sequence of a Lyme disease spirochaete, *Borrelia burgdorferi*. *Nature* **390**, 580 (Dec 11, 1997).

240. D. J. Grab, R. Kennedy, M. T. Philipp, *Borrelia burgdorferi* possesses a collagenolytic activity. *FEMS Microbiology Letters* **144**, 39 (1996).
241. M. S. Klempner, R. Noring, R. A. Rogers, Invasion of human skin fibroblasts by the Lyme disease spirochete, *Borrelia burgdorferi*. *J Infect Dis* **167**, 1074 (May, 1993).
242. A. K. Behera, E. Hildebrand, J. Szafranski, H. H. Hung, A. J. Grodzinsky *et al.*, Role of aggrecanase 1 in Lyme arthritis. *Arthritis Rheum* **54**, 3319 (Oct, 2006).
243. A. S. Kolaskar, P. C. Tongaonkar, A semi-empirical method for prediction of antigenic determinants on protein antigens. *FEBS Lett* **276**, 172 (Dec 10, 1990).
244. L. A. Solchaga, K. J. Penick, J. F. Welter, Chondrogenic differentiation of bone marrow-derived mesenchymal stem cells: tips and tricks. *Methods Mol Biol* **698**, 253 (2011).
245. S. R. Tew, A. D. Murdoch, R. P. Rauchenberg, T. E. Hardingham, Cellular methods in cartilage research: primary human chondrocytes in culture and chondrogenesis in human bone marrow stem cells. *Methods* **45**, 2 (May, 2008).
246. N. Parveen, J. M. Leong, Identification of a candidate glycosaminoglycan-binding adhesin of the Lyme disease spirochete *Borrelia burgdorferi*. *Mol Microbiol* **35**, 1220 (Mar, 2000).
247. N. Parveen, M. Caimano, J. D. Radolf, J. M. Leong, Adaptation of the Lyme disease spirochaete to the mammalian host environment results in enhanced glycosaminoglycan and host cell binding. *Mol Microbiol* **47**, 1433 (Mar, 2003).
248. N. Parveen, K. A. Cornell, J. L. Bono, C. Chamberland, P. Rosa *et al.*, Bgp, a secreted glycosaminoglycan-binding protein of *Borrelia burgdorferi* strain N40, displays nucleosidase activity and is not essential for infection of immunodeficient mice. *Infect Immun* **74**, 3016 (May, 2006).
249. K. A. Cornell, S. Primus, J. A. Martinez, N. Parveen, Assessment of methylthioadenosine/S-adenosylhomocysteine nucleosidases of *Borrelia burgdorferi* as targets for novel antimicrobials using a novel high-throughput method. *J Antimicrob Chemother* **63**, 1163 (Jun, 2009).

250. D. S. Saidac, S. A. Marras, N. Parveen, Detection and quantification of Lyme spirochetes using sensitive and specific molecular beacon probes. *BMC Microbiol* **9**, 43 (2009).
251. R. G. Cluss, D. A. Silverman, T. R. Stafford, Extracellular secretion of the *Borrelia burgdorferi* Oms28 porin and Bgp, a glycosaminoglycan binding protein. *Infect Immun* **72**, 6279 (Nov, 2004).
252. M. Pinne, Doctoral, Umeå universitet (2006).
253. Z. Ouyang, M. Kumar, T. Kariu, S. Haq, M. Goldberg *et al.*, BosR (BB0647) governs virulence expression in *Borrelia burgdorferi*. *Mol Microbiol* **74**, 1331 (Dec, 2009).
254. T. Krojer, M. Garrido-Franco, R. Huber, M. Ehrmann, T. Clausen, Crystal structure of DegP (HtrA) reveals a new protease-chaperone machine. *Nature* **416**, 455 (Mar 28, 2002).
255. C. H. Jones, P. Dexter, A. K. Evans, C. Liu, S. J. Hultgren *et al.*, Escherichia coli DegP Protease Cleaves between Paired Hydrophobic Residues in a Natural Substrate: the PapA Pilin. *Journal of Bacteriology* **184**, 5762 (2002).
256. B. Lipinska, M. Zylicz, C. Georgopoulos, The HtrA (DegP) protein, essential for Escherichia coli survival at high temperatures, is an endopeptidase. *J Bacteriol* **172**, 1791 (Apr, 1990).
257. A. Jomaa, J. Iwanczyk, J. Tran, J. Ortega, Characterization of the autocleavage process of the Escherichia coli HtrA protein: implications for its physiological role. *J Bacteriol* **191**, 1924 (Mar, 2009).
258. S. M. Loosmore, Y. P. Yang, R. Oomen, J. M. Shortreed, D. C. Coleman *et al.*, The Haemophilus influenzae HtrA protein is a protective antigen. *Infect Immun* **66**, 899 (Mar, 1998).
259. H. Schuhmann, P. F. Huesgen, C. Gietl, I. Adamska, The DEG15 serine protease cleaves peroxisomal targeting signal 2-containing proteins in Arabidopsis. *Plant Physiol* **148**, 1847 (Dec, 2008).
260. T. M. Hering, J. Kollar, T. D. Huynh, Complete coding sequence of bovine aggrecan: comparative structural analysis. *Arch Biochem Biophys* **345**, 259 (Sep 15, 1997).

261. H. E. Miwa, T. A. Gerken, T. D. Huynh, L. R. Duesler, M. Cotter *et al.*, Conserved sequence in the aggrecan interglobular domain modulates cleavage by ADAMTS-4 and ADAMTS-5. *Biochim Biophys Acta* **1790**, 161 (Mar, 2009).
262. R. V. Iozzo, R. V. Iozzo, Ed. (Crc Press, 2000).
263. H. Nakamura, Y. Fujii, I. Inoki, K. Sugimoto, K. Tanzawa *et al.*, Brevican is degraded by matrix metalloproteinases and aggrecanase-1 (ADAMTS4) at different sites. *J Biol Chem* **275**, 38885 (Dec 8, 2000).
264. G. A. Homandberg, R. Meyers, J. M. Williams, Intraarticular injection of fibronectin fragments causes severe depletion of cartilage proteoglycans in vivo. *J Rheumatol* **20**, 1378 (Aug, 1993).
265. A. N. Tladen, M. Klawitter, V. Lux, A. Mirsaidi, G. Bahrenberg *et al.*, Detrimental Role for Human High Temperature Requirement Serine Protease A1 (HTRA1) in the Pathogenesis of Intervertebral Disc (IVD) Degeneration. *J Biol Chem* **287**, 21335 (Jun 15, 2012).
266. N. Sofat, S. D. Robertson, R. Wait, Fibronectin III 13-14 domains induce joint damage via Toll-like receptor 4 activation and synergize with interleukin-1 and tumour necrosis factor. *J Innate Immun* **4**, 69 (2012).
267. R. A. Oldershaw, M. A. Baxter, E. T. Lowe, N. Bates, L. M. Grady *et al.*, Directed differentiation of human embryonic stem cells toward chondrocytes. *Nature Biotechnology* **28**, 1187 (2010).
268. B. T. Estes, B. O. Diekman, J. M. Gimble, F. Guilak, Isolation of adipose-derived stem cells and their induction to a chondrogenic phenotype. *Nature Protocols* **5**, 1294 (2010).
269. A. D. Murdoch, L. M. Grady, M. P. Ablett, T. Katopodi, R. S. Meadows *et al.*, Chondrogenic Differentiation of Human Bone Marrow Stem Cells in Transwell Cultures: Generation of Scaffold-Free Cartilage. *Stem Cells* **25**, 2786 (2007).
270. J. Welter, L. Solchaga, K. Penick, Simplification of aggregate culture of human mesenchymal stem cells as a chondrogenic screening assay. *BioTechniques* **42**, 732 (2007).
271. B. Beutler, Tlr4: central component of the sole mammalian LPS sensor. *Curr Opin Immunol* **12**, 20 (Feb, 2000).

272. C. Guyard, J. M. Battisti, S. J. Raffel, M. E. Schruppf, A. R. Whitney *et al.*, Relapsing fever spirochaetes produce a serine protease that provides resistance to oxidative stress and killing by neutrophils. *Mol Microbiol* **60**, 710 (May, 2006).
273. L. T. Hu, G. Perides, R. Noring, M. S. Klempner, Binding of human plasminogen to *Borrelia burgdorferi*. *Infect Immun* **63**, 3491 (Sep, 1995).
274. X. Yang, K. Promnares, J. Qin, M. He, D. Y. Shroder *et al.*, Characterization of multiprotein complexes of the *Borrelia burgdorferi* outer membrane vesicles. *J Proteome Res* **10**, 4556 (Oct 7, 2011).
275. B. Gesslbauer, A. Poljak, C. Handwerker, W. Schuler, D. Schwendenwein *et al.*, Comparative membrane proteome analysis of three *Borrelia* species. *Proteomics* **12**, 845 (Mar, 2012).
276. S. Bergstrom, W. R. Zuckert, in *Borrelia: Molecular Biology, Host Interaction and Pathogenesis*, J. S. Samuels, Radolf, J.D., Ed. (Caister Academic Press, Norfolk, UK, 2010), pp. 139-166.
277. S. J. Norris, J. K. Howell, E. A. Odeh, T. Lin, L. Gao *et al.*, High-throughput plasmid content analysis of *Borrelia burgdorferi* B31 by using Luminex multiplex technology. *Appl Environ Microbiol* **77**, 1483 (Feb, 2011).
278. J. Iwanczyk, V. Leong, J. Ortega, Factors Defining the Functional Oligomeric State of Escherichia coli DegP Protease. *PLoS One* **6**, e18944 (2011).
279. J. Skórko-Glonek, D. Żurawa, F. Tanfani, A. Scirè, A. Wawrzynów *et al.*, The N-terminal region of HtrA heat shock protease from Escherichia coli is essential for stabilization of HtrA primary structure and maintaining of its oligomeric structure. *Biochimica et Biophysica Acta (BBA) - Proteins & Proteomics* **1649**, 171 (2003).
280. X. C. Bai, X. J. Pan, X. J. Wang, Y. Y. Ye, L. F. Chang *et al.*, Characterization of the structure and function of Escherichia coli DegQ as a representative of the DegQ-like proteases of bacterial HtrA family proteins. *Structure* **19**, 1328 (Sep 7, 2011).
281. Y. J. Wu, D. P. La Pierre, J. Wu, A. J. Yee, B. B. Yang, The interaction of versican with its binding partners. *Cell Res* **15**, 483 (Jul, 2005).

282. R. Frischknecht, C. I. Seidenbecher, The crosstalk of hyaluronan-based extracellular matrix and synapses. *Neuron Glia Biol* **4**, 249 (Aug, 2008).
283. A. D. Berendsen, L. W. Fisher, T. M. Kilts, R. T. Owens, P. G. Robey *et al.*, Modulation of canonical Wnt signaling by the extracellular matrix component biglycan. *Proc Natl Acad Sci U S A* **108**, 17022 (Oct 11, 2011).
284. R. V. Iozzo, L. Schaefer, Proteoglycans in health and disease: novel regulatory signaling mechanisms evoked by the small leucine-rich proteoglycans. *FEBS J* **277**, 3864 (Oct, 2010).
285. P. Singh, C. Carraher, J. E. Schwarzbauer, Assembly of fibronectin extracellular matrix. *Annu Rev Cell Dev Biol* **26**, 397 (Nov 10, 2010).
286. T. J. Moriarty, M. U. Norman, P. Colarusso, T. Bankhead, P. Kubes *et al.*, Real-time high resolution 3D imaging of the lyme disease spirochete adhering to and escaping from the vasculature of a living host. *PLoS Pathog* **4**, e1000090 (Jun, 2008).
287. K. Midwood, S. Sacre, A. M. Piccinini, J. Inglis, A. Trebault *et al.*, Tenascin-C is an endogenous activator of Toll-like receptor 4 that is essential for maintaining inflammation in arthritic joint disease. *Nat Med* **15**, 774 (Jul, 2009).
288. J. I. Pulai, H. Chen, H. J. Im, S. Kumar, C. Hanning *et al.*, NF-kappa B mediates the stimulation of cytokine and chemokine expression by human articular chondrocytes in response to fibronectin fragments. *J Immunol* **174**, 5781 (May 1, 2005).
289. R. Pankov, K. M. Yamada, Fibronectin at a glance. *J Cell Sci* **115**, 3861 (Oct 15, 2002).
290. S. L. Su, C. D. Tsai, C. H. Lee, D. M. Salter, H. S. Lee, Expression and regulation of Toll-like receptor 2 by IL-1beta and fibronectin fragments in human articular chondrocytes. *Osteoarthritis Cartilage* **13**, 879 (Oct, 2005).
291. M. Gouwy, S. Struyf, P. Proost, J. Van Damme, Synergy in cytokine and chemokine networks amplifies the inflammatory response. *Cytokine Growth Factor Rev* **16**, 561 (Dec, 2005).
292. F. T. Afshari, J. C. Kwok, L. White, J. W. Fawcett, Schwann cell migration is integrin-dependent and inhibited by astrocyte-produced aggrecan. *Glia* **58**, 857 (May, 2010).

293. A. K. Behera, E. Durand, C. Cugini, S. Antonara, L. Bourassa *et al.*, *Borrelia burgdorferi* BBB07 interaction with integrin alpha3beta1 stimulates production of pro-inflammatory mediators in primary human chondrocytes. *Cell Microbiol* **10**, 320 (Feb, 2008).
294. M. Guerau-de-Arellano, B. T. Huber, Chemokines and Toll-like receptors in Lyme disease pathogenesis. *Trends Mol Med* **11**, 114 (Mar, 2005).
295. Z. Szekanecz, A. Vegvari, Z. Szabo, A. E. Koch, Chemokines and chemokine receptors in arthritis. *Front Biosci (Schol Ed)* **2**, 153 (2010).
296. R. R. Mullegger, T. K. Means, J. J. Shin, M. Lee, K. L. Jones *et al.*, Chemokine signatures in the skin disorders of Lyme borreliosis in Europe: predominance of CXCL9 and CXCL10 in erythema migrans and acrodermatitis and CXCL13 in lymphocytoma. *Infect Immun* **75**, 4621 (Sep, 2007).
297. Z. Zhao, B. McCloud, R. Fleming, M. S. Klempner, *Borrelia burgdorferi*-induced monocyte chemoattractant protein-1 production in vivo and in vitro. *Biochem Biophys Res Commun* **358**, 528 (Jun 29, 2007).
298. K. Strle, E. E. Drouin, S. Shen, J. E. Khoury, G. McHugh *et al.*, *Borrelia burgdorferi* stimulates macrophages to secrete higher levels of cytokines and chemokines than *Borrelia afzelii* or *Borrelia garinii*. *J Infect Dis* **200**, 1936 (Dec 15, 2009).
299. S. Grygorczuk, J. Zajkowska, R. Swierzbinska, S. Pancewicz, M. Kondrusik *et al.*, Concentration of interferon-inducible T cell chemoattractant and monocyte chemotactic protein-1 in serum and cerebrospinal fluid of patients with Lyme borreliosis. *Rocz Akad Med Bialymst* **50**, 173 (2005).
300. K. Strle, J. J. Shin, L. J. Glickstein, A. C. Steere, Association of a Toll-like receptor 1 polymorphism with heightened Th1 inflammatory responses and antibiotic-refractory Lyme arthritis. *Arthritis Rheum* **64**, 1497 (May, 2012).
301. G. A. Homandberg, Cartilage damage by matrix degradation products: fibronectin fragments. *Clin Orthop Relat Res*, S100 (Oct, 2001).
302. FDA, (2012), *FDA Approved medical devices for in vitro Lyme disease diagnostics*. U.S. Food and Drug Administration, Retrieved October 18, 2012. <http://www.accessdata.fda.gov/scripts/cdrh/devicesatfda/index.cfm>

303. R. M. Bacon, B. J. Biggerstaff, M. E. Schriefer, R. D. Gilmore, Jr., M. T. Philipp *et al.*, Serodiagnosis of Lyme disease by kinetic enzyme-linked immunosorbent assay using recombinant VlsE1 or peptide antigens of *Borrelia burgdorferi* compared with 2-tiered testing using whole-cell lysates. *J Infect Dis* **187**, 1187 (Apr 15, 2003).